

## GWTC-4.0: Tests of General Relativity. II. Parameterized Tests

THE LIGO SCIENTIFIC COLLABORATION, THE VIRGO COLLABORATION, AND THE KAGRA COLLABORATION

(Compiled: 18 March 2026)

### ABSTRACT

In this second of three papers on tests of general relativity (GR) applied to the compact binary coalescence signals in the fourth Gravitational-Wave Transient Catalog (GWTC-4.0), we present the results of the parameterized tests of GR and constraints on line-of-sight acceleration. We include events up to and including the first part of the fourth observing run (O4a) of the LIGO–Virgo–KAGRA detectors. As in the other two papers in this series, we restrict our analysis to the 42 confident signals, measured by at least two detectors, that have false alarm rates  $\leq 10^{-3} \text{ yr}^{-1}$  from O4a, in addition to the 49 such events from previous observing runs. This paper focuses on the eight tests that constrain parameterized deviations from the expected GR (or unaccelerated) values. These include modifications of post-Newtonian (PN) parameters, spin-induced quadrupole moments different from those of a binary black hole, and possible dispersive or birefringent propagation effects. Overall, we find no evidence for physics beyond GR, for spin-induced quadrupole moments different from those of a Kerr black hole in GR, or for line of sight acceleration, with more than 90% of the events including the null result (no deviation) within their 90% credible intervals. We discuss possible systematics affecting the other events and tests, even though they are statistically not surprising, given noise. We improve the bounds on deviations from the GR PN coefficients by factors of 1.2–5.5 and provide illustrative translations to constraints on some modified theories. Also, we update the bound on the mass of the graviton, at 90% credibility, to  $m_g \leq 1.92 \times 10^{-23} \text{ eV}/c^2$ . Thus, we see that GR holds, and many of the bounds on possible deviations derived from our events are the best to date.

### 1. OVERVIEW

This paper is the second of three papers examining the nature of gravity through tests of general relativity (GR)—and more generally of physics beyond the usual assumption of quasi-circular, isolated binaries composed of black holes (BHs) and/or neutron stars (NSs)—performed on the gravitational wave (GW) signals as reported by the LIGO–Virgo–KAGRA Collaboration (LVK) in the fourth Gravitational-Wave Transient Catalog (GWTC-4.0; Abac et al. 2025a,b). Paper I (Abac et al. 2025c) gives an introduction and overview of our suite of events, tests, and shared methods, and also presents the results of the consistency tests. Paper III (Abac et al. 2025d) focuses on tests of the remnants, considering the ringdown and possible echoes. This paper describes the various parameterized tests performed to place quantitative bounds on possible deformations of the GWs observed from compact binary coalescence (CBC) sources, relative to those calculated in GR. Specifically, we apply these tests to binary BH (BBH), NS–BH binary (NSBH), and binary NS (BNS) systems. Where applicable, we describe the improved bounds

relative to previous GW catalogs and to existing bounds in the literature.

Specifically, we first examine deviations in post-Newtonian (PN) coefficients. The PN approximation (e.g., Einstein et al. 1938; Chandrasekhar 1965; Maggiore 2007; Poisson & Will 2014) is the standard framework for computing and testing corrections to Newtonian gravity. Tests of gravity in the PN framework have commonly been carried out in the weak field (e.g., Solar System tests; Will 2014, 2018). However, for CBCs, the PN approximation has been iterated to an impressively high order in perturbation theory (Blanchet 2024), so one can even use it to test highly relativistic effects during the end of inspiral (e.g., Blanchet & Sathyaprakash 1994, 1995; Arun et al. 2006a,b). For a binary system, the PN approximation describes corrections to the binary’s dynamics as a series in powers of  $v/c$ , where  $v$  is the binary’s orbital velocity. The coefficients we test appear in the GW phase, and thus describe a combination of the binary’s conservative and dissipative dynamics.

The lowest few PN parameters can be constrained with binary-pulsar observations (e.g., Taylor & Weisberg 1982, 1989; Kramer et al. 2021), while higher PN orders can only be constrained meaningfully with GW observations, since these allow one to probe the strong-field, dynamical portion of the binary’s evolution close to merger. We use two frameworks (TIGER and FTI, both defined and described below) to place bounds on deviations in individual PN coefficients, and also

**Table 1.** Event selection table for the analyses in this paper, from first part of the fourth observing run (O4a) and the previous observing runs O1–O3

Run	Event Name	SNR	$(1+z)\mathcal{M}/M_{\odot}$	$\chi_{\text{eff}}$	$q$	Parameterized			SIM			PRP	
						TIGER	FTI	PCA	Phenom	EOB	LOSA	MDR	SSB
O1	GW150914	$26.0^{+0.1}_{-0.2}$	$30.7^{+1.8}_{-1.6}$	$-0.04^{+0.12}_{-0.14}$	$0.88^{+0.11}_{-0.22}$	✓	++	...	...	...	...	✓	+
	GW151012*	$9.3^{+0.3}_{-0.5}$	$18.8^{+3.4}_{-1.5}$	$0.13^{+0.30}_{-0.22}$	$0.57^{+0.36}_{-0.34}$	++	...	...	...	...	...	++	+
	GW151226	$12.7^{+0.3}_{-0.3}$	$9.71^{+0.08}_{-0.06}$	$0.20^{+0.23}_{-0.08}$	$0.53^{+0.41}_{-0.34}$	✓I	++	...	✓	...	...	✓	+
O2	GW170104	$13.8^{+0.2}_{-0.3}$	$25.7^{+1.7}_{-1.7}$	$-0.04^{+0.15}_{-0.19}$	$0.73^{+0.24}_{-0.26}$	✓	++	...	...	...	...	✓	+
	GW170608	$15.3^{+0.2}_{-0.3}$	$8.50^{+0.05}_{-0.05}$	$0.05^{+0.13}_{-0.05}$	$0.74^{+0.23}_{-0.33}$	✓I	++	...	...	...	...	✓	+
	GW170729*	$10.7^{+0.4}_{-0.5}$	$52.5^{+9.2}_{-12.0}$	$0.33^{+0.23}_{-0.32}$	$0.58^{+0.35}_{-0.23}$	++	...	...	...	...	...	++	+
	GW170809	$12.8^{+0.2}_{-0.3}$	$29.9^{+2.4}_{-2.0}$	$0.07^{+0.17}_{-0.17}$	$0.71^{+0.25}_{-0.25}$	✓PI	...	...	...	...	...	✓	+
	GW170814	$17.7^{+0.2}_{-0.3}$	$27.0^{+1.5}_{-1.3}$	$0.08^{+0.13}_{-0.13}$	$0.81^{+0.16}_{-0.23}$	✓	++	...	...	...	...	✓	+
	GW170817	$32.7^{+0.1}_{-0.1}$	$1.1976^{+0.0004}_{-0.0002}$	$0.02^{+0.06}_{-0.02}$	$0.72^{+0.24}_{-0.21}$	++	++	+	...	...	✓	++	...
	GW170818	$12.0^{+0.3}_{-0.4}$	$32.7^{+2.8}_{-2.5}$	$-0.05^{+0.19}_{-0.22}$	$0.80^{+0.18}_{-0.24}$	✓PI	...	...	...	...	...	✓	+
	GW170823	$12.2^{+0.2}_{-0.3}$	$39.1^{+5.4}_{-4.7}$	$0.07^{+0.21}_{-0.22}$	$0.78^{+0.20}_{-0.30}$	✓PI	...	...	...	...	...	✓	+
O3a	GW190408_181802	$14.6^{+0.2}_{-0.3}$	$23.8^{+1.2}_{-1.5}$	$-0.03^{+0.13}_{-0.17}$	$0.75^{+0.21}_{-0.26}$	✓	++	...	...	...	...	✓	+
	GW190412	$19.8^{+0.2}_{-0.3}$	$15.24^{+0.37}_{-0.23}$	$0.21^{+0.12}_{-0.13}$	$0.325^{+0.172}_{-0.097}$	✓	++	✓	✓	...	...	✓	+
	GW190421_213856	$10.7^{+0.2}_{-0.4}$	$45.9^{+5.7}_{-6.3}$	$-0.10^{+0.21}_{-0.27}$	$0.78^{+0.20}_{-0.32}$	✓PI	...	...	...	...	...	✓	+
	GW190425	$12.4^{+0.3}_{-0.4}$	$1.4873^{+0.0008}_{-0.0006}$	$0.06^{+0.11}_{-0.05}$	$0.67^{+0.29}_{-0.25}$	...	...	...	...	...	✓	...	...
	GW190503_185404	$12.1^{+0.2}_{-0.4}$	$37.8^{+6.1}_{-6.7}$	$-0.05^{+0.23}_{-0.30}$	$0.69^{+0.27}_{-0.29}$	✓PI	...	...	...	...	...	✓	+
	GW190512_180714	$12.7^{+0.3}_{-0.4}$	$18.58^{+0.69}_{-0.66}$	$0.02^{+0.13}_{-0.14}$	$0.54^{+0.36}_{-0.18}$	✓	++	...	...	...	...	✓	+
	GW190513_205428	$12.5^{+0.3}_{-0.4}$	$30.7^{+6.1}_{-3.4}$	$0.18^{+0.29}_{-0.22}$	$0.52^{+0.41}_{-0.20}$	✓PI	...	...	...	...	...	✓	+
	GW190517_055101	$10.8^{+0.5}_{-0.6}$	$36.2^{+4.2}_{-4.9}$	$0.52^{+0.20}_{-0.26}$	$0.64^{+0.30}_{-0.30}$	✓PI	...	...	...	...	...	✓	+
	GW190519_153544	$15.9^{+0.2}_{-0.3}$	$65.1^{+8.7}_{-10.9}$	$0.33^{+0.20}_{-0.24}$	$0.63^{+0.26}_{-0.22}$	✓PI	...	...	...	...	...	✓	+
	GW190521	$14.3^{+0.4}_{-0.3}$	$101^{+29}_{-34}$	$-0.14^{+0.50}_{-0.45}$	$0.59^{+0.33}_{-0.38}$	✓PI	...	...	...	...	...	...	...
	GW190521_074359	$25.9^{+0.1}_{-0.2}$	$39.8^{+3.2}_{-2.7}$	$0.10^{+0.13}_{-0.13}$	$0.77^{+0.19}_{-0.21}$	✓	++	...	...	...	...	✓	+
	GW190602_175927	$13.2^{+0.2}_{-0.3}$	$73^{+12}_{-18}$	$0.12^{+0.25}_{-0.28}$	$0.63^{+0.32}_{-0.34}$	✓PI	...	...	...	...	...	✓	+
	GW190630_185205	$16.4^{+0.2}_{-0.3}$	$29.5^{+2.1}_{-1.7}$	$0.10^{+0.14}_{-0.13}$	$0.68^{+0.28}_{-0.22}$	✓	++	...	...	...	...	✓	+
	GW190706_222641	$13.4^{+0.2}_{-0.4}$	$77^{+12}_{-18}$	$0.32^{+0.24}_{-0.30}$	$0.56^{+0.34}_{-0.25}$	✓PI	...	...	...	...	...	✓	+
	GW190707_093326	$13.1^{+0.2}_{-0.4}$	$9.90^{+0.11}_{-0.10}$	$-0.04^{+0.10}_{-0.09}$	$0.66^{+0.28}_{-0.20}$	✓I	++	...	...	...	...	✓	+
	GW190708_232457	$13.4^{+0.2}_{-0.3}$	$15.48^{+0.25}_{-0.24}$	$0.05^{+0.11}_{-0.10}$	$0.58^{+0.36}_{-0.18}$	✓	++	...	...	...	...	✓	+
	GW190720_000836	$10.9^{+0.3}_{-0.8}$	$10.37^{+0.11}_{-0.11}$	$0.19^{+0.14}_{-0.11}$	$0.53^{+0.35}_{-0.24}$	✓I	++	...	✓	...	...	✓	+
	GW190727_060333	$11.7^{+0.2}_{-0.5}$	$45.2^{+5.8}_{-5.5}$	$0.11^{+0.26}_{-0.26}$	$0.79^{+0.18}_{-0.29}$	✓PI	...	...	...	...	...	✓	+
	GW190728_064510	$13.1^{+0.3}_{-0.4}$	$10.14^{+0.11}_{-0.08}$	$0.13^{+0.20}_{-0.07}$	$0.64^{+0.30}_{-0.36}$	✓I	++	...	✓	...	...	✓	+
	GW190814	$25.3^{+0.1}_{-0.2}$	$6.42^{+0.02}_{-0.02}$	$0.00^{+0.07}_{-0.07}$	$0.111^{+0.012}_{-0.011}$	✓	++	✓	...	...	...	✓	+
	GW190828_063405	$16.5^{+0.2}_{-0.3}$	$34.6^{+3.5}_{-2.9}$	$0.19^{+0.16}_{-0.17}$	$0.82^{+0.15}_{-0.26}$	✓	++	...	✓	...	...	✓	+
	GW190828_065509	$10.2^{+0.4}_{-0.5}$	$17.33^{+0.61}_{-0.71}$	$0.05^{+0.16}_{-0.17}$	$0.44^{+0.38}_{-0.16}$	✓I	++	...	...	...	...	✓	+
	GW190910_112807	$14.5^{+0.2}_{-0.3}$	$43.6^{+4.4}_{-4.0}$	$0.00^{+0.17}_{-0.19}$	$0.80^{+0.18}_{-0.23}$	✓PI	...	...	...	...	...	✓	+
GW190915_235702	$13.1^{+0.2}_{-0.3}$	$32.5^{+3.1}_{-3.1}$	$-0.02^{+0.19}_{-0.23}$	$0.76^{+0.21}_{-0.29}$	✓PI	...	...	...	...	...	✓	+	

**Table 1** continued

Table 1 (continued)

Run	Event Name	SNR	$(1+z)\mathcal{M}/M_{\odot}$	$\chi_{\text{eff}}$	$q$	Parameterized			SIM			PRP	
						TIGER	FTI	PCA	Phenom	EOB	LOSA	MDR	SSB
	GW190924_021846	$12.0^{+0.3}_{-0.4}$	$6.44^{+0.03}_{-0.02}$	$0.03^{+0.20}_{-0.08}$	$0.58^{+0.32}_{-0.30}$	✓ I	++	...	...	...	...	✓	+
O3b	GW191109_010717	$17.2^{+0.5}_{-0.5}$	$60.1^{+9.8}_{-9.3}$	$-0.29^{+0.42}_{-0.31}$	$0.73^{+0.21}_{-0.24}$	✓ PI	...	...	...	...	...	✓	...
	GW191129_134029	$13.1^{+0.2}_{-0.3}$	$8.49^{+0.06}_{-0.05}$	$0.06^{+0.16}_{-0.08}$	$0.63^{+0.31}_{-0.29}$	✓ I	++	...	...	...	...	✓	+
	GW191204_171526	$17.5^{+0.2}_{-0.2}$	$9.69^{+0.05}_{-0.05}$	$0.16^{+0.08}_{-0.05}$	$0.69^{+0.25}_{-0.26}$	✓ I	++	✓	✓	...	...	✓	+
	GW191215_223052	$11.2^{+0.3}_{-0.4}$	$24.9^{+1.5}_{-1.4}$	$-0.03^{+0.17}_{-0.21}$	$0.73^{+0.24}_{-0.27}$	✓	...	...	...	...	...	✓	+
	GW191216_213338	$18.6^{+0.2}_{-0.2}$	$8.94^{+0.05}_{-0.05}$	$0.11^{+0.13}_{-0.06}$	$0.63^{+0.31}_{-0.29}$	✓	++	✓	✓	...	...	✓	+
	GW191222_033537	$12.5^{+0.2}_{-0.3}$	$51.0^{+7.2}_{-6.5}$	$-0.04^{+0.20}_{-0.25}$	$0.79^{+0.18}_{-0.32}$	✓ PI	...	...	...	...	...	✓	+
	GW200115_042309	$11.3^{+0.3}_{-0.5}$	$2.58^{+0.01}_{-0.01}$	$-0.15^{+0.24}_{-0.41}$	$0.243^{+0.432}_{-0.097}$	✓ I	++	...	...	...	✓	...	...
	GW200129_065458	$26.8^{+0.2}_{-0.2}$	$32.1^{+1.8}_{-2.6}$	$0.11^{+0.11}_{-0.16}$	$0.85^{+0.12}_{-0.41}$	✓	++	...	++	...	...	✓	+
	GW200202_154313	$10.8^{+0.2}_{-0.4}$	$8.15^{+0.05}_{-0.05}$	$0.04^{+0.13}_{-0.06}$	$0.72^{+0.24}_{-0.31}$	✓ I	++	...	...	...	...	✓	+
	GW200208_130117	$10.8^{+0.3}_{-0.5}$	$38.8^{+5.2}_{-4.8}$	$-0.07^{+0.22}_{-0.27}$	$0.73^{+0.23}_{-0.29}$	✓ PI	...	...	...	...	...	✓	+
	GW200219_094415	$10.7^{+0.3}_{-0.5}$	$43.7^{+6.3}_{-6.2}$	$-0.08^{+0.23}_{-0.29}$	$0.77^{+0.21}_{-0.32}$	✓ PI	...	...	...	...	...	✓	+
	GW200224_222234	$20.0^{+0.2}_{-0.2}$	$41.1^{+3.6}_{-3.8}$	$0.11^{+0.15}_{-0.15}$	$0.82^{+0.16}_{-0.26}$	✓ PI	...	...	...	...	...	✓	+
	GW200225_060421	$12.5^{+0.3}_{-0.4}$	$17.65^{+0.98}_{-1.97}$	$-0.12^{+0.17}_{-0.28}$	$0.73^{+0.23}_{-0.28}$	✓	++	...	...	...	...	✓	+
	GW200311_115853	$17.8^{+0.2}_{-0.2}$	$32.7^{+2.7}_{-2.8}$	$-0.02^{+0.16}_{-0.20}$	$0.82^{+0.16}_{-0.27}$	✓	++	...	...	...	...	✓	+
	GW200316_215756	$10.3^{+0.4}_{-0.7}$	$10.68^{+0.12}_{-0.12}$	$0.13^{+0.27}_{-0.10}$	$0.59^{+0.34}_{-0.38}$	✓ I	++	...	✓	...	...	✓	...
O4a	GW230518_125908	$14.2^{+0.2}_{-0.4}$	$2.94^{+0.00}_{-0.00}$	$-0.01^{+0.09}_{-0.11}$	$0.18^{+0.04}_{-0.03}$	✓ I	✓	...	...	...	...	...	...
	GW230601_224134	$12.3^{+0.2}_{-0.3}$	$73.0^{+8.3}_{-11.8}$	$-0.03^{+0.27}_{-0.32}$	$0.69^{+0.26}_{-0.30}$	✓ PI	...	...	...	...	...	✓	✓
	GW230605_065343	$10.5^{+0.3}_{-0.4}$	$14.44^{+0.28}_{-0.24}$	$0.06^{+0.16}_{-0.10}$	$0.65^{+0.31}_{-0.29}$	✓	✓	...	...	...	...	✓	✓
	GW230606_004305	$10.3^{+0.3}_{-0.4}$	$39.5^{+5.9}_{-5.8}$	$-0.11^{+0.26}_{-0.31}$	$0.70^{+0.27}_{-0.33}$	✓ PI	...	...	...	...	...	✓	✓
	GW230609_064958	$9.8^{+0.3}_{-0.5}$	$40.1^{+5.7}_{-5.9}$	$-0.14^{+0.22}_{-0.27}$	$0.73^{+0.24}_{-0.30}$	✓ PI	...	...	...	...	...	✓	✓
	GW230624_113103	$9.7^{+0.4}_{-0.5}$	$24.5^{+3.1}_{-2.4}$	$0.17^{+0.29}_{-0.25}$	$0.59^{+0.35}_{-0.29}$	✓ PI	...	...	...	...	...	✓	✓
	GW230627_015337	$28.5^{+0.1}_{-0.1}$	$6.41^{+0.01}_{-0.01}$	$0.02^{+0.08}_{-0.03}$	$0.69^{+0.25}_{-0.21}$	✓	✓	✓	...	...	...	✓	✓
	GW230628_231200	$15.5^{+0.2}_{-0.3}$	$35.8^{+2.8}_{-2.7}$	$-0.01^{+0.16}_{-0.16}$	$0.85^{+0.14}_{-0.24}$	✓	✓	...	...	...	...	✓	✓
	GW230630_234532	$9.4^{+0.3}_{-0.5}$	$8.57^{+0.06}_{-0.09}$	$-0.04^{+0.16}_{-0.08}$	$0.67^{+0.29}_{-0.28}$	✓ I	...	...	...	...	...	✓	✓
	GW230702_185453	$9.5^{+0.3}_{-0.5}$	$33.0^{+4.8}_{-3.9}$	$0.05^{+0.29}_{-0.26}$	$0.45^{+0.45}_{-0.25}$	✓ PI	...	...	...	...	...	✓	✓
	GW230731_215307	$11.9^{+0.2}_{-0.3}$	$9.46^{+0.07}_{-0.06}$	$-0.05^{+0.11}_{-0.06}$	$0.76^{+0.22}_{-0.29}$	✓ I	✓	...	...	...	...	✓	✓
	GW230811_032116	$12.8^{+0.3}_{-0.4}$	$33.3^{+3.0}_{-2.6}$	$0.02^{+0.18}_{-0.18}$	$0.63^{+0.31}_{-0.22}$	✓	✓	...	...	...	...	✓	✓
	GW230814_061920	$9.4^{+0.3}_{-0.5}$	$77^{+12}_{-18}$	$0.05^{+0.29}_{-0.28}$	$0.62^{+0.32}_{-0.29}$	✓ PI	...	...	...	...	...	✓	✓
	GW230824_033047	$10.0^{+0.2}_{-0.4}$	$65.8^{+8.0}_{-12.7}$	$-0.00^{+0.23}_{-0.27}$	$0.71^{+0.26}_{-0.34}$	✓ PI	...	...	...	...	...	✓	✓
	GW230904_051013	$10.2^{+0.3}_{-0.5}$	$9.06^{+0.06}_{-0.06}$	$0.05^{+0.15}_{-0.07}$	$0.68^{+0.29}_{-0.31}$	✓ I	...	...	...	...	...	✓	✓
	GW230914_111401	$16.2^{+0.2}_{-0.3}$	$59.4^{+7.8}_{-11.3}$	$0.12^{+0.19}_{-0.20}$	$0.62^{+0.32}_{-0.26}$	✓ PI	...	...	...	...	...	✓	✓
	GW230919_215712	$15.7^{+0.2}_{-0.3}$	$26.4^{+1.2}_{-1.2}$	$0.18^{+0.12}_{-0.13}$	$0.79^{+0.18}_{-0.25}$	✓	✓	...	✓	✓	...	✓	✓
	GW230920_071124	$10.1^{+0.3}_{-0.4}$	$35.8^{+4.1}_{-3.4}$	$0.00^{+0.22}_{-0.23}$	$0.75^{+0.22}_{-0.30}$	✓ PI	...	...	...	...	...	✓	✓
	GW230922_020344	$11.8^{+0.3}_{-0.4}$	$38.2^{+3.6}_{-3.2}$	$0.03^{+0.20}_{-0.21}$	$0.75^{+0.22}_{-0.26}$	✓ PI	✓	...	...	...	...	✓	✓
	GW230922_040658	$11.4^{+0.2}_{-0.4}$	$105^{+15}_{-29}$	$0.31^{+0.25}_{-0.32}$	$0.71^{+0.26}_{-0.43}$	✓ PI	...	...	...	...	...	✓	✓
	GW230924_124453	$12.9^{+0.2}_{-0.3}$	$31.7^{+2.4}_{-2.0}$	$0.02^{+0.18}_{-0.18}$	$0.81^{+0.17}_{-0.24}$	✓	✓	...	...	...	...	✓	✓

Table 1 continued

Table 1 (continued)

Run	Event Name	SNR	$(1+z)\mathcal{M}/M_{\odot}$	$\chi_{\text{eff}}$	$q$	Parameterized			SIM			PRP	
						TIGER	FTI	PCA	Phenom	EOB	LOSA	MDR	SSB
	GW230927_043729	$10.5^{+0.2}_{-0.4}$	$41.0^{+4.3}_{-3.8}$	$0.01^{+0.20}_{-0.22}$	$0.80^{+0.18}_{-0.27}$	✓ <sub>PI</sub>	...	...	...	...	...	✓	✓
	GW230927_153832	$19.7^{+0.2}_{-0.2}$	$20.14^{+0.41}_{-0.41}$	$0.03^{+0.08}_{-0.08}$	$0.75^{+0.21}_{-0.19}$	✓	✓	✓	...	...	...	✓	✓
	GW230928_215827	$8.9^{+0.4}_{-0.6}$	$61^{+10}_{-14}$	$0.40^{+0.20}_{-0.28}$	$0.56^{+0.35}_{-0.27}$	✓ <sub>PI</sub>	...	...	...	...	...	✓	✓
	GW231001_140220	$9.6^{+0.3}_{-0.5}$	$81^{+17}_{-20}$	$-0.04^{+0.33}_{-0.35}$	$0.54^{+0.36}_{-0.26}$	✓ <sub>PI</sub>	...	...	...	...	...	✓	✓
	GW231020_142947	$10.5^{+0.3}_{-0.4}$	$9.99^{+0.10}_{-0.10}$	$0.15^{+0.25}_{-0.12}$	$0.61^{+0.35}_{-0.40}$	✓ <sub>I</sub>	✓	...	✓	✓	...	✓	✓
	GW231028_153006	$21.0^{+0.2}_{-0.2}$	$107^{+10}_{-27}$	$0.44^{+0.16}_{-0.20}$	$0.63^{+0.33}_{-0.35}$	✓ <sub>PI</sub>	...	...	...	...	...	✓	✓
	GW231102_071736	$13.3^{+0.2}_{-0.3}$	$71.7^{+7.8}_{-10.5}$	$0.06^{+0.23}_{-0.22}$	$0.72^{+0.25}_{-0.27}$	✓ <sub>PI</sub>	...	...	...	...	...	✓	✓
	GW231104_133418	$11.0^{+0.2}_{-0.4}$	$11.31^{+0.10}_{-0.10}$	$0.14^{+0.12}_{-0.07}$	$0.70^{+0.26}_{-0.31}$	✓ <sub>I</sub>	✓	...	✓	✓	...	✓	✓
	GW231108_125142	$12.4^{+0.2}_{-0.3}$	$23.79^{+0.96}_{-0.97}$	$-0.08^{+0.13}_{-0.15}$	$0.75^{+0.22}_{-0.23}$	✓	✓	...	...	...	...	✓	✓
	GW231110_040320	$11.0^{+0.3}_{-0.4}$	$18.02^{+0.69}_{-0.48}$	$0.17^{+0.13}_{-0.12}$	$0.65^{+0.30}_{-0.25}$	✓	✓	...	✓	✓	...	✓	✓
	GW231113_200417	$10.1^{+0.3}_{-0.5}$	$9.82^{+0.08}_{-0.08}$	$0.13^{+0.14}_{-0.08}$	$0.65^{+0.31}_{-0.31}$	✓ <sub>I</sub>	✓	...	✓	✓	...	✓	✓
	GW231114_043211	$9.8^{+0.3}_{-0.5}$	$14.61^{+0.37}_{-0.31}$	$0.08^{+0.22}_{-0.16}$	$0.36^{+0.27}_{-0.17}$	✓ <sub>I</sub>	...	...	...	...	...	✓	✓
	GW231118_005626	$10.5^{+0.3}_{-0.5}$	$17.62^{+0.40}_{-0.54}$	$0.37^{+0.10}_{-0.11}$	$0.55^{+0.37}_{-0.22}$	✓	...	...	✓	...	...	✓	✓
	GW231118_090602	$10.9^{+0.4}_{-0.4}$	$10.53^{+0.12}_{-0.09}$	$0.08^{+0.36}_{-0.09}$	$0.56^{+0.38}_{-0.41}$	✓ <sub>I</sub>	✓	...	✓	✓	...	✓	✓
	GW231123_135430	$20.7^{+0.2}_{-0.3}$	$137^{+21}_{-27}$	$0.31^{+0.25}_{-0.41}$	$0.74^{+0.22}_{-0.38}$	...	...	...	...	...	...	✗	✗
	GW231206_233134	$11.0^{+0.3}_{-0.4}$	$41.9^{+4.7}_{-4.9}$	$-0.09^{+0.22}_{-0.24}$	$0.81^{+0.17}_{-0.28}$	✓ <sub>PI</sub>	...	...	...	...	...	✓	✓
	GW231206_233901	$21.0^{+0.1}_{-0.2}$	$36.1^{+2.3}_{-2.3}$	$-0.05^{+0.14}_{-0.15}$	$0.76^{+0.21}_{-0.25}$	✓	✓	...	...	...	...	✓	✓
	GW231213_111417	$9.7^{+0.2}_{-0.4}$	$44.4^{+7.2}_{-6.5}$	$0.06^{+0.24}_{-0.23}$	$0.79^{+0.19}_{-0.30}$	✓ <sub>PI</sub>	...	...	...	...	...	✓	✓
	GW231223_032836	$8.8^{+0.3}_{-0.5}$	$55.0^{+9.3}_{-15.0}$	$-0.15^{+0.33}_{-0.37}$	$0.71^{+0.26}_{-0.41}$	✓ <sub>PI</sub>	...	...	...	...	...	✓	✓
	GW231224_024321	$12.9^{+0.2}_{-0.3}$	$8.48^{+0.06}_{-0.06}$	$-0.01^{+0.08}_{-0.06}$	$0.79^{+0.19}_{-0.26}$	✓ <sub>I</sub>	✓	...	...	...	...	✓	✓
	GW231226_101520	$33.7^{+0.1}_{-0.1}$	$39.8^{+1.6}_{-1.6}$	$-0.09^{+0.09}_{-0.10}$	$0.88^{+0.11}_{-0.19}$	✓	...	...	...	...	...	✓	✓

NOTE— Event selection table for the analyses in this paper, from O4a (Abac et al. 2025b) and the previous observing runs O1 (Abbott et al. 2016a), O2 (Abbott et al. 2019a), O3a (Abbott et al. 2021a, 2024), and O3b (Abbott et al. 2023), with binary parameters from each observing run’s catalog paper. TIGER, FTI, and MDR results for GW170817 were published in Abbott et al. (2019b). The starred events GW151012 and GW170729 had previously been used for the indicated tests of GR in Abbott et al. (2016a, 2019c), but do not meet the current selection criteria. The O3a event GW190425 does meet the current selection criteria, but was previously excluded from most tests as a binary neutron star. A ✓ indicates an event meeting our selection criteria for an analysis and thus included in our results; only these have been used to generate the bounds on GR deviations presented in this paper. A ++ indicates previous results by the LVK exist, but are not used for the new bounds here, while a + indicates existing results in external works. A ... indicates events not meeting selection criteria. For the TIGER tests, further subscripts I/PI indicate where the test is only applied to the inspiral/post-inspiral stages, respectively. A few events have ✗ signs, indicating they had originally met the selection criteria, but technical difficulties in their analysis prevented obtaining meaningful results.

69 illustrate how such bounds can be translated (with significant  
70 caveats) into constraints on some alternative theories.

71 We also test for deviations in phenomenological post-  
72 inspiral coefficients with TIGER, in combinations of multiple  
73 PN coefficients using principal component analysis (PCA),  
74 and in the spin-induced multipole (SIM) PN coefficients.

75 Additionally, we place bounds on the line-of-sight accel-  
76 eration (LOSA) of the source systems and on modifications  
77 to the propagation (PRP) of GWs to Earth, including in the  
78 GWs’ dispersion relation (MDR), and of spacetime symme-  
79 try breaking (SSB) leading to anisotropic birefringence. The  
80 LOSA analysis is not a test of GR, but rather tests for astro-

81 physics not included in the standard analyses performed in  
82 Abac et al. (2025b). However, the LOSA analysis is included  
83 in this paper as such effects could appear as a GR deviation  
84 in other tests. Similarly, the LOSA analysis is also sensitive  
85 to other deviations from the assumption of quasi-circular iso-  
86 lated binaries, including deviations from GR, and provides a  
87 test of deviations starting at  $-4\text{PN}$  (see Section 2.4) that is  
88 complementary to other analyses.

89 We apply these tests to the GW events from GWTC-4.0 that  
90 were observed with at least two detectors, and with a false-  
91 alarm rate of  $\leq 10^{-3} \text{ yr}^{-1}$ , as described in Paper I. These  
92 include 42 events from O4a, which are new, as well as some

93 events from previous runs, O1 (Abbott et al. 2016a,b), O2  
 94 (Abbott et al. 2019a,b,c), O3a (Abbott et al. 2021b, 2024),  
 95 and O3b (Abbott et al. 2023, 2025), which have been used  
 96 for a subset of the tests, in particular in creating combined  
 97 results. Table 1 details which events were analyzed by each  
 98 test. Table 1 also provides each binary’s redshifted chirp mass  
 99  $(1+z)\mathcal{M}$ , effective inspiral spin  $\chi_{\text{eff}}$ , and mass ratio  $q$ , as  
 100 convenient combinations of the masses and spins (Abac et al.  
 101 2025a).

102 The rest of this paper is organized as follows: Section 2  
 103 describes the parameterized tests of modifications in the gener-  
 104 ation of the GWs from the CBC systems, with the constraints  
 105 on deviations in individual PN and post-inspiral coefficients  
 106 given in Section 2.1 and the PCA multiparameter analysis  
 107 given in Section 2.2, while Section 2.3 presents the SIM test  
 108 and Section 2.4 the LOSA test. The propagation tests are  
 109 given in Section 3 (MDR in Section 3.1 and SSB in Sec-  
 110 tion 3.2). We provide final conclusions along with a summary  
 111 of the bounds and some of their implications in Section 4. In  
 112 Appendix A, we discuss the check of waveform systematics  
 113 (i.e., systematic biases due to waveform modeling uncertain-  
 114 ties) for the TIGER analysis of GW231028.153006, while in  
 115 Appendix B, we discuss how prior effects lead to the apparent  
 116 GR deviation found in the MDR analysis of that event. In Ap-  
 117 pendix C, we discuss the waveform systematics found in the  
 118 MDR analysis of GW231123.135430 (henceforth shortened  
 119 to GW231123).

## 120 2. TESTS OF GW GENERATION

### 121 2.1. FTI and TIGER: Single-parameter tests

122 Alternative theories of gravity may lead to modifications  
 123 of a binary’s binding energy and angular momentum and the  
 124 corresponding fluxes, which lead to changes in the orbital  
 125 motion of the binary (e.g., Sotiriou & Barausse 2007; Yagi  
 126 et al. 2012; Mirshekari & Will 2013; Lang 2014, 2015; Julié  
 127 2018; Bernard et al. 2022; Shiralilou et al. 2022). This means  
 128 that the inspiral portion of the GW signal emitted by the  
 129 binary differs from GR. Such deviations from GR can be  
 130 captured by introducing extra parameters in the waveform. In  
 131 this section, we focus on constraining deviations from GR  
 132 by introducing parametric deviations in the inspiral, post-  
 133 inspiral, and merger–ringdown part of a waveform model. We  
 134 will focus on deviations in the frequency domain GW phase,  
 135 since GW observations are less sensitive to deviations in the  
 136 amplitude (see, e.g., Cutler & Flanagan 1994).

137 The GW signal from the early inspiral of compact binar-  
 138 ies can be well described using the PN formalism (Blanchet  
 139 2024). In the PN approximation, the waveform is expanded in  
 140 powers of dimensionless velocity  $v/c$ , where  $\mathcal{O}([v/c]^n)$  rela-  
 141 tive to the leading order is referred to as the  $(n/2)$ PN order.  
 142 Given the intrinsic parameters of a binary, the coefficients at  
 143 each PN order are uniquely determined in GR. Measuring  
 144 these coefficients by allowing them to differ from their GR  
 145 value can therefore be used as a null test of GR (Blanchet &  
 146 Sathyaprakash 1994, 1995; Arun et al. 2006a,b; Yunes & Pre-  
 147 torius 2009; Mishra et al. 2010; Li et al. 2012a,b). Although  
 148 many alternative theories of gravity admit a PN expansion and

149 can therefore be captured in this form, this is not always the  
 150 case. For example, abrupt changes in the waveform such as  
 151 dynamical scalarization do not admit a PN expansion (Samp-  
 152 son et al. 2014; Khalil et al. 2019). However, such a null test  
 153 may still be able to detect such deviations from GR.

154 The frequency domain phase of the GW signal during  
 155 early inspiral can be obtained from the PN expanded time  
 156 domain waveform using the stationary phase approxima-  
 157 tion (Sathyaprakash & Dhurandhar 1991; Cutler & Flanagan  
 158 1994; Buonanno et al. 2009). For quasi-circular, spin-aligned  
 159 binaries, it has the form

$$160 \quad \Psi_{\ell m}(f) = 2\pi f t_c - \phi_c - \frac{\pi}{4} \\ 161 \quad + \frac{3c^5}{128\eta v^5} \frac{|m|}{2} \sum_{n=0}^7 \left( \psi_n + \psi_{nl} \log \frac{v}{c} \right) \frac{v^n}{c^n}, \quad (1)$$

162 where  $v = [2\pi G(1+z)Mf/|m|]^{1/3}$  with  $f$  the GW fre-  
 163 quency,  $M$  the total mass,  $\eta$  the symmetric mass ratio,  $z$   
 164 the redshift, and  $t_c, \phi_c$  the time and phase at coalescence  
 165 (Abac et al. 2025a). The coefficients  $\psi_n$  and  $\psi_{nl}$  (where the  
 166  $l$  denotes the coefficients of the logarithmic terms) are the  
 167  $(n/2)$ PN coefficients and depend on the masses and spins of  
 168 the binary. The subscript  $\ell m$  denotes the  $(\ell, m)$  multipole in  
 169 the spherical harmonic decomposition of the waveform. The  
 170 PN coefficients are fully known up to 4.5PN (Blanchet et al.  
 171 2023), but we only include the ones up to 3.5PN here since  
 172 we do not test for higher orders.

173 Deviations from GR can then be modeled by introducing  
 174 parametric deviations to the non-spinning part of the PN coef-  
 175 ficients in GR  $\psi_i^{\text{GR,NS}}$ , i.e., of the form

$$176 \quad \psi_i \rightarrow (1 + \delta\hat{\varphi}_i) \psi_i^{\text{GR,NS}} + \psi_i^{\text{GR,S}}, \quad (2)$$

177 where  $\delta\hat{\varphi}_i$  is the deviation parameter and  $\psi_i^{\text{GR,S}}$  is the spin-  
 178 dependent part of the PN coefficient in GR. This is the  
 179 same parameterization that was previously used (Abbott et al.  
 180 2016b, 2019b,c, 2021b; Sanger et al. 2024; Abbott et al. 2025),  
 181 and avoids possible singularities when the spin-dependent  
 182 terms cancel with the non-spinning terms. Since the spin  
 183 terms are still included in the GR part of the model, excluding  
 184 the spin terms from the normalization of the deviations does  
 185 not lead to any problems even for highly spinning systems.  
 186 The full set of inspiral parameters that we constrain is then

$$187 \quad \{\delta\hat{\varphi}_{-2}, \delta\hat{\varphi}_0, \delta\hat{\varphi}_1, \delta\hat{\varphi}_2, \delta\hat{\varphi}_3, \delta\hat{\varphi}_4, \delta\hat{\varphi}_{5l}, \delta\hat{\varphi}_6, \delta\hat{\varphi}_{6l}, \delta\hat{\varphi}_7\}. \quad (3)$$

188 The non-logarithmic 2.5PN term is degenerate with the co-  
 189 alescence phase, so it cannot be constrained. In GR, the  $-1$ PN  
 190 and 0.5PN terms vanish, so we instead treat  $\delta\hat{\varphi}_{-2}$  and  $\delta\hat{\varphi}_1$  as  
 191 absolute deviations with a normalization factor equal to the  
 192 0PN coefficient. All other deviation parameters are fractional  
 193 deviations relative to the GR values.

194 We use two different frameworks to constrain these inspiral  
 195 deviation parameters. They use a different approach for how  
 196 exactly the corrections are added to the GR waveform, and  
 197 differ in the underlying GR waveform model used. Using two

different implementations of the parameterized inspiral test with two different GR waveform models makes the test more robust against waveform systematics coming from approximations made in the models.

The first framework is called the Flexible Theory-Independent (FTI) method (Mehta et al. 2023) and can use any frequency-domain, aligned-spin GR waveform as a baseline model. In this work, we use the SEOB-NRV5HM\_ROM (Pompili et al. 2023) waveform approximant for BBHs. For NSBHs (only GW230518\_125908 in O4a), we use SEOBNRV4\_ROM\_NRTIDALV2\_NSBH (Dietrich et al. 2019; Matas et al. 2020). Previous papers used SEOBNRV4\_ROM (Bohé et al. 2017) for both BBHs and NSBHs, as well as SEOBNRV4HM\_ROM (Cotesta et al. 2020) for a few BBHs, and additionally used SEOB-NRV4\_ROM\_NRTIDALV2 (Dietrich et al. 2019) for the BNSs GW170817. In FTI, the beyond GR corrections are added to the phase of an inspiral–merger–ringdown frequency-domain waveform. The frequency-domain phase is computed for the inspiral part and then smoothly tapered off to zero towards merger–ringdown so that the post-inspiral part of the signal remains the same as in GR. The tapering happens using a windowing function that is centered around a tapering frequency, which is a free parameter of the model together with the window width. We choose the tapering frequency to be the frequency at the peak of the (2, 2) multipole  $f_{\text{tape}} = f_{\text{peak}}^{22}$  (using the fit from Bohé et al. 2017) and the window width to be one GW cycle  $\mathcal{N}_{\text{GW}} = 1$ .

The settings used for FTI in previous papers (Abbott et al. 2016b, 2019b,c, 2021b, 2025) were different than those employed here. Specifically, the choice of the tapering frequency changed from  $f_{\text{tape}} = 0.35 f_{\text{peak}}^{22}$  in GWTC-3.0 to  $f_{\text{tape}} = 1.0 f_{\text{peak}}^{22}$  in this work. The motivation for increasing the tapering frequency is that this captures more of the late inspiral, which is especially important for higher PN orders and more massive systems (Mehta et al. 2023). Since the bounds obtained depend on the tapering frequency used, it is not possible to directly compare the GWTC-3.0 and O4a bounds. Typically, the increase in tapering frequency leads to tighter bounds on higher PN coefficients since more of the late inspiral is considered in the analysis. For low total-mass systems like BNSs, the tapering frequency lies outside the sensitive band of the detectors and therefore does not significantly influence the results. Only new events from O4a were analyzed with the updated FTI model, so any results obtained by combining events only use the events marked with a  $\checkmark$  in Table 1.

In the second framework, the Test Infrastructure for General Relativity (TIGER; Agathos et al. 2014; Meidam et al. 2018; Roy et al. 2026), the parameterized deviations are directly added to the PN phase coefficients in the IMRPHENOMXAS (Pratten et al. 2020) waveform model. This means that it can only be used by waveforms in that family, and the corrections are propagated to the spin-precessing waveform with higher order multipole moments IMRPHENOMX-PHM\_SPINTAYLOR (IMRPHENOMXPHM for brevity; Prat-

ten et al. 2021; Colleoni et al. 2025b), which is used in this work. However, the corrections do not affect the spin precession. By implementing the corrections directly into the PN coefficients of the model, a smooth connection to the post-inspiral part of the waveform is guaranteed by construction. Previous versions of TIGER used the same construction for the IMRPHENOMPv2 (Hannam et al. 2014; Bohé et al. 2016; Husa et al. 2016; Khan et al. 2016) and IMRPHENOMPv3HM (Khan et al. 2019, 2020) waveform models.

The TIGER framework also allows for parameterized deviations in the post-inspiral part of the waveform, similarly to Cornish et al. (2011). The IMRPHENOMXAS waveform has analytical expressions for the GW phase in the intermediate and merger–ringdown regimes which contain coefficients that can be parameterized much like the inspiral PN coefficients. The main difference is that the post-inspiral coefficients come from calibrating the waveform to numerical relativity (NR) simulations in GR instead of from analytical results. The parameters  $\delta\hat{b}_1, \delta\hat{b}_2, \delta\hat{b}_3, \delta\hat{b}_4$  capture deviations in the NR-calibrated coefficients in the intermediate regime, and the parameters  $\delta\hat{c}_1, \delta\hat{c}_2, \delta\hat{c}_4, \delta\hat{c}_\ell$  capture deviations in the merger–ringdown calibration coefficients (Pratten et al. 2020; Roy et al. 2026).

For the inspiral parameters, combined TIGER results are obtained using IMRPHENOMPv2 for GWTC-2.0 events (Abbott et al. 2021b), except for GW190412 and GW190814. For these two events and all others, we apply the new TIGER framework based on IMRPHENOMXPHM. For the (significantly revised) post-inspiral parameters, all analyses use the new framework. GW191109\_010717 was excluded from the combined analysis despite meeting the post-inspiral selection criteria. We found apparent deviations for this event, similar to the findings reported in the GWTC-3.0 tests of GR paper (Abbott et al. 2025), with the apparent tension explained as being driven by data-quality issues in both LIGO detectors rather than by genuine departures from GR.

In this section, we vary only one deviation parameter

$$\delta\hat{p}_i \in \left\{ \underbrace{\delta\hat{\varphi}_{-2}, \delta\hat{\varphi}_0, \dots, \delta\hat{\varphi}_7}_{\text{Inspiral}}, \underbrace{\delta\hat{b}_1, \dots, \delta\hat{b}_4}_{\text{Intermediate}}, \underbrace{\delta\hat{c}_1, \delta\hat{c}_2, \delta\hat{c}_4, \delta\hat{c}_\ell}_{\text{Merger-ringdown}} \right\} \quad (4)$$

at a time. This is sufficient to detect and constrain deviations from GR, even when the deviations are present in multiple PN orders (Sampson et al. 2013; Meidam et al. 2018; Perkins & Yunes 2022). Testing for multiple deviation parameters at the same time would lead to less informative posteriors due to correlations between the parameters (Abbott et al. 2016b; Gupta et al. 2020). In Section 2.2, such a multi-parameter test is performed using the principal component analysis approach. For both FTI and TIGER, we use priors that are uniform in  $\delta\hat{p}_i$  and symmetric around zero. For the TIGER analyses, we adopt the following prior ranges:  $\delta\hat{\varphi}_{-2} \in [-0.1, 0.1]$ ,  $\delta\hat{\varphi}_{0,1,2,3} \in [-5, 5]$ ,  $\delta\hat{\varphi}_{4,5\ell,6} \in [-20, 20]$ ,  $\delta\hat{\varphi}_{6\ell,7} \in [-30, 30]$ , and for the post-inspiral parameters,  $[-20, 20]$ . We use the following prior ranges for FTI:  $\delta\hat{\varphi}_{-2} \in [-1, 1]$  ( $[-0.01, 0.01]$  for GW230518\_125908) and  $\delta\hat{\varphi}_i \in [-20, 20]$  for all other param-

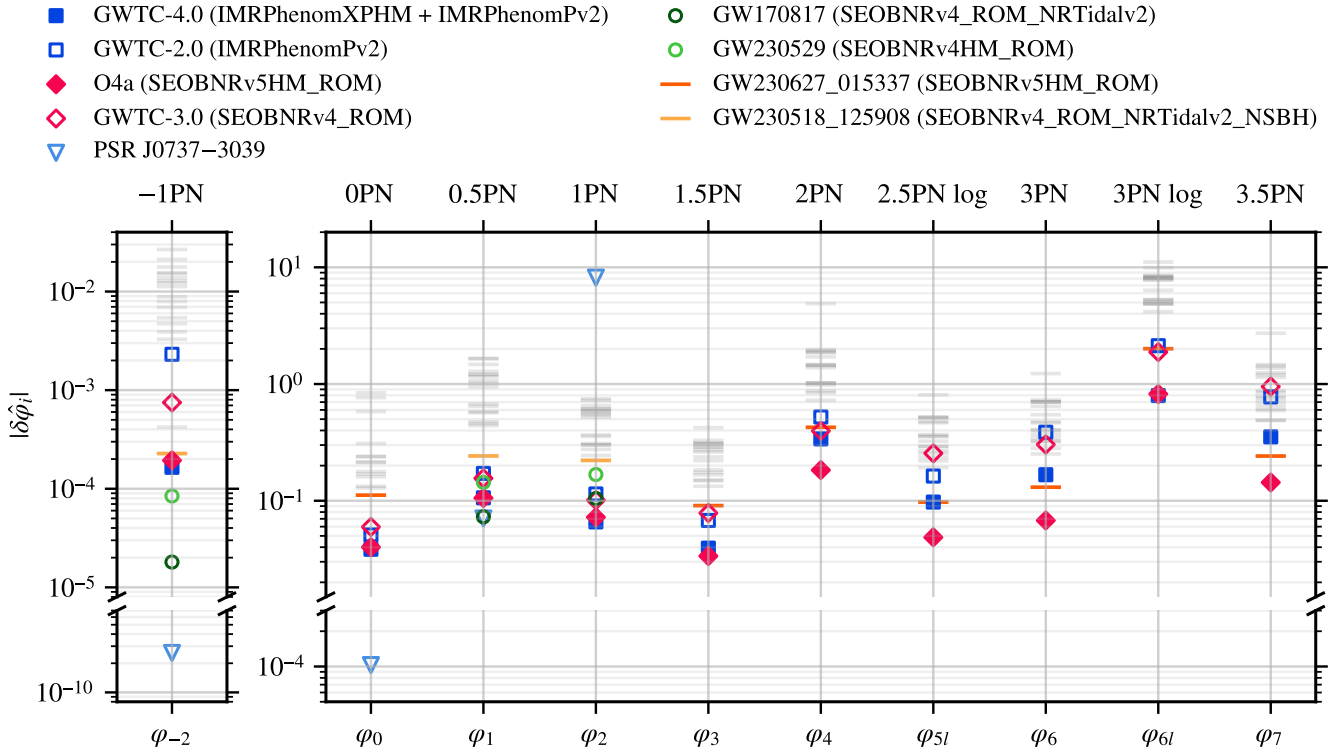


**Figure 1.** Results for the magnitudes of the inspiral deviation coefficients (from  $-1\text{PN}$  to  $3.5\text{PN}$ ) in terms of 90% upper limits, compared with previous combined results from GWTC-2.0 (Abbott et al. 2021b) and GWTC-3.0 (Abbott et al. 2025), as appropriate. The horizontal stripes mark the results from individual events obtained with the SEOBNRv5HM\_ROM waveform model using the FTI analysis. Marginalizing over all results from O4a (GWTC-3.0), while assuming that all events share the same values for the violation coefficients, results in the filled (unfilled) red diamonds for the SEOBNRv5HM\_ROM waveform model. These bounds cannot be directly compared due to changes in the tapering frequency and waveform model used in the analysis. Marginalizing over all results from GWTC-4.0 (GWTC-2.0) for the IMRPHEMXPXM (IMRPHEMXPV2) waveform model using the TIGER analysis results in the filled (unfilled) blue squares. The dark and light orange stripes highlight BBH GW230627.015337 and NSBH GW230518.125908, respectively, when they give the best individual event constraints on the inspiral parameters. The green circles show the bounds obtained with BNS GW170817 (Abbott et al. 2019b) and NSBH GW230529 (Sänger et al. 2024) when competitive; those two events are not included in the combined bounds. The blue upside-down triangles indicate bounds obtained with the double pulsar J0737–3039 (Kramer et al. 2021) when competitive. Starting from  $1.5\text{PN}$  the pulsar bounds get much worse than the bounds from GWs and are therefore not shown.

eters. These broad priors are chosen to avoid prior-railing issues (i.e., significant posterior probability density right up to at least one prior boundary), which often arise from degeneracies between the deviation parameters and the GR parameters. Since the priors we use are wide enough to avoid truncating the posterior, the exact choice of range does not impact the constraints on deviation parameters, though it does impact the values of Bayes factors (quoted below for TIGER).

The FTI test is only applied to events that have a significant inspiral signal. The inspiral part of the signal is in this case defined in the frequency domain as the frequencies up to the tapering frequency used. The selection criteria are then a signal-to-noise ratio (SNR) of at least 10 in the inspiral and at least 5 GW cycles in the inspiral to ensure there is enough inspiral signal. The inspiral SNR and cycles are calculated using the maximum likelihood parameters from the GR analysis (Abac et al. 2025b) with IMRPHEMXPXM. In

the TIGER analysis, we impose an SNR threshold of greater than 6 in the inspiral part of the signal to select an event for testing inspiral phasing coefficients. An identical criterion is applied in the post-inspiral regime to determine whether an event qualifies for the analysis of post-inspiral phasing coefficients. Following the prescription of the IMRPHEMXPAS model, we use the  $(2, 2)$  multipole frequency at the minimum energy circular orbit (MECO; Cabero et al. 2017) to divide the waveform between the inspiral and post-inspiral regimes. (There are small corrections to the MECO used to obtain the exact end-of-inspiral frequency in IMRPHEMXPAS, but these are less than a 3% correction for the range of mass ratios and spins allowed by our priors.) This prescription gives an end-of-inspiral frequency that is between 1.4 and 3.6 times smaller than the one used by FTI, with the largest differences occurring for negative effective inspiral spins (defined in Abac et al. 2025a). The median SNR values are computed using

341 posterior samples obtained from the standard GR analysis  
342 with the IMRPHENOMXPHM model.

343 The results for the inspiral deviation parameters  $\delta\hat{\varphi}_i$  are  
344 consistent with GR for all events analyzed. There are two  
345 events where GR is outside the 90% credible interval for  
346 some parameters for FTI. For the parameters with the largest  
347 deviations, GR is still found within the 92.7% credible inter-  
348 val for GW230628\_231200 and the 98.2% credible interval  
349 for GW231110\_040320. However, for GW230628\_231200,  
350 TIGER finds the GR value within the 90% credible interval  
351 for the inspiral parameters, though it is found outside that  
352 interval for some post-inspiral parameters, but still within  
353 the 94.3% credible interval. For GW231110\_040320, TIGER  
354 finds that GR lies outside the 90% credible interval for all  
355 the inspiral parameters except  $-1\text{PN}$ , and for all of the inter-  
356 mediate parameters. However, GR is still found within the  
357 98.9% credible interval. Additionally, the TIGER Bayes fac-  
358 tors prefer GR for both events for all the deviation parameters.  
359 In general, we expect to find GR outside the 90% credible  
360 interval for a few events due to noise fluctuations, given the  
361 number of events under consideration.

362 For four of the events, namely GW230518\_125908,  
363 GW231020\_142947, GW231104\_133418, and  
364 GW231113\_200417, we were unable to obtain constraints on  
365 the 0PN deviation parameter for FTI. These are all low-mass  
366 events with low SNR where strong correlations between  $\delta\hat{\varphi}_0$   
367 and the chirp mass lead to problems in the analysis (Sänger  
368 et al. 2024). The higher tapering frequency in FTI, compared  
369 to the lower end-of-inspiral frequency in TIGER, implies  
370 that this degeneracy is stronger for FTI. The TIGER re-  
371 sults do not show this issue for these events, except for  
372 GW230518\_125908 and one O3b event, GW200115\_042309.  
373 This is likely because the lower cutoff frequency leaves a few  
374 unmodified GW cycles in band that break the degeneracy. The  
375 exceptional behavior in these two events is specifically due to  
376 a strong degeneracy between  $\delta\hat{\varphi}_0$  and the chirp mass, leading  
377 to a significantly larger chirp mass compared to the GR case  
378 and, consequently, to an apparent deviation in the 0PN term  
379 with a positive value, as seen in Sänger et al. (2024). The FTI  
380 analysis of GW200115\_042309 in Abbott et al. (2025) also  
381 exhibits a degeneracy with the chirp mass, resulting in a bias  
382 in the posterior distribution of the 0PN deviation parameter.  
383 Since a lower tapering frequency was used in that analysis,  
384 the bias was less severe, and the event was not excluded from  
385 the combined analysis.

386 TIGER finds the GR value near the boundary of 90% credi-  
387 bility for the high-mass event GW231028\_153006, where the  
388 GR analysis (Abac et al. 2025b) finds significant systematic  
389 modeling uncertainties. As discussed in Appendix A, we find  
390 that the largest shifts away from GR (for the intermediate  
391 coefficients) are likely attributable to waveform modeling un-  
392 certainties, but the smaller shifts for the merger–ringdown  
393 coefficients seem instead to be attributable primarily to a prior  
394 effect.

395 In Figure 1, we show the 90% upper bounds on the mag-  
396 nitude of the PN deviation parameters in the inspiral; the  
397 analogous plot for the TIGER post-inspiral coefficients is

398 Figure 2. The bounds for individual events obtained with  
399 FTI are shown as grey stripes. We highlight the event  
400 GW230627\_015337, which is the BBH signal that gives the  
401 best constraints. This event is particularly good for inspiral  
402 tests of GR because its low masses means there is a long  
403 inspiral while it also has a relatively high SNR of  $28.5^{+0.1}_{-0.1}$ .  
404 We also show the bounds for the BNS GW170817 (Abbott  
405 et al. 2019b) and NSBH GW230529\_181500 (abbreviated to  
406 GW230529; Sänger et al. 2024) for comparison when their  
407 bounds are competitive. GW230529 does not meet the selec-  
408 tion criteria for inclusion in this paper because it was detected  
409 by only one detector and therefore is excluded from the com-  
410 bined results we present here. The high-SNR single-detector  
411 event GW230814\_230901 (Abac et al. 2025e) is not shown,  
412 however, since its bounds do not stand out compared to those  
413 of other events, though the more recent even higher-SNR  
414 event GW250114 (Abac et al. 2025f) from the second part  
415 of the fourth observing run (O4b) does provide even better  
416 constraints on its own (Abac et al. 2026).

417 We also show the combined bounds for both FTI and  
418 TIGER obtained under the assumption that deviations have  
419 the same value for each event. When combining events, we  
420 exclude the BNS GW170817 due to the different nature of  
421 its source. For comparison, we also include the combined  
422 FTI and TIGER results from previous catalogs. For TIGER,  
423 we plot the results from the GWTC-2.0 paper (Abbott et al.  
424 2021b) since there are no TIGER results in the GWTC-3.0  
425 paper (Abbott et al. 2025); however, we quote the GWTC-4.0  
426 improvement factor in Table 1 of Paper I relative to the re-  
427 cent IMRPHENOMXPHM reanalysis of GWTC-3.0 in Roy  
428 et al. (2026). All combined bounds improve with the largest  
429 improvements seen for FTI for the high-PN parameters. As  
430 discussed before, the change in tapering frequency is contribut-  
431 ing to this improvement. The list of events included in the  
432 combined bounds is different between FTI and TIGER, mak-  
433 ing it impossible to directly compare the combined bounds  
434 between the two. The differences between the bounds for  
435 individual events from FTI and TIGER should be seen as an  
436 estimate for the systematic uncertainties that can be expected  
437 from inspiral tests, with FTI pushing the transition from in-  
438 spirals to post-inspirals to the highest possible frequency and  
439 TIGER providing more conservative bounds. The best bound  
440 from GWs at  $-1\text{PN}$  is still from GW170817, and is an order  
441 of magnitude better than the combined constraints from O4a  
442 (FTI) or GWTC-4.0 (TIGER).

443 It is also possible to put constraints on the PN deviation  
444 parameters using binary pulsars (Yunes & Hughes 2010). The  
445 best overall bound on dipole radiation comes from the double  
446 pulsar PSR J0737–3039A/B (Kramer et al. 2021), with a  
447 90% upper bound corresponding to  $|\delta\hat{\varphi}_{-2}| \leq 2.6 \times 10^{-10}$ .  
448 This double pulsar also puts the most stringent constraint  
449 on deviations from GR at Newtonian order with  $|\delta\hat{\varphi}_0| \leq$   
450  $1.0 \times 10^{-4}$ . At 0.5PN, the double pulsar bound is  $|\delta\hat{\varphi}_1| \leq$   
451  $7.0 \times 10^{-2}$ , which is on par with the bound from GW170817.  
452 From 1PN onwards the bounds from the double pulsar are  
453 less constraining than the bounds from GWs. The bounds

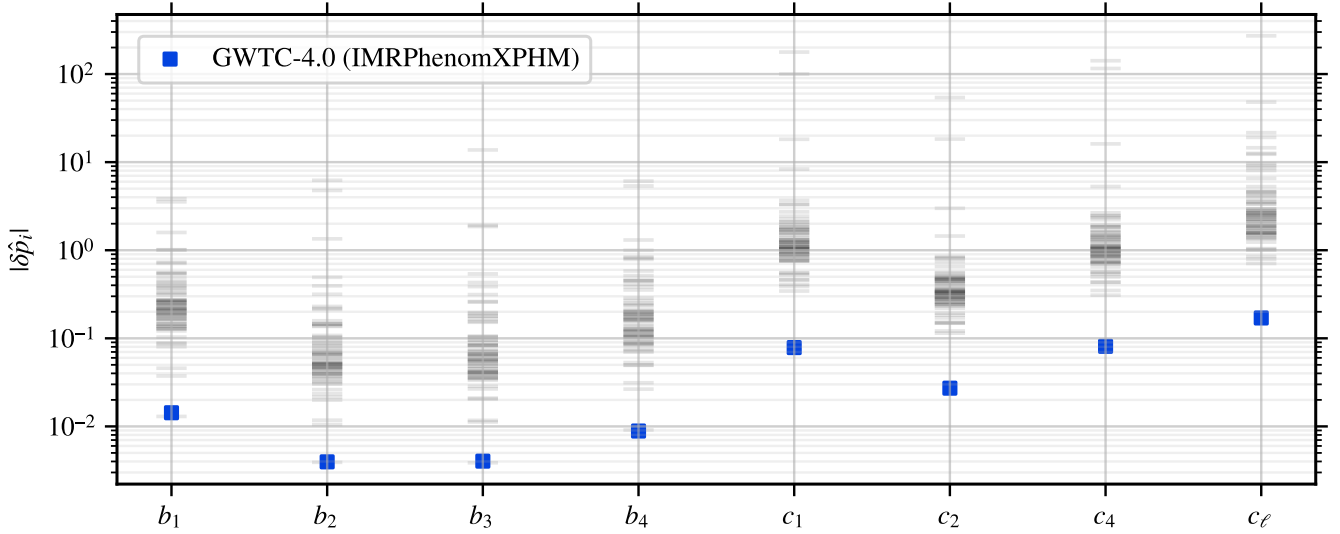


**Figure 2.** Results for the magnitudes of the post-inspiral deviation coefficients using TIGER. The horizontal stripes mark the results from individual events obtained with the IMRPHENOMXPHM waveform model. Marginalizing over all analyzed events in GWTC-4.0, while assuming that all events share the same values for the violation coefficients, results in the blue squares.

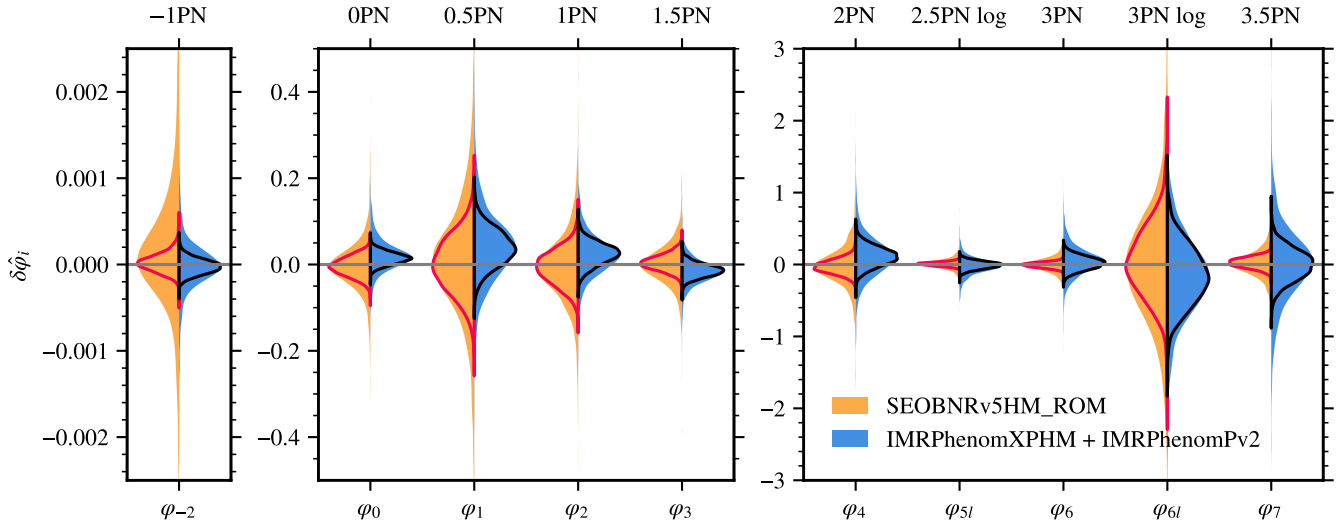


**Figure 3.** The constraints on the GR violation parameters in the inspiral, marginalized over all analyzed events, in orange on the left for the SEOBNRv5HM\_ROM waveform model (FTI analysis) and in blue on the right for the IMRPHENOMXPHM waveform model (TIGER analysis). Consistency of GR corresponds to vanishing parameters (the horizontal line). Assuming independent violation parameters between events, using a hierarchical analysis, results in the filled probability densities. Instead, assuming that the violation parameters share the same values between different events leads to the unfilled distributions.

454 from PSR J0737–3039A/B are shown as blue upside-down  
455 triangles in Figure 1.

456 The combined posteriors for the inspiral deviation param-  
457 eters are shown in Figure 3 (unfilled violins) and are consistent  
458 with GR at the 90% credible level for all parameters. The  
459 combined posteriors are dominated by GW230627\_015337  
460 because of its tight constraints. The posteriors for this event  
461 are centered around zero, a trait inherited by the displayed  
462 combined posteriors. This is reflected in the GR quantiles

463 shown in Table 2 being between 40% and 60%. Here the GR  
464 quantile is defined as the fraction of samples with  $\delta\hat{\varphi}_i < 0$ , so  
465 a posterior perfectly centered on GR gives a quantile of 50%.  
466 We also combined the posteriors from the different events  
467 using a hierarchical approach to get the combined posteriors  
468 shown in Figure 3 (filled violins). This approach allows  
469 the deviation parameters to take independent values for each  
470 event, modeling their distribution as a Gaussian described by  
471 a mean  $\mu$  and standard deviation  $\sigma$ . We again see that the

**Table 2.** Results from parametrized tests of GW generation).

$p_i$	pipeline	waveform	Hierarchical				Restricted	
			$\mu$	$\sigma$	$\delta\hat{\varphi}_i$	$Q_{\text{GR}}$	$\delta\hat{\varphi}_i$	$Q_{\text{GR}}$
$\varphi_{-2}$ ( $\times 500$ )	FTI	EOB	$0.06^{+0.47}_{-0.27}$	$< 0.66$	$0.05^{+0.81}_{-0.57}$	40%	$0.01^{+0.10}_{-0.08}$	44%
	TIGER	Phenom	$-0.01^{+0.15}_{-0.16}$	$< 0.30$	$-0.01^{+0.31}_{-0.35}$	55%	$-0.01^{+0.08}_{-0.07}$	63%
$\varphi_0$	FTI	EOB	$0.00^{+0.05}_{-0.04}$	$< 0.08$	$0.00^{+0.09}_{-0.09}$	54%	$-0.01^{+0.04}_{-0.04}$	59%
	TIGER	Phenom	$0.02^{+0.03}_{-0.02}$	$< 0.06$	$0.02^{+0.06}_{-0.06}$	24%	$0.02^{+0.02}_{-0.02}$	10%
$\varphi_1$	FTI	EOB	$0.01^{+0.13}_{-0.12}$	$< 0.22$	$0.01^{+0.24}_{-0.24}$	46%	$0.00^{+0.11}_{-0.11}$	50%
	TIGER	Phenom	$0.04^{+0.08}_{-0.07}$	$< 0.13$	$0.04^{+0.15}_{-0.12}$	26%	$0.04^{+0.06}_{-0.07}$	18%
$\varphi_2$	FTI	EOB	$-0.01^{+0.07}_{-0.07}$	$< 0.13$	$-0.01^{+0.13}_{-0.13}$	55%	$-0.01^{+0.06}_{-0.07}$	57%
	TIGER	Phenom	$0.03^{+0.05}_{-0.04}$	$< 0.08$	$0.03^{+0.09}_{-0.09}$	25%	$0.03^{+0.04}_{-0.04}$	15%
$\varphi_3$	FTI	EOB	$0.00^{+0.04}_{-0.03}$	$< 0.07$	$0.00^{+0.08}_{-0.08}$	51%	$0.00^{+0.03}_{-0.03}$	43%
	TIGER	Phenom	$-0.01^{+0.03}_{-0.03}$	$< 0.05$	$-0.02^{+0.06}_{-0.05}$	71%	$-0.01^{+0.03}_{-0.02}$	82%
$\varphi_4$	FTI	EOB	$-0.02^{+0.21}_{-0.19}$	$< 0.40$	$-0.02^{+0.45}_{-0.43}$	54%	$-0.03^{+0.16}_{-0.15}$	62%
	TIGER	Phenom	$0.09^{+0.24}_{-0.24}$	$< 0.42$	$0.09^{+0.45}_{-0.46}$	34%	$0.11^{+0.23}_{-0.23}$	21%
$\varphi_{51}$	FTI	EOB	$0.01^{+0.05}_{-0.05}$	$< 0.11$	$0.01^{+0.13}_{-0.12}$	45%	$0.01^{+0.04}_{-0.05}$	40%
	TIGER	Phenom	$-0.02^{+0.08}_{-0.09}$	$< 0.14$	$-0.02^{+0.14}_{-0.18}$	61%	$-0.01^{+0.08}_{-0.09}$	61%
$\varphi_6$	FTI	EOB	$0.00^{+0.09}_{-0.08}$	$< 0.15$	$0.00^{+0.18}_{-0.18}$	51%	$-0.01^{+0.06}_{-0.06}$	58%
	TIGER	Phenom	$0.04^{+0.16}_{-0.16}$	$< 0.29$	$0.04^{+0.34}_{-0.31}$	41%	$0.02^{+0.15}_{-0.14}$	41%
$\varphi_{61}$	FTI	EOB	$-0.04^{+0.79}_{-0.81}$	$< 1.23$	$-0.01^{+1.45}_{-1.40}$	51%	$0.01^{+0.83}_{-0.75}$	49%
	TIGER	Phenom	$-0.18^{+0.60}_{-0.59}$	$< 0.97$	$-0.17^{+1.11}_{-1.16}$	62%	$-0.20^{+0.69}_{-0.57}$	68%
$\varphi_7$	FTI	EOB	$0.01^{+0.15}_{-0.14}$	$< 0.29$	$0.01^{+0.33}_{-0.34}$	47%	$0.03^{+0.11}_{-0.12}$	38%
	TIGER	Phenom	$-0.06^{+0.40}_{-0.35}$	$< 0.72$	$-0.04^{+0.77}_{-0.81}$	56%	$-0.03^{+0.36}_{-0.34}$	55%
$b_1$	TIGER	Phenom	$0.01^{+0.01}_{-0.01}$	$< 0.02$	$0.01^{+0.02}_{-0.02}$	28%	$0.00^{+0.01}_{-0.01}$	17%
$b_2$	TIGER	Phenom	$0.00^{+0.00}_{-0.00}$	$< 0.01$	$0.00^{+0.01}_{-0.01}$	75%	$0.00^{+0.00}_{-0.00}$	79%
$b_3$	TIGER	Phenom	$0.00^{+0.00}_{-0.00}$	$< 0.01$	$0.00^{+0.01}_{-0.01}$	27%	$0.00^{+0.00}_{-0.00}$	22%
$b_4$	TIGER	Phenom	$0.00^{+0.01}_{-0.01}$	$< 0.01$	$0.00^{+0.01}_{-0.01}$	67%	$0.00^{+0.01}_{-0.01}$	78%
$c_1$	TIGER	Phenom	$0.02^{+0.05}_{-0.06}$	$< 0.08$	$0.02^{+0.08}_{-0.10}$	34%	$0.03^{+0.04}_{-0.05}$	16%
$c_2$	TIGER	Phenom	$-0.01^{+0.02}_{-0.02}$	$< 0.03$	$-0.01^{+0.03}_{-0.03}$	66%	$-0.01^{+0.02}_{-0.02}$	79%
$c_4$	TIGER	Phenom	$0.04^{+0.05}_{-0.05}$	$< 0.08$	$0.04^{+0.09}_{-0.09}$	21%	$0.04^{+0.04}_{-0.04}$	10%
$c_\ell$	TIGER	Phenom	$0.02^{+0.18}_{-0.15}$	$< 0.23$	$0.02^{+0.28}_{-0.27}$	43%	$0.00^{+0.16}_{-0.15}$	53%

NOTE—Combined constraints on the deviation parameters obtained by marginalizing over all analyzed events in GWTC-4.0 using the analyses FTI (which uses the SEOBNRV5HM\_ROM waveform) and TIGER (which uses the IMRPHENOMXPHM and IMRPHENOMPV2 waveforms). Hierarchical (restricted) constraints are obtained under the assumption that deviation coefficients can (cannot) vary across the observed events. The one-sided quantile corresponding to the GR value for the distributions plotted in Figures 3 and 5 is indicated by  $Q_{\text{GR}}$ . For hierarchical constraints, we also provide the mean  $\mu$  and standard deviation  $\sigma$  of the inferred hyperdistribution. For  $\delta\hat{\varphi}_i$  and  $\mu$ , we report the median as well as the 90%-credible intervals, while for  $\sigma$  we only present 90% upper bounds.

472 posteriors are consistent with GR at the 90% credible level for  
473 all PN deviation parameters. The 90% contours for the hyper-  
474 parameters  $\mu$  and  $\sigma$  of the hierarchical approach are shown in  
475 Figure 4 for each PN deviation parameter. GR corresponds to  
476  $\mu = \sigma = 0$ , which is enclosed by the contours for all inspiral  
477 parameters. The medians, 90% credible intervals, and GR  
478 quantiles for all  $\delta\hat{\varphi}_i$  and both approaches to combine results

479 are listed in Table 2, as well as the medians and 90% credible  
480 intervals for  $\mu$  and the 90% upper limits on  $\sigma$ .

481 Figure 2 shows the 90% upper bounds on the magnitude of  
482 the post-inspiral deviation parameters obtained with TIGER  
483 for each O4a event (grey stripes). The blue squares are the  
484 bounds obtained by combining all events assuming that devia-  
485 tions have the same value for each event. Figure 5 shows the  
486 combined posteriors for the post-inspiral parameter obtained

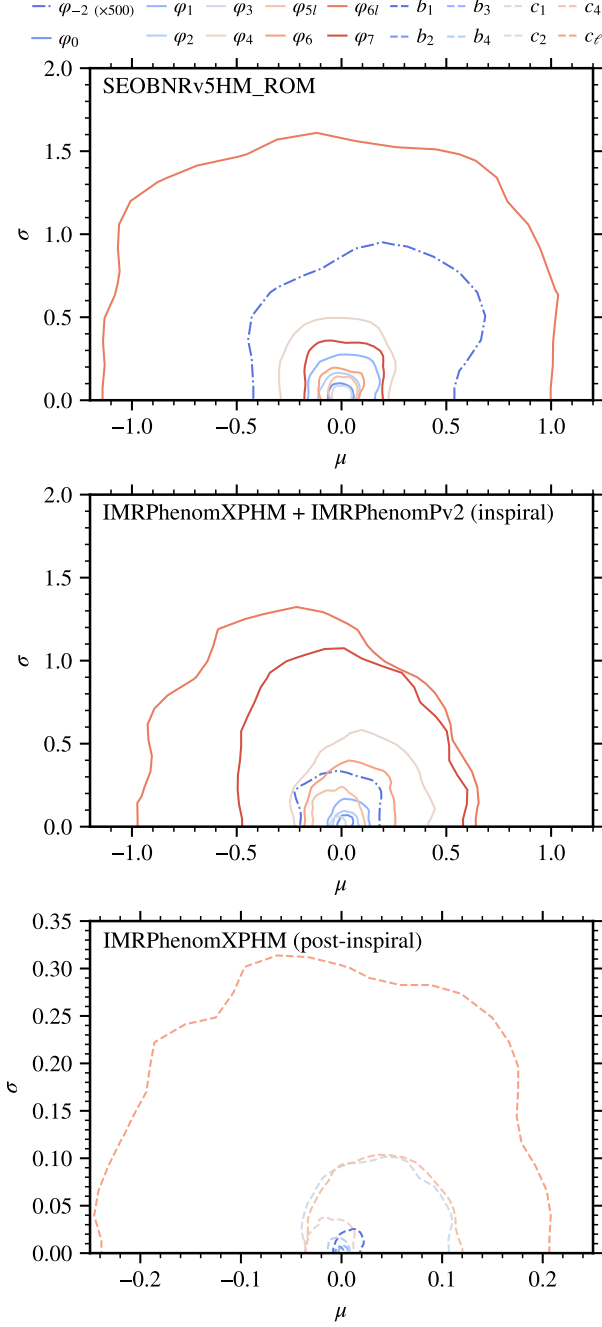


**Figure 4.** Inferred hyperparameters  $\mu$  and  $\sigma$  of the GR violation coefficients. For each testing coefficient, the contours mark 90% credible regions. The inspiral parameters for the two waveform models SEOBNRv5HM\_ROM (using the FTI analysis) and IMRPHENOMXPHM (along with IMRPHENOMPv2; using the TIGER analysis) are considered in the top and middle panel respectively. The bottom panel shows the post-inspiral parameters for the IMRPHENOMXPHM waveform model. All contours enclose the GR expectation of  $\mu = \sigma = 0$ ; the  $\delta\hat{\varphi}_{-2}$  values are rescaled  $\times 500$  to improve visibility.

487 with both the restricted (unfilled violins) and hierarchical  
 488 (filled violins) approaches. The 90% contours for the hyper-  
 489 parameters of the hierarchical analysis are shown in the  
 490 bottom panel of Figure 4. Table 2 gives the median and 90%  
 491 credible intervals on the post-inspiral deviation parameters  
 492 for the combined constraints using both approaches, as well  
 493 as the medians and 90% credible intervals for  $\mu$  and the 90%  
 494 upper limits on  $\sigma$ . All results for the TIGER post-inspiral  
 495 parameters are consistent with GR at the 90% credible level.

496 To give some intuition on the physical significance of the  
 497 constraints on deviations in the PN parameters and how they  
 498 roughly compare to other constraints, we provide illustrative  
 499 translations to constraints on parameters of specific modified  
 500 gravity theories in Table 3. The example theories included  
 501 are: scalar–tensor theories with an evolving scalar field (Ja-  
 502 cobson 1999; Horbatsch & Burgess 2012), Einstein–dilaton–  
 503 Gauss–Bonnet (Gross & Sloan 1987; Kanti et al. 1996), dy-  
 504 namical Chern–Simons (Alexander & Yunes 2009), Einstein–  
 505 Maxwell with black hole charge, and dirty black holes or  
 506 pseudo-complex GR (Hess & Greiner 2009; Caspar et al.  
 507 2012; Hess 2016; Maimon et al. 2025). In order to map a PN  
 508 parameter constraint to a parameter in a given theory, we map  
 509 the posteriors of leading-order agnostic constraints to specific  
 510 parameters, using posteriors of intrinsic parameters for each  
 511 analyzed O4a event and the PN expressions in Khalil et al.  
 512 (2018); Nielsen & Birnholtz (2018); Tatura & Yagi (2018).  
 513 When mapping posteriors, we also need to reweight the sam-  
 514 ples to account for differing priors. The bounds on theories  
 515 we quote in Table 3 are the 90% upper bound for the GW  
 516 event that gives the tightest constraint on a given parameter,  
 517 except for pseudo-complex GR, where the combined results  
 518 are used. For comparison, we also provide existing bounds  
 519 on each theory. Current constraints on scalar–tensor theories  
 520 come from observations of the quasar OJ287 (Horbatsch &  
 521 Burgess 2012). For Einstein–dilaton–Gauss–Bonnet gravity  
 522 and Einstein–Maxwell, the strongest bound arises from the  
 523 low-mass, long-inspiral signal GW230529 (Sanger et al. 2024,  
 524 not included here because it is a single-detector event). For  
 525 dynamical Chern–Simons gravity, current bounds come from  
 526 NICER observations of a pulsar (Silva et al. 2021) which is  
 527  $\gtrsim 4$  times lighter than the BHs that provide the results in  
 528 Table 3. In order to obtain better constraints from GW obser-  
 529 vations, one would need a low-mass binary with at least one  
 530 rapidly spinning object.

531 The values given in Table 3 are for the purposes of illustra-  
 532 tion, and there are several caveats to them being directly taken  
 533 as constraints on the specific theories. To begin with, a given  
 534 modified gravity theory will give deviations in multiple PN  
 535 parameters, while the analyses consider each PN parameter  
 536 deviation in isolation. In addition, these analyses make use  
 537 of the merger–ringdown signal, but without taking into ac-  
 538 count how a specific theory would modify that portion of the  
 539 GW signal from GR. For instance, Johnson-McDaniel et al.  
 540 (2022) analyzes phenomenological non-GR signals with FTI  
 541 and TIGER, finding that these methods can yield constraints  
 542 on a PN deviation parameter that are much smaller than the

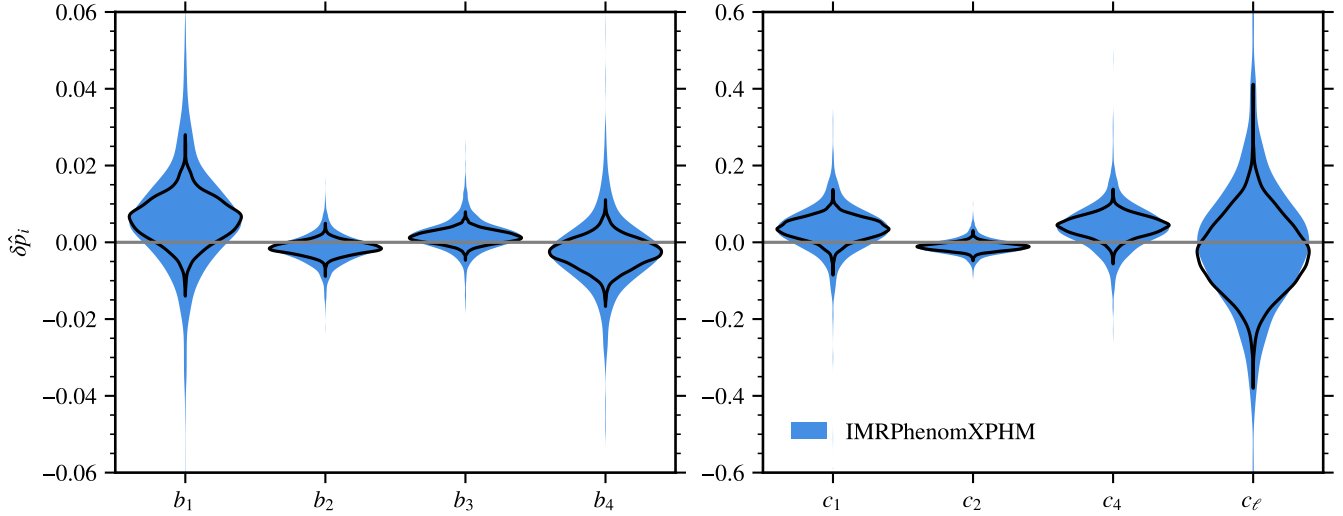


**Figure 5.** The constraints on the GR violation parameters in the post-inspiral using TIGER, marginalized over all analyzed events in GWTC-4.0. Consistency of GR corresponds to vanishing parameters (the horizontal line). Assuming independent violation parameters between events, using a hierarchical analysis, results in the colored probability densities. Instead, assuming that the violation parameters share the same values between different events leads to the unfilled distributions.

**Table 3.** Illustrative mappings of parametrized tests of GW generation to specific theories of gravity.

Theory	$\varphi_i$	Parameter	FTI bound	TIGER bound	Existing bound
Scalar–tensor	$\varphi_{-2}$	$ \dot{\phi} $ [ $\text{s}^{-1}$ ]	$1.1 \times 10^3$	$1.1 \times 10^3$	$10^{-6}$ (Horbatsch & Burgess 2012)
Einstein–dilaton–Gauss–Bonnet	$\varphi_{-2}$	$\sqrt{\alpha_{\text{EdGB}}}$ [km]	0.98	1.07	0.28 (Sänger et al. 2024)
Einstein–Maxwell	$\varphi_{-2}$	$\zeta = \left  \frac{q_1}{m_1} - \frac{q_2}{m_2} \right $	0.047	0.052	0.024 (Gao et al. 2024)
dynamical Chern–Simons	$\varphi_4$	$\sqrt{\alpha_{\text{dCS}}}$ [km]	35.9	39.6	8.5 (Silva et al. 2021)
pseudo-complex GR $n = 2$	$\varphi_4$	$b_c/b$	1.18	0.44	0.29 (Maimon et al. 2025)
pseudo-complex GR $n = 3$	$\varphi_6$	$b_c/b$	0.62	0.16	0.084 (Maimon et al. 2025)

NOTE—The results of the FTI and TIGER tests for specific O4a GW events and PN coefficients are mapped to 90% upper bounds on parameters in modified theories using the leading order correction to the waveform in a particular theory and posteriors of binary parameters. Specifically the binary parameters used are those of GW230518\_125908, except for dynamical Chern–Simons where GW231224\_024321 and GW231118\_090602 lead to better bounds for FTI and TIGER, respectively, and for pseudo-complex GR, where bounds are calculated using all events’ posteriors. For comparison, we also provide existing bounds on a given theory. This table illustrates the size of the constraints on the PN coefficient, but should not be interpreted as claimed constraints on alternative theories of gravity (e.g., since several PN coefficients, as well as the merger–ringdown are modified in alternative theories). For pseudo-complex GR, larger values correspond to better constraints and a  $b_c/b$  bound above 1 rules out horizonless objects for that  $n$  (see  $n = 2$  in our illustrative translation).

543 true deviation. Thus, these mappings will not be equivalent to  
544 those obtained with an analysis that assumes a specific theory.

## 545 2.2. FTI and TIGER: Multiparameter PN coefficient tests 546 with PCA

547 The parametrized tests of GR aim to identify potential de-  
548 viations by modifying the GW phasing with dimensionless  
549 deviation parameters. This approach is implemented in the  
550 FTI and TIGER frameworks, as discussed before. Focusing  
551 on the inspiral part of the GW signal, the null parametrization

552  $\delta\hat{\varphi}_i$  is introduced at each PN order, with  $i$  denoting the PN in-  
553 dex, in Equation (2). Considering the inspiral phase up to the  
554 3.5PN order with non-vanishing PN coefficients in GR gives  
555 rise to eight deviation parameters, i.e., by dropping  $\delta\hat{\varphi}_{-2}$  and  
556  $\delta\hat{\varphi}_1$  in Equation (3). However, all the deviation parameters  
557 are not measured simultaneously since such *multi-parameter*  
558 tests give rise to uninformative posteriors. This is caused by  
559 the correlations between the deviation parameters and other  
560 GR parameters, which can be mitigated by increasing detector

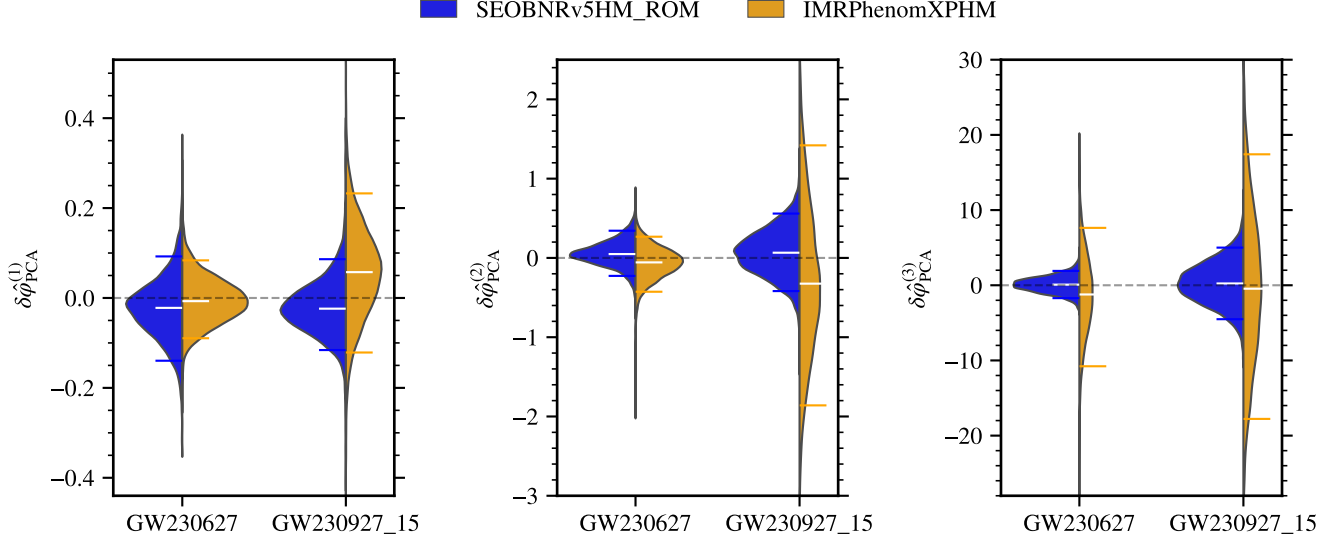


**Figure 6.** Violin plots showing the posterior probability distribution of the first three leading PCA parameters, from the O4a events listed in the PCA column of Table 1 (GW230627.015337 and GW230927.153832, abbreviated as GW230627 and GW230927\_15), passing the selection criteria described in Section 2.2. In each violin plot, the colored horizontal bars and the horizontal white solid line denote the 90% credible intervals and the posterior median, respectively. We mark the GR value of zero with dashed grey lines.

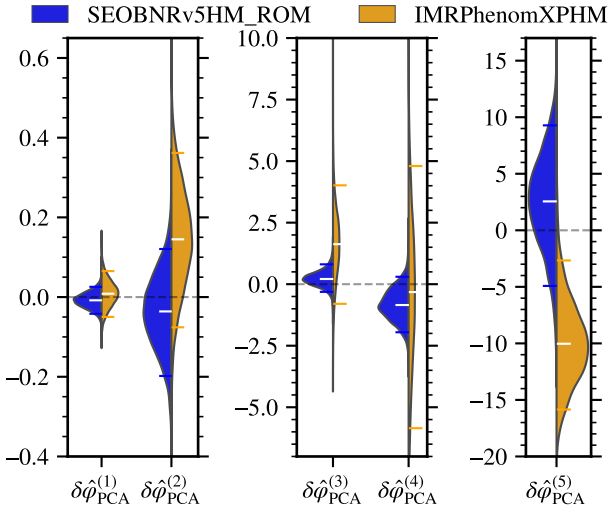


**Figure 7.** The joint posterior probability distributions on the first five leading PCA parameters from all the selected GWTC-4.0 events are shown. The joint bounds are obtained through the marginalized-likelihood multiplication technique. The markers have the same meaning as in Figure 6. All PCA parameters are statistically consistent with GR at the 90% credible level, except for the fifth parameter in the TIGER framework. This deviation may stem from instrumental noise features or from waveform-modeling systematic uncertainties.

**Table 4.** Combined constraints on the leading five PCA parameters from all selected GWTC-4.0 events.

$\delta\hat{\varphi}_{\text{PCA}}^{(k)}$	Median & 90% errors		GR quantile	
	FTI	TIGER	FTI	TIGER
$\delta\hat{\varphi}_{\text{PCA}}^{(1)}$	$-0.01^{+0.04}_{-0.03}$	$0.01^{+0.06}_{-0.06}$	66%	41%
$\delta\hat{\varphi}_{\text{PCA}}^{(2)}$	$-0.04^{+0.16}_{-0.16}$	$0.14^{+0.22}_{-0.22}$	64%	14%
$\delta\hat{\varphi}_{\text{PCA}}^{(3)}$	$0.21^{+0.60}_{-0.52}$	$1.63^{+2.39}_{-2.43}$	24%	14%
$\delta\hat{\varphi}_{\text{PCA}}^{(4)}$	$-0.85^{+1.15}_{-1.10}$	$-0.32^{+5.12}_{-5.53}$	88%	54%
$\delta\hat{\varphi}_{\text{PCA}}^{(5)}$	$2.56^{+6.72}_{-7.48}$	$-10.03^{+7.36}_{-5.82}$	28%	98%

NOTE—We give the median, 90% credible intervals, and the GR quantile, i.e.,  $P(\delta\hat{\varphi}_{\text{PCA}}^{(i)} < 0)$ , of the combined PCA posteriors.

561 network sensitivity (Gupta et al. 2020; Datta et al. 2021) or  
 562 by basing the parametrization on the radiative multipole mo-  
 563 ments (Kastha et al. 2018, 2019; Mahapatra 2024; Mahapatra  
 564 & Kastha 2024; Mahapatra et al. 2024). While deviation from

565 GR can occur at any PN order and hence the eight deviation  
 566 parameters should be measured simultaneously, to avoid the  
 567 aforementioned problem with uninformative posteriors, the  
 568 FTI and TIGER analyses each perform eight *single param-*  
 569 *eter* tests, where only one deviation parameter is measured  
 570 with the others being consistent with GR. However, we will  
 571 instead use principal component analysis (PCA; Arun & Pai  
 572 2013; Pai & Arun 2013; Saleem et al. 2022; Shoom et al.  
 573 2023; Datta et al. 2024; Mahapatra et al. 2025) to identify the  
 574 best-measured linear combinations of a set of PN deviation pa-  
 575 rameters. The bounds so obtained are more constraining than  
 576 the single parameter tests since they contain the information  
 577 from multiple PN orders.

578 In a multi-parameter test, along with the 15 GR parameters,

the six deviation parameters, introduced from 1.5PN to 3.5PN, are included:

$$\{\delta\hat{\varphi}_3, \delta\hat{\varphi}_4, \delta\hat{\varphi}_{5\ell}, \delta\hat{\varphi}_6, \delta\hat{\varphi}_{6\ell}, \delta\hat{\varphi}_7\}, \quad (5)$$

with the assumption that  $\{\delta\hat{\varphi}_0, \delta\hat{\varphi}_1, \delta\hat{\varphi}_2\}$ , the leading-order PN deviation parameters, are consistent with GR. While current GW detectors are sensitive enough to distinguish lower-order fractional deviations from intrinsic binary parameters in single-parameter tests for several events, in particular distinguishing 0PN and 1PN deviations from chirp mass and mass ratio, this is not the case for multi-parameter tests. Moreover, since the  $-1$ PN and 0PN deviations are already well-constrained by binary pulsar measurements (Yunes & Hughes 2010; Kramer et al. 2021), our analysis focuses instead on a six-dimensional test with fractional deviation parameters ranging from 1.5PN to 3.5PN (Mahapatra et al. 2025). This results in a 21-dimensional parameter space; hence, these analyses are computationally expensive. After obtaining the marginalized posteriors on the six deviation parameters, we post-process the posteriors using PCA to transition to a new basis. This new basis is a linear combination of the original deviation parameters with suitable weights, expressed as

$$\delta\hat{\varphi}_{\text{PCA}}^{(k)} = \sum_i \alpha^{ki} \delta\hat{\varphi}_i, \quad (6)$$

where the summation index runs over the six deviation parameters in Equation (5). The coefficient  $\alpha^{ki}$  corresponds to elements of the transformation matrix that diagonalizes the covariance matrix (Arun & Pai 2013; Pai & Arun 2013; Saleem et al. 2022; Datta et al. 2024; Mahapatra et al. 2025). Hence, shifting to the PCA basis reduces the correlations and provides better constraints. The PN coefficients that contribute relatively more to the observed inspiral signal have better-constrained fractional deviation parameters and therefore contribute dominantly to the leading informative PCA components, making the PCA method sensitive to the relative normalization of the different deviation parameters. PCA has inherent sign ambiguity because the direction of eigenvectors is not uniquely determined; their signs can be flipped without affecting the variance they explain. To resolve this, we adopt a sign convention where each eigenvector and each principal component is adjusted so that the largest element is always positive (Mahapatra et al. 2025).

We implement the PCA on GW events observed during the O4a run that meet specific selection criteria and constrain the deviations from GR. Due to the high computational cost of multi-parameter runs, we use strict selection criteria of inspiral SNR  $\geq 14.5$  and detector-frame chirp mass  $(1+z)\mathcal{M} < 20.5M_\odot$  to ensure longer inspiral signals. The inspiral SNR in the FTI and TIGER frameworks is defined in Section 2.1. For chirp mass, we use the median of the chirp mass posterior from the GR analysis with IMRPHENOMXPHM. Imposing this criterion results in two qualifying events from O3a (GW190412 and GW190814), two from O3b (GW191204\_171526 and GW191216\_213338), and two from O4a (GW230627\_015337 and GW230927\_153832) selected for PCA analysis in both the FTI and TIGER frameworks.

We perform a multi-parameter run on the selected events using the parametrized extension of the SEOBNRv5HM\_ROM waveform for FTI and the IMRPHENOMXPHM waveform for TIGER, as in the single-parameter analyses in Section 2.1. Both waveforms give consistent results in the PCA basis. In Figure 6, we show the violin plots of the posterior probability distributions for the first three leading PCA parameters corresponding to the selected O4a events. The results from PCA analysis on the O3a and O3b events are presented in Mahapatra et al. (2025). We restrict our attention to the first three PCA parameters since they carry the most information. The higher-order PCA parameters receive relatively larger contributions from those original deviation parameters that have uninformative posteriors (i.e., are dominated by the priors). Consequently, the higher-order PCA parameters, which have wide posteriors, are not considered. We find that for both events, the posteriors are consistent with GR at the 90% credible level for all PCA parameters within both the FTI and TIGER frameworks.

To combine information from multiple events, we use the marginalized-likelihood multiplication technique applied to the original deviation parameters (Saleem et al. 2022; Mahapatra et al. 2025), where the likelihoods are constructed by sampling from six-dimensional kernel density estimator fits using a Gaussian mixture model (as implemented in SCIKIT-LEARN; Pedregosa et al. 2011). Subsequently, we apply PCA to the combined posteriors of the original deviation parameters in order to obtain the PCA parameters for multiple events. We find that higher PCA parameters for multiple events contain useful information, even though they do not for the individual events: The leading three PCA parameters in the FTI framework and the leading two in the TIGER framework are informative in all individual event analyses, as the Jensen–Shannon (JS) divergence (Lin 1991) between the posterior and prior distributions exceeds 0.1 bit. An exception is GW230627\_015337 in the TIGER framework, where the JS divergence for the third PCA parameter also exceeds 0.1 bit. However, in the joint analysis, the leading five PCA parameters are informative, with the JS divergence exceeding 0.1 bit in both frameworks.

The combined posterior probability distributions on the first five leading PCA parameters from all the GW events passing the selection criteria are displayed in Figure 7. The median values, 90% credible intervals, and GR quantiles for combined PCA posteriors are listed in Table 4. The combined posterior distributions of the PCA parameters are statistically consistent with GR within the 90% credible interval, except for the fifth PCA parameter in the TIGER framework. The fifth PCA parameter in the TIGER framework exhibits a significant offset from zero, with a GR quantile of 98%. Furthermore, the fourth PCA parameter in the FTI framework, as well as the second and third PCA parameters in the TIGER framework, are offset from zero. These offsets are all driven by the event GW190814 (Abbott et al. 2020b), for which we observed a similar offset in the PCA posteriors (Mahapatra et al. 2025). If GW190814 is excluded from the combined results, they do not have any notable offsets from zero. The deviations found for GW190814 could possibly be caused by noise artifacts

present in the data or by systematic errors from the waveform model and parameterization framework (Mahapatra et al. 2025). The difference between the FTI and TIGER results is an estimate of the latter. We deduce a joint bound (at 90% credibility) on the leading PCA parameter to be  $-0.01^{+0.04}_{-0.03}$  (0.01<sup>+0.06</sup><sub>-0.06</sub>) in the FTI (TIGER) framework, consistent with GR predictions. The loud O4b event GW250114 (Abac et al. 2025f) also provides tight constraints on the first two PCA parameters (Abac et al. 2026).

### 2.3. Spin-induced multipole moment coefficient null test

The gravitational field of a spinning object includes contributions from the object’s quadrupole and higher multipole moments, which arise from rotationally induced deformations. These higher-order contributions leave unique imprints on gravitational waveforms, encoding the values of the spin-induced multipole moments of the binary’s constituent objects. For black holes, these moments take specific values that are uniquely determined by the mass and spin, as dictated by the no-hair conjecture (Carter 1971; Hansen 1974). Inferring the values of these moments from their imprints on gravitational waveforms can allow one to distinguish exotic compact objects from black holes. In this analysis, we model the spin-induced quadrupole moment of each compact object using the parameterization

$$Q_i = -\kappa_i \chi_i^2 m_i^3, \quad (7)$$

where  $Q_i$ , representing the quadrupole-moment scalar, appears in the leading-order 2PN term in the GW phase and  $\kappa_i$  encodes the response of the object’s shape to its spin for object  $i = 1, 2$ . Here  $m_i$  and  $\chi_i$  are the mass and the dimensionless spin of the compact object  $i$ . Along with the 2PN leading-order term, we also include the spin-induced quadrupole-moment terms at 3PN in the binary inspiral phase (Arun et al. 2009; Mishra et al. 2016). For a given family of exotic compact objects, the value of  $\kappa_i$ , the dimensionless spin-induced quadrupole-moment coefficient, is primarily determined by the mass of the compact object, with a subdominant dependence on the object’s spin, but the value can be significantly different for different classes of exotic compact objects.

For Kerr black holes, the value is  $\kappa_{\text{BH}} = 1$  (Carter 1971; Hansen 1974); for other compact stars, the value of  $\kappa$  is different due to the stars’ internal structure. For models of spinning neutron stars,  $\kappa$  can vary between  $\sim 2$  and  $\sim 14$  (Pappas & Apostolatos 2012a,b; Harry & Hinderer 2018). For available models of spinning boson stars,  $\kappa$  can have values of  $\sim 10$ – $150$  (Ryan 1997), and  $\kappa$  can even be negative for exotic stars such as gravastars (Uchikata & Yoshida 2016). One expects any compact object that has a spin-induced quadrupole different from that of a black hole to have a nonzero tidal deformability (e.g., Sennett et al. 2017; Johnson-McDaniel et al. 2020; Pacilio et al. 2020; Narikawa et al. 2021) as well as differences in the tidal heating (Cardoso et al. 2017; Maselli et al. 2018; Datta & Bose 2019; Datta et al. 2020; Chia et al. 2025) and modifications to the merger–ringdown part of the signal compared to that from an BBH. However, including

these effects is not essential for the effectiveness of the null test presented here. While we do not explicitly test signals from non-black hole objects, the measurement of the spin-induced quadrupole coefficient  $\kappa$  from GW data serves as a physics-motivated null test: deviations from the Kerr prediction  $\kappa = 1$  may indicate the presence of exotic compact objects or deviations from GR.

The coefficients  $\kappa_i$  represent the primary and secondary components’ spin-induced quadrupole moment parameters for a spinning compact binary system. Although we include the 3PN spin-quadrupole contributions in our waveform model, the estimation of individual spin-induced quadrupole parameters  $\kappa_1$  and  $\kappa_2$  remains challenging due to their strong correlations with the component masses and spins. In principle, higher-order corrections beyond 3PN could help disentangle these parameters. Given the current detector sensitivities, at least the additional 3.5PN term (where the spin-induced octupole first enters Marsat 2015) does not significantly improve constraints, which remain broad. For this reason, we limit our analysis to the leading and next-to-leading spin-quadrupole terms. However, with a combination of  $\kappa_i$  values one can proceed further (Krishnendu et al. 2017, 2019a,b; Abbott et al. 2021b; Divyajyoti et al. 2024). We consider the symmetric and anti-symmetric combinations of  $\kappa_i$ ,

$$\kappa_{\text{S}} = \frac{\kappa_1 + \kappa_2}{2}, \quad (8)$$

$$\kappa_{\text{a}} = \frac{\kappa_1 - \kappa_2}{2}. \quad (9)$$

For binary black holes in general relativity,  $\kappa_{\text{S}} = 1$  and  $\kappa_{\text{a}} = 0$ . In this analysis, we assume  $\kappa_{\text{a}} = 0$  in order to construct a more constraining null test for the Kerr nature of compact objects by measuring deviations from the expected value via  $\kappa_{\text{S}} = 1 + \delta\kappa_{\text{S}}$ . This assumption simplifies the parameter space and enhances our ability to detect deviations from the black hole prediction, though it does not capture possible asymmetries in the spin-induced quadrupole moments of the two components. However, for the loud O4b event GW241011 (Abac et al. 2025g), whose source was an unequal-mass binary, we have been able to constrain deviations in  $\kappa_1$ , allowing it and  $\kappa_2$  to vary independently.

We introduce the parameterized deviations  $\delta\kappa_{\text{S}}$  to the inspiral phase for both the IMRPHEMXPHEM\_MSA and SEOBNRv5HM\_ROM waveform models, similar to the introduction of generic deviations of PN coefficients for these waveform models in Section 2.1. Here IMRPHEMXPHEM\_MSA denotes that we use the version of this model in which precession is modeled using a multiscale analysis (Pratten et al. 2021), which was previously studied on GWTC-3.0 events (Divyajyoti et al. 2024), instead of the SpinTaylor variant used throughout the rest of this paper.

We apply selection criteria based on the measurability of  $\delta\kappa_{\text{S}}$ , requiring that the posterior distribution is sufficiently constrained to distinguish potential deviations from the black hole value  $\kappa_{\text{S}} = 1$ . For the IMRPHEMXPHEM\_MSA analysis, we require (i) an inspiral network SNR of at least 6 and (ii)  $\chi_{\text{eff}} > 0$  at the 90% credible level. To compute

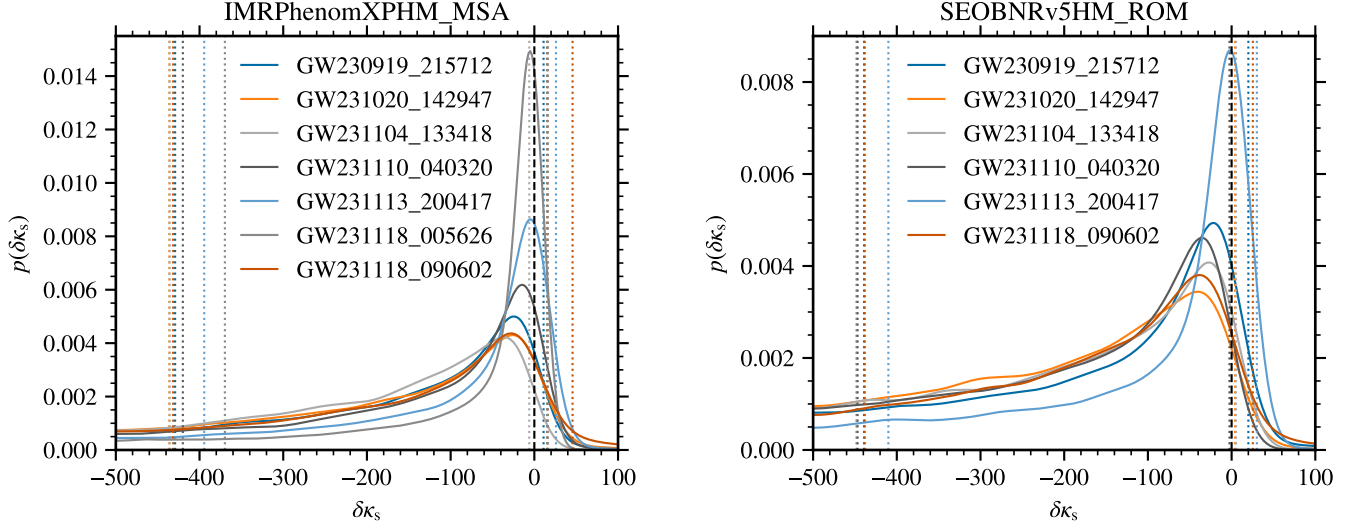


**Figure 8.** The posterior probability distribution on the spin-induced quadrupole moment parameter  $\delta\kappa_s$  using the IMRPHENOMXPHM\_MSA (left panel) and SEOBNRv5HM\_ROM (right panel) waveform models. The black dashed vertical line indicates the BBH value ( $\delta\kappa_s = 0$ ). The colored vertical lines show the 90% symmetric bounds on  $\delta\kappa_s$  calculated from the individual events assuming a uniform prior ranging between  $[-500, 500]$  on  $\delta\kappa_s$ .

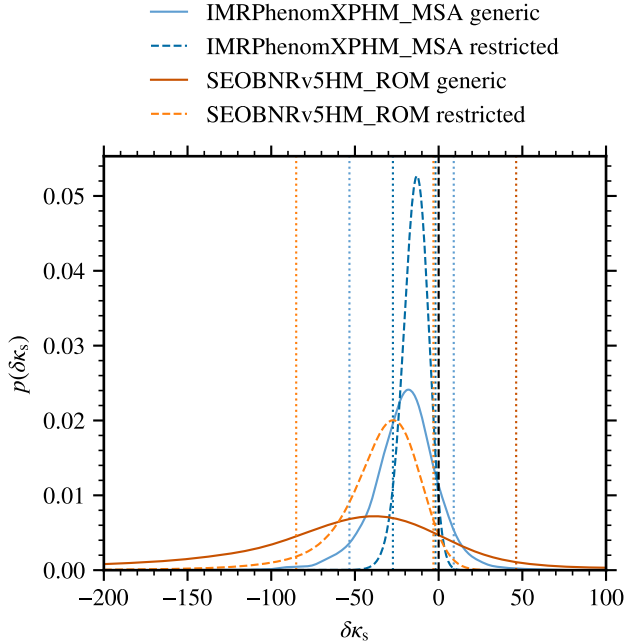


**Figure 9.** Joint posterior probability distribution on the spin-induced quadrupole moment parameter  $\delta\kappa_s$  from the GWTC-4.0 events. Bounds obtained by multiplying the likelihoods (restricted) and by hierarchically combining events (generic) are shown. The analysis is performed assuming a uniform prior ranging between  $[-500, 500]$  on  $\delta\kappa_s$ . The dashed line indicates the BBH value of  $\delta\kappa_s$ , while the dotted lines mark the 90% symmetric credible intervals. The BBH value is found slightly outside of the 90% credible interval for the restricted results, due to correlations with  $\chi_{\text{eff}}$ .

798 the combined bounds, we include events reported in [Abbott](#)  
 799 [et al. \(2021b\)](#) that satisfy both selection criteria. This results  
 800 in a total of seven events from O4a and eight events from  
 801 GWTC-3.0. The event selection criterion on  $\chi_{\text{eff}}$  is stricter  
 802 than the one imposed for GWTC-3.0, so GW200129\_065458  
 803 is no longer selected for this test.

804 Besides the spin-induced quadrupole-moment test previ-  
 805 ously used in [Abbott et al. \(2021b\)](#), we also employ a new test  
 806 based on the FTI framework used for parameterized inspiral  
 807 tests (see Section 2.1). For this version of the test, the correc-  
 808 tions due to  $\delta\kappa_s$  are added at 2PN and 3PN in the frequency-  
 809 domain phase during inspiral ([Mehta et al. 2023](#)). In order  
 810 to only apply the corrections to the inspiral portion of the  
 811 waveform, the corrections are tapered off towards the merger-  
 812 ringdown, which is left the same as in GR, as described in  
 813 Section 2.1. This test uses the SEOBNRv5HM\_ROM wave-  
 814 form model and is applied only to events that satisfy the FTI  
 815 event selection criteria of having an inspiral SNR of at least  
 816 10 and at least 5 GW cycles in the inspiral. Additionally, as  
 817 for the IMRPHENOMXPHM\_MSA analysis, we require that  
 818 zero effective inspiral spin  $\chi_{\text{eff}} = 0$  is outside the 90% credi-  
 819 ble interval of the GR posterior. Overall, six events from O4a  
 820 pass these selection criteria.

821 Figure 8 shows the posterior distributions of  $\delta\kappa_s$  for indi-  
 822 vidual events. They are derived under the assumption of a  
 823 uniform prior on  $\delta\kappa_s$  between  $[-500, 500]$ . As the parameter  
 824  $\delta\kappa_s$  is correlated with  $\chi_{\text{eff}}$ , individual events constrain posi-  
 825 tive values of  $\delta\kappa_s$  more strongly for positive effective inspiral  
 826 spin and often have a long tail for negative  $\delta\kappa_s$  ([Krishnendu](#)  
 827 [et al. 2019b](#)). Since most events observed have small but  
 828 positive  $\chi_{\text{eff}}$  ([Abac et al. 2025h](#)), it is expected that the com-  
 829 bined posterior and the 90% bounds will have more stringent  
 830 constraints on positive values of  $\delta\kappa_s$  than negative values.

831 The combined posterior distribution on  $\delta\kappa_s$  from all selected GW events is shown in Figure 9. The 90% credible interval on  $\delta\kappa_s$  from the hierarchical analysis is  $\delta\kappa_s = -19^{+28}_{-34}$  833 for IMRPHENOMXPHM\_MSA and  $\delta\kappa_s = -49^{+95}_{-176}$  834 for SEOBNRV5HM\_ROM. When restricted to the positive 835 prior region, this analysis places a 90% credibility constraint of  $\delta\kappa_s < 26$  for IMRPHENOMXPHM\_MSA and 836  $\delta\kappa_s < 127$  for SEOBNRV5HM\_ROM. The combined IMR- 837 PHENOMXPHM\_MSA bounds are tighter than the SEOB- 838 NRv5HM\_ROM ones because the GWTC-3.0 events have 839 not yet been included in the SEOBNRv5HM\_ROM analysis, 840 due to computational constraints. However, the IMRPHE- 841 NOMXPHM\_MSA and SEOBNRv5HM\_ROM results for 842 individual events in Figure 8 agree quite well.

845 The distribution hyperparameters are just consistent with 846 the null hypothesis ( $\mu = \sigma = 0$ ), with  $\mu = -19^{+20}_{-22}$  847 and  $\sigma < 25$  for IMRPHENOMXPHM\_MSA, and with 848  $\mu = -51^{+53}_{-128}$  and  $\sigma < 119$  for SEOBNRv5HM\_ROM. 849 Both  $\mu$  and the population-marginalized posterior in Figure 9 850 inherit the asymmetry of the individual events, which tend to 851 be skewed toward  $\delta\kappa_s < 0$ . This explains why the results are 852 marginally consistent with the null hypothesis and suggests 853 that negative values of  $\delta\kappa_s$  are harder to constrain.

854 The dashed curves in Figure 9 shows the joint-likelihood 855 posterior obtained under the assumption that all events share 856 a common value of  $\delta\kappa_s$ . Within this framework, we obtain 857  $\delta\kappa_s = -14^{+12}_{-14}$  for IMRPHENOMXPHM\_MSA and  $\delta\kappa_s =$  858  $-32^{+29}_{-53}$  for SEOBNRv5HM\_ROM. The combined results 859 of the restricted analysis are not consistent with  $\delta\kappa_s = 0$  860 at the 90% credible level due to the correlation with  $\chi_{\text{eff}}$ , 861 just like the hierarchical results. When restricted to positive 862 values, the constraint becomes  $\delta\kappa_s < 5.7$  for IMRPHENOMX- 863 PHM\_MSA and  $\delta\kappa_s < 13$  for SEOBNRv5HM\_ROM.

864 Overall, the results are consistent with BBHs described by 865 GR.

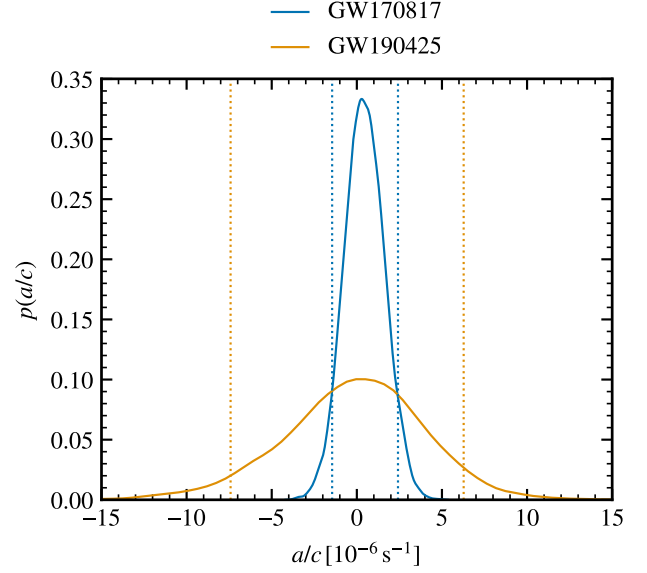
#### 866 2.4. LOSA: Line-of-Sight Acceleration

867 Motion of a CBC relative to a GW detector will cause the 868 signal to be Doppler shifted. Uniform (constant velocity) 869 motion will cause a constant Doppler shift, the measurement 870 of which is perfectly degenerate with the intrinsic mass of the 871 CBC following the mass–redshift degeneracy in GW signals 872 (Abac et al. 2025a). However, a CBC moving with a *time-* 873 *varying* relative velocity caused, e.g., by a constant LOSA  $a$  874 such as due to a nearby supermassive black hole, will cause 875 a  $-4\text{PN}$  modulation (Vijaykumar et al. 2023; Tiwari et al. 876 2025) at the leading order: the strength of this modulation 877 is proportional to the magnitude of the LOSA. Tiwari et al. 878 (2025) discusses how LOSA compares to other effects like 879 repeated lensing by a supermassive black hole.

880 The modulated inspiral GW waveform in the frequency 881 domain can be written as

$$882 \quad \tilde{h}(f) = \tilde{h}_{\text{non-acc}}(f) \left( 1 + \frac{\Delta\mathcal{A}_{\text{LOSA}}}{\mathcal{A}_{\text{non-acc}}} \right) e^{i\Delta\Psi_{\text{LOSA}}}, \quad (10)$$

883 where  $\tilde{h}_{\text{non-acc}}(f)$  is the waveform without the effects of 884 LOSA,  $\Delta\mathcal{A}_{\text{LOSA}}/\mathcal{A}_{\text{non-acc}} \propto a/v^8$  is the modulation in the



885 **Figure 10.** The posterior probability distributions for events satisfying the LOSA selection criteria. The colored dotted lines represent the 90% credible levels.

885 amplitude, and  $\Delta\Psi_{\text{LOSA}} \propto a/v^{13}$  is the phase correction 886 due to LOSA. Here  $v = [\pi G(1+z)Mf]^{1/3}$  is the binary's 887 orbital velocity, where  $z$  is the binary's redshift and  $M$  is its 888 total mass. The phase correction contains contributions from 889 point-particle, aligned spin, and tidal effect terms (Vijaykumar 890 et al. 2023; Tiwari et al. 2025).

891 The LOSA corrections have been derived assuming 892  $|a/c|t_{\text{sd}} \ll 1$ , where  $t_{\text{sd}}$  is the signal duration in the detector's 893 sensitive band, so we can linearize in  $|a/c|t_{\text{sd}}$ . Additionally, 894 the current setup of phase corrections due to LOSA only has 895 corrections to the dominant  $(2, \pm 2)$  multipoles of the wave- 896 form and does not include contributions from precessing spins. 897 For a precessing binary, the aligned spin LOSA corrections 898 are computed using the spin components at the reference 899 frequency.

900 We impose a set of selection criteria (Tiwari et al. 2025) to 901 identify events to which to apply the LOSA analysis, where 902 we evaluate these criteria using the intrinsic parameters of 903 the binary based on the GR analyses (Abac et al. 2025b), in 904 addition to using the LOSA results themselves in the final two 905 a posteriori criteria:

- 906 1. We ensure that the median of the redshifted total mass 907  $(1+z)M$  of the CBC is  $\leq 10 M_{\odot}$ , since lower-mass 908 binaries have longer signals in the detectors sensitive 909 band, with many cycles at relatively small  $v$ , which give 910 the best constraints on the LOSA.
- 911 2. We ensure the median value of mass ratio  $q \geq 0.25$ , to 912 avoid biased LOSA recovery due to higher multipole 913 content.

- 914 3. We ensure the median value of  $\chi_p \leq 0.4$ , to avoid  
 915 biased LOSA recovery due to precession, since the  
 916 LOSA corrections used are only for aligned spins.
- 917 4. After we perform LOSA inference on the events pass-  
 918 ing the above selection criteria, we calculate the quan-  
 919 tity  $|a/c|t_{\text{sd}}$  to ensure it is  $\leq 0.01$  at the 90% credi-  
 920 ble level. Here we compute  $t_{\text{sd}}$  using the Newtonian-  
 921 order expression for the time to coalescence,  $5G(1 +$   
 922  $z)Mc^5/(256\eta v^8)$  (e.g., [Buonanno et al. 2009](#)), starting  
 923 from the low frequency used in the analysis.

924 We use precessing waveforms IMRPHEMOMXP\_MSA ([Prat-](#)  
 925 [ten et al. 2021](#)) and IMRPHEMOMXP\_NRTIDALV2 ([Colleoni](#)  
 926 [et al. 2025a](#)) as the base waveforms for BBHs and BNSs,  
 927 respectively, while we use IMRPHEMOMNSBH ([Thompson](#)  
 928 [et al. 2020](#)), which is non-precessing, for NSBHs.

929 Among the O4 events, we find GW230518\_125908 to have  
 930 a total redshifted mass very close to the cutoff, so the first  
 931 selection criteria is only satisfied for the results using some  
 932 waveform models. We thus restrict consideration to the IMR-  
 933 PHENOMNSBH analysis, where we found that the median total  
 934 mass of GW230518\_125908 is slightly above the threshold.  
 935 However, three pre-O4 events fulfilled the first three selection  
 936 criteria regardless of the waveform model used in the analysis,  
 937 namely GW170817, GW190425, and GW200115\_042309.  
 938 We find GW170817 and GW190425 to also fulfill the fourth  
 939 criterion and to be non-accelerating (see [Figure 10](#)):  $a/c$  is  
 940 constrained to be  $0.42^{+2.00}_{-1.87} \times 10^{-6} \text{ s}^{-1}$  for GW170817 and  
 941  $-0.01^{+6.29}_{-7.40} \times 10^{-6} \text{ s}^{-1}$  for GW190425. We also find that  
 942 GW200115\_042309 is consistent with zero LOSA at slightly  
 943 less than 90% credibility. However, these results fail criterion  
 944 four, so we cannot claim a reliable constraint on LOSA, and  
 945 thus do not provide quantitative results.

### 946 3. TESTS OF GW PROPAGATION

947 This section is dedicated to plausible modification (beyond  
 948 GR) of the GW signal as it propagates between the source  
 949 and the detector. As discussed in [Abbott et al. \(2019c\)](#), we  
 950 assume that GR accurately models the generation of GWs  
 951 near the source in its local wave zone ([Thorne 1980](#)), or that  
 952 the deviations from GR during the generation or due to non-  
 953 linearity of the field in the near zone are not observable. This  
 954 is an excellent assumption in many cases. For instance, for  
 955 the massive graviton, the constraints from propagation mean  
 956 that the Yukawa length scale  $\lambda_g$  that determines the correc-  
 957 tions to the Newtonian potential is  $\lambda_g/r \gtrsim 10^{11}$  times the  
 958 maximum separation of the binary  $r$  in the sensitive band  
 959 of ground-based detectors, thus leading to corrections to the  
 960 binary's GR dynamics from a massive graviton that are of  
 961 order  $r^2/(2\lambda_g^2) \lesssim 10^{-22}$  (bounds on  $m_g$  from individual  
 962 events would lead to corrections at most an order of magni-  
 963 tude higher). We also assume that the GW signal is described  
 964 sufficiently accurately by two (tensorial) polarizations similar  
 965 to GR. In [Section 3.1](#), we consider a phenomenological model  
 966 where the modification in the propagation of GW is caused  
 967 by a modification to the dispersion relation. In [Section 3.2](#),

968 we consider modifications in GW signal caused by the dif-  
 969 ference in propagation of each polarization. For both of the  
 970 above tests, the modification to the GR waveform scales with  
 971 the distance to the source. As such, GWTC-4.0, containing  
 972 many events at  $> 1$  Gpc ([Abac et al. 2025b](#)), is well suited to  
 973 improve constraints on the modified propagation theories.

974 The companion paper focusing on the inference of cosmo-  
 975 logical parameters with GWTC-4.0 ([Abac et al. 2025i](#)), also  
 976 constrains a broad class of theoretical models that allow for  
 977 violations of GR. In that work, we concentrate on a specific  
 978 effect often referred to as GW friction, which manifests itself  
 979 as a modification of the GW amplitude and thus alters the  
 980 inferred luminosity distance. We place constraints on the ratio  
 981 of gravitational-wave to electromagnetic luminosity distances  
 982 by using the distribution of source-frame BBH masses and  
 983 assuming luminal GW propagation, finding results consistent  
 984 with GR.

#### 985 3.1. Tests of a modified GW dispersion relation

986 GR predicts that the gravitational interaction (graviton)  
 987 propagates with the speed of light, and the corresponding  
 988 energy-momentum relation takes a simple form  $E^2 = p^2 c^2$ .  
 989 However, in the case of massive graviton and Lorentz in-  
 990 variance violating theories of gravity, we have a modified  
 991 dispersion relation (MDR) with an extra term:

$$992 E^2 = p^2 c^2 + A_\alpha p^\alpha c^\alpha, \quad (11)$$

993 where the phenomenological parameter  $A_\alpha$  governs the  
 994 strength of the violation and  $\alpha$  controls the frequency depen-  
 995 dence of the dispersion ([Will 1998](#); [Mirshekari et al. 2012](#)).  
 996 The modified dispersion causes different frequency compo-  
 997 nents of the signal to travel with different group velocities,  
 998 changing the morphology of the signal, which can be ex-  
 999 pressed as a frequency-dependent phase modification of the  
 1000 GR waveform  $\tilde{h}(f) = \tilde{h}_{\text{GR}}(f) \exp(i\delta\Psi(f))$ , with the modi-  
 1001 fication ([Ezquiaga et al. 2022](#)):

$$1002 \delta\Psi(f) = -\frac{\pi D_\alpha h^{\alpha-2} (1+z)^{\alpha-1}}{c} A_\alpha f^{\alpha-1}. \quad (12)$$

1003 Here  $h$  is the Planck constant,  $z$  is the redshift of the source,  
 1004 and  $D_\alpha$  is a modified distance parameter, defined by:

$$1005 D_\alpha = \frac{c(1+z)^{1-\alpha}}{H_0} \int_0^z \frac{(1+\bar{z})^{\alpha-2}}{\sqrt{\Omega_m(1+\bar{z})^3 + \Omega_\Lambda}} d\bar{z}, \quad (13)$$

1006 where  $H_0$  is the Hubble constant,  $\Omega_m$  is the matter density  
 1007 parameter, and  $\Omega_\Lambda$  is the dark energy density parameter. Here,  
 1008 we use the  $\Lambda$ CDM cosmological model given in [Abac et al.](#)  
 1009 [\(2025a\)](#). As such, we neglect the radiation density in the  
 1010 expression for our distance parameter.

1011 Previous tests of MDR performed by the LVK ([Abbott](#)  
 1012 [et al. 2017, 2019c, 2021b, 2025](#)) quoted the results using  
 1013 the particle velocity, for which the constraints on  $A_\alpha$  are  
 1014  $1 - \alpha$  times larger than those obtained with the group velocity  
 1015 for  $\alpha \neq 1$ ; for  $\alpha = 1$  the particle velocity yields a devia-  
 1016 tion with a different frequency dependence than the group-  
 1017 velocity results. [Ezquiaga et al. \(2022\)](#) showed that the phase

modification obtained using the group velocity is consistent with that obtained through the Wentzel–Kramers–Brillouin approach (Beltrán Jiménez et al. 2020), which is why we use the group-velocity expressions here.

The MDR given in Equation (11) provides a simple phenomenological parametrization to a broad class of modified theories. Different values of  $\alpha$  describe the leading dispersive effect in different non-GR theories. Particular predictions correspond to  $\alpha = 0$  (massive graviton; Will 1998),  $\alpha = 2.5$  (multi-fractal spacetime; Calcagni 2010),  $\alpha = 3$  (doubly special relativity; Amelino-Camelia 2002), and  $\alpha = 4$  (Hořava–Lifshitz and extra dimensional theories; Hořava 2009; Sefiedgar et al. 2011).

Following the phenomenological approach, we test  $\alpha \in \{-3, -2, -1, 0, 0.5, 1.5, 2.5, 3, 3.5, 4\}$ . The case  $\alpha = 2$  is excluded, as this choice is equivalent to changing the overall speed of GW propagation and results in no dispersion. Compared with GWTC-3.0, we drop the test of  $\alpha = 1$ ; in this case the GW group velocity is equal to the speed of light at leading order and the amplitude  $A_{\alpha=1}$  cannot be constrained (Baka et al. 2025). However, we now also include negative values of  $\alpha$ , which can result from a dark energy phase transition (de Rham & Melville 2018; Baker et al. 2022; Harry & Noller 2022).

We have introduced two novelties in the analysis after GWTC-3.0 (Abbott et al. 2025). First, we use IMRPHENOMXPHM for the underlying GR waveform. Second, for each value of  $\alpha$ , we sample in the effective amplitude parameter  $A_{\text{eff}}$  (which decouples the sampling parameter from the choice of cosmology) and reweight the final result to a prior flat in  $A_\alpha$ , instead of sampling separately for the positive and negative values of  $A_\alpha$  using the logarithm of an effective wavelength parameter (Abbott et al. 2019c; Baka et al. 2025). For  $\alpha = 0$ , we additionally sample in the effective graviton mass (Baka et al. 2025). For the combined bounds on the graviton mass, we opt to transform the  $A_0$  posterior to a prior flat in graviton mass (Baka et al. 2025), to ensure consistency between our bounds on  $A_0$  and  $m_g$ .

Contrary to the tests of GW generation, where the deviation from GR is expected to depend on the parameters of each individual source, we assume that the modification in the propagation of the gravitational waves themselves is universal to all events, and independent of their SNR or parameters. Therefore, we do not perform a hierarchical analysis as in Section 2. Instead, we just apply kernel density estimation to the  $A_\alpha$  posteriors and combine the posteriors from different events by multiplying together the individual likelihoods (which are proportional to the posteriors as the priors were chosen to be flat) and renormalizing the result. Finally, we estimate bounds on the amplitude parameters using the combined results.

We use all 43 events analyzed for MDR in GWTC-3.0 (Abbott et al. 2025), as well as all new BBH events in GWTC-4.0 that pass the general selection criteria described in Section 1. BNS and NSBH events are excluded due to computational constraints, as these signals have long durations. Additionally, these relatively nearby events provide limited information on dispersion, with only loosely constrained posteriors,

as demonstrated for GW170817 (Abbott et al. 2019b). We exclude GW230518\_125908 due to its likely NSBH nature. Although we analyzed GW231123, we omit it from our combined analysis due to significant waveform systematic uncertainties (Abac et al. 2025j), which led to an apparent GR violation when analyzed with the IMRPHENOMXPHM waveform model. We give details of our studies of the systematic errors from waveform modeling for this event and MDR in Appendix C.

Therefore, we include 40 new events from O4a in our combined analysis. In Baka et al. (2025), the authors reanalyze the GWTC-3.0 data using all of the improvements described above and provide a more detailed explanation of the methods. All comparisons to the GWTC-4.0 results are made with respect to these reanalyzed GWTC-3.0 results, to ensure that any differences are driven only by the inclusion of results from the new mergers, and not by changes in methodology.

Figure 11 shows the violin plots describing the combined bounds on the amplitude parameters  $A_\alpha$ . The shaded gray region shows the result for 43 events from GWTC-3.0 (Abbott et al. 2025; Baka et al. 2025), while the blue posteriors show the result for the 83 cumulative events in GWTC-4.0 (i.e., after adding the events from O4a). Overall, the new results are more constraining than those from GWTC-3.0 and more consistent with the GR prediction (zero) for positive values of  $\alpha$ . On average, the new posteriors are narrower by a factor 1.96 compared to the factor of 1.39 improvement expected from the multiplication of Gaussian distributions. Although for  $\alpha = -3$  and  $\alpha = -2$  cases, GR lands outside the central 90% credible interval, this is driven primarily by GW231028\_153006 for which prior effects lead to the apparent GR violations. The deviations disappear if this event is excluded and therefore we find no evidence for dispersion of GWs. See Appendix B for details about the prior effects for GW231028\_153006.

In Table 5 we summarize the data from Figure 11. For each tested value of  $\alpha$ , we report the 5% and 95% quantiles together with the quantile at which GR was found,  $Q_{\text{GR}} = P(A_\alpha < 0)$ . These values show the difference in width of the marginalised posteriors and consistency with GR between GWTC-3.0 and its extension to GWTC-4.0.

We applied a special treatment for  $\alpha = 0$ , which can be interpreted as giving the dispersion due to a massive graviton, and obtained the 90% upper bound on the graviton mass,  $1.92 \times 10^{-23} \text{ eV}/c^2$ . The new result gives a factor of 1.16 improvement compared to the GWTC-3.0 bound  $2.23 \times 10^{-23} \text{ eV}/c^2$  (Abbott et al. 2025; Baka et al. 2025). The bound on the graviton mass from planetary ephemerides is  $1.01 \times 10^{-24} \text{ eV}/c^2$  at the 99.7% confidence level (Mariani et al. 2023), which is an order of magnitude better than our constraint. However, these results are complementary, since they use different set of observations (GW versus astrometry) and focus on different phenomenologies (wave propagation versus orbital motion).

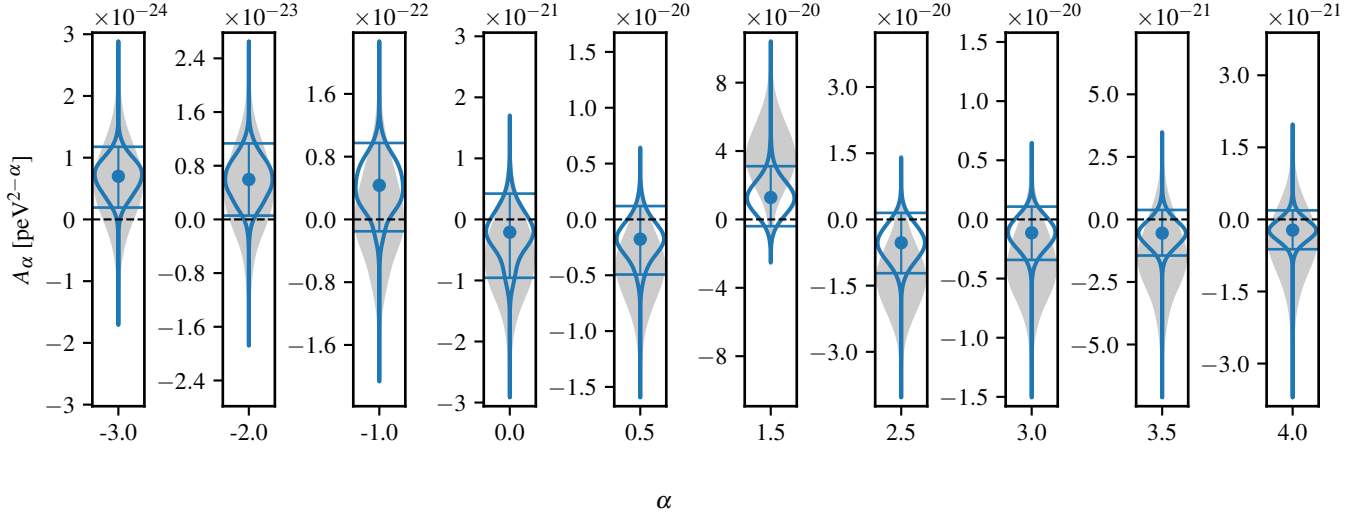


**Figure 11.** Posteriors on the MDR amplitude parameters  $A_\alpha$ . Results from GWTC-3.0 (Abbott et al. 2025; Baka et al. 2025) are indicated by a shaded light-gray area, while the new results in GWTC-4.0 are represented by blue curves. The error bars indicate 90% credible intervals. The significant shifts away from zero for  $\alpha = -3, -2$  are driven by prior effects for GW231028\_153006.

**Table 5.** Combined results for the MDR analysis

	$\bar{m}_g$	$\bar{A}_{-3.0}$		$\bar{A}_{-2.0}$		$\bar{A}_{-1.0}$		$\bar{A}_{0.0}$		$\bar{A}_{0.5}$	
	90% [ $10^{-23}$ ]	90% [ $10^{-84}$ ]	$Q_{GR}$ %	90% [ $10^{-71}$ ]	$Q_{GR}$ %	90% [ $10^{-58}$ ]	$Q_{GR}$ %	90% [ $10^{-45}$ ]	$Q_{GR}$ %	90% [ $10^{-39}$ ]	$Q_{GR}$ %
GWTC-3.0	2.23	-0.38 – 1.59	15.7	-0.53 – 1.42	22.3	-0.86 – 1.04	45.5	-1.63 – 0.41	84.1	-9.40 – 0.66	92.2
GWTC-4.0	1.92	0.19 – 1.18	1.1	0.06 – 1.13	3.4	-0.15 – 0.97	10.3	-0.96 – 0.42	71.7	-4.94 – 1.20	84.8
		$\bar{A}_{1.5}$		$\bar{A}_{2.5}$		$\bar{A}_{3.0}$		$\bar{A}_{3.5}$		$\bar{A}_{4.0}$	
		[ $10^{-26}$ ]	%	[ $10^{-14}$ ]	%	[ $10^{-9}$ ]	%	[ $10^{-3}$ ]	%	[ $10^3$ ]	%
GWTC-3.0		0.95 – 6.83	1.3	-2.50 – -0.11	96.4	-8.53 – 0.95	90.4	-3.89 – 0.85	85.0	-1.69 – 0.64	75.3
GWTC-4.0		-0.40 – 3.11	10.5	-1.22 – 0.15	90.0	-3.42 – 1.08	79.8	-1.44 – 0.38	84.2	-0.62 – 0.19	82.5

NOTE—We compare the results for GWTC-4.0 with those for GWTC-3.0 (Abbott et al. 2025; Baka et al. 2025). The table shows 90% credible intervals for the dimensionless graviton mass  $\bar{m}_g = m_g/(\text{eV}/c^2)$  and the dimensionless amplitude parameters  $\bar{A}_\alpha = A_\alpha/\text{eV}^{2-\alpha}$ . We also include the quantiles of the GR hypothesis  $Q_{GR} = P(A_\alpha < 0)$ . The significant shifts away from zero for  $\alpha = -3, -2$  are driven by prior effects for GW231028\_153006.

### 1129 3.2. Tests of anisotropic birefringence from the Standard 1130 Model Extension

1131 The effective field theory referred to as the Standard Model  
1132 Extension (SME) is a phenomenological framework for deriv-  
1133 ing observational constraints of SSB, such as violations  
1134 of Lorentz invariance and charge–parity–time (CPT) symme-  
1135 try (Colladay & Kostelecký 1998; Kostelecký 2004). For  
1136 GWs, Lorentz and CPT violation can result in anisotropic and  
1137 dispersive propagation. One particular prediction of SME is  
1138 birefringence, which can cause the two polarizations to travel  
1139 at different speeds in vacuum.

1140 Within the SME’s gravity sector, all symmetry-breaking  
1141 operators that appear in the Lagrangian are associated with  
1142 a certain mass dimension  $d$ . Operators at higher mass di-

1143 mensions are suppressed by larger powers of the natural en-  
1144 ergy scale (Kostelecký & Mewes 2016). For gauge-invariant  
1145 theories that allow SSB, the leading order manifestation of  
1146 anisotropic birefringence appears at mass-dimension  $d = 5$ .  
1147 This introduces a frequency-dependent birefringent dispersion  
1148 relation (Kostelecký & Mewes 2016; Mewes 2019), which  
1149 changes the frequency-domain waveform,

$$1150 \tilde{h}_+(f) = \tilde{h}_+^{\text{GR}}(f) \cos(\beta f^2) - \tilde{h}_\times^{\text{GR}}(f) \sin(\beta f^2), \quad (14)$$

$$1151 \tilde{h}_\times(f) = \tilde{h}_+^{\text{GR}}(f) \sin(\beta f^2) + \tilde{h}_\times^{\text{GR}}(f) \cos(\beta f^2). \quad (15)$$

1152 Here  $\tilde{h}_+^{\text{GR}}(f)$  and  $\tilde{h}_\times^{\text{GR}}(f)$  are the polarization components  
1153 in GR and  $\beta$  is the deviation parameter directly related to  
1154 the symmetry breaking operators that appear in the SME

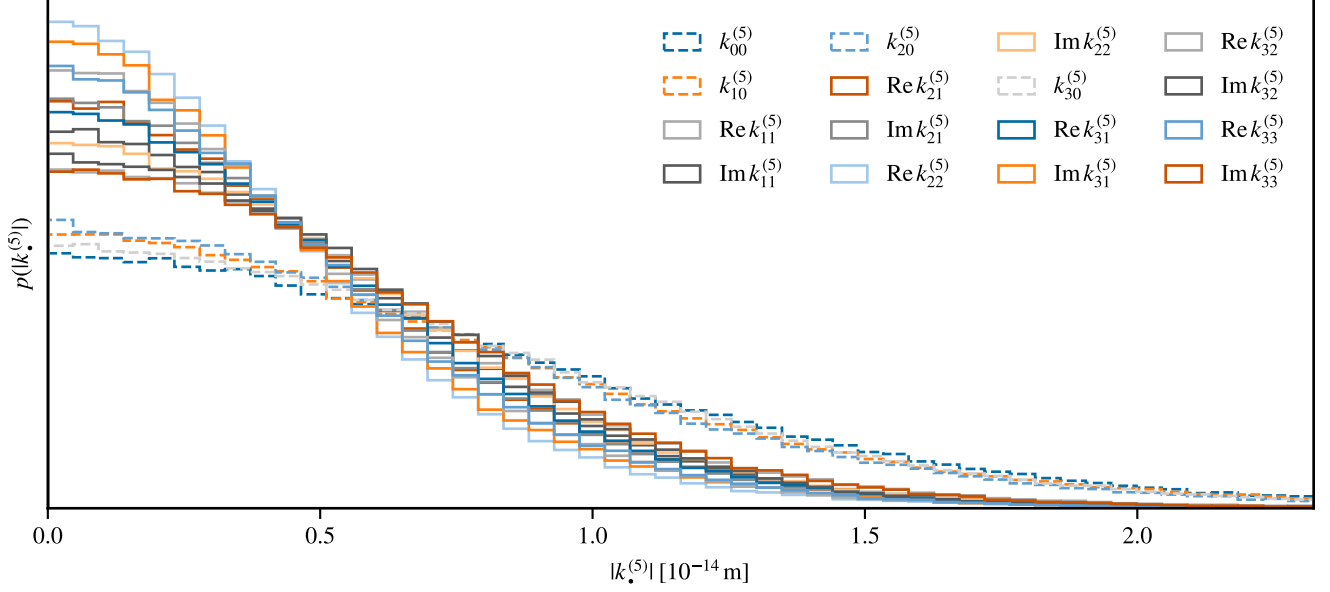


**Figure 12.** The combined posterior probability on the 16 anisotropic dispersion and birefringence coefficients  $k_{\ell m}^{(5)}$  from O4a. We highlight the  $m = 0$  coefficients, which have weaker constraints than the others.

Lagrangian at  $d = 5$ :

$$\beta = \frac{4\pi^2}{c} |k_{\text{eff}}^{(5)}| \tau(z), \quad k_{\text{eff}}^{(5)} = \sum_{\ell, m} Y_{\ell m}(\hat{\mathbf{n}}) k_{\ell m}^{(5)}, \quad (16)$$

$$\tau(z) = \int_0^z \frac{1 + \bar{z}}{H_0 \sqrt{\Omega_m(1 + \bar{z})^3 + \Omega_\Lambda}} d\bar{z}. \quad (17)$$

where the superscript (5) denotes parameters related to dimension  $d = 5$  and the parameters  $k_{\ell m}^{(5)}$  often appear as  $k_{(\ell m)}^{(5)}$  in other papers (Kostelecký & Mewes 2016; O’Neal-Ault et al. 2021; Haegel et al. 2023). Here  $\ell = 0, 1, \dots, d - 2 = 3$  and  $-\ell \leq m \leq \ell$ , while  $\hat{\mathbf{n}}$  is the direction of the source in spherical polar coordinates centered on the Earth and  $\tau(z)$  is the effective propagation time associated with cosmological redshift  $z$ , where we use the cosmological model given in Abac et al. (2025a). Similarly to MDR, we only consider the propagation effect and neglect any modifications in the GWs that could arise during their generation.

Since CBC sources are isotropically distributed over the sky (Essick et al. 2023), we have sufficiently many GW detections to extract all 16  $k_{\ell m}^{(5)}$  parameters to determine all the degrees of freedom possible in  $d = 5$  symmetry breaking operators in the Lagrangian.

We place a uniform prior on  $k_{\text{eff}}^{(5)} \tau(z)$  and use IMRPHENOMXPHM as the baseline GR waveform model. We then derive the posteriors on  $k_{\text{eff}}^{(5)}$  and perform the singular value decomposition of the matrix of spherical harmonics to obtain the posteriors of the 16  $k_{\ell m}^{(5)}$  parameters we are interested in. While we do not have uniform priors on the individual  $k_{\ell m}^{(5)}$  parameters, we have checked that we obtain almost identical results when placing a uniform prior on  $k_{\text{eff}}^{(5)}$ . These post-

processing details can be found in Haegel et al. (2023), which provides the limits obtained from 45 events in GWTC-3.0. However, there were some typographic errors in their calculations, and the actual constraint is  $(Y_{00}(\hat{\mathbf{n}}))^2$  times the original constraint, which is about one order of magnitude tighter. We do not provide results on GWTC-3.0, awaiting re-analysis with the updated BILBY implementation.

Figure 12 shows the marginalized posteriors of the absolute values of the 16  $k_{\ell m}^{(5)}$  coefficients from 40 events in O4a. Here we omit GW231123 from the combined results due to the waveform modeling uncertainties discussed in Abac et al. (2025j) and also illustrated for MDR in Appendix C. For GW231028-153006, the SSB analysis finds the same prior-driven shifts away from GR found by MDR (see Appendix B), and we thus include this event in the combined results, as does MDR. The posteriors for all parameters peak at zero, which corresponds to GR. In Table 6 we summarize the data from Figure 12. Compared to the original GWTC-3.0 results in Haegel et al. (2023), the constraints from just O4a are about a factor of two tighter, after accounting for the correction mentioned above. These are thus the current best constraints on these coefficients—see Table D51 in Kostelecký & Russell (2026), which also shows results from other studies that have obtained more constraining illustrative bounds by varying the coefficients one at a time, though this procedure is only valid for the purposes of illustration.

#### 4. CONCLUSIONS

We have presented the results of eight tests of GR or physics beyond isolated, quasi-circular binaries, four of which are new (and one, TIGER, has been significantly updated), all testing

**Table 6.** Combined results for the SSB analysis

$ k_{ij}^{(5)}  [10^{-14}\text{m}]$	90%
$ k_{00}^{(5)} $	1.52
$ k_{10}^{(5)} $	1.46
$ \text{Re } k_{11}^{(5)} $	1.05
$ \text{Im } k_{11}^{(5)} $	0.98
$ k_{20}^{(5)} $	1.39
$ \text{Re } k_{21}^{(5)} $	0.95
$ \text{Im } k_{21}^{(5)} $	0.94
$ \text{Re } k_{22}^{(5)} $	0.81
$ \text{Im } k_{22}^{(5)} $	0.99
$ k_{30}^{(5)} $	1.42
$ \text{Re } k_{31}^{(5)} $	0.95
$ \text{Im } k_{31}^{(5)} $	0.85
$ \text{Re } k_{32}^{(5)} $	0.87
$ \text{Im } k_{32}^{(5)} $	0.98
$ \text{Re } k_{33}^{(5)} $	0.88
$ \text{Im } k_{33}^{(5)} $	1.05

NOTE—We give the 90% upper bounds for the magnitudes of all 16  $k_{\ell m}^{(5)}$  SSB coefficients from the O4a marginalized posteriors in Figure 12.

various parameterized modifications to GR, and placing constraints on such deviations.

Overall, our tests find that the signals conform to our expectations from GR. We provide highlights of the bounds and improvements in Table 1 of Paper I. In particular, we improve the constraints on deviations in the PN coefficients compared to GWTC-3.0 by up to a factor of 5.5. We also provide illustrative translations (with caveats) of the PN coefficient constraints to constraints on a variety of alternative theories in Table 3. The loudest event during O4a, GW230814\_230901, can by itself place a tight bound on some PN deviations (Abac et al. 2025e), but it is excluded from this paper’s analysis because it is a single-detector event; even without it, the PN coefficient constraints obtained from the full catalog are better. However, the loud O4b event GW250114 (Abac et al. 2025f) provides even better constraints than the full catalog (Abac et al. 2026). Additionally, the MDR analysis updates the bound on the graviton mass to  $m_g \leq 1.92 \times 10^{-23} \text{ eV}/c^2$  at 90% credibility.

Since we apply these tests to 91 events in GWTC-4.0, statistically a few should display apparent deviations from GR expectations. Of the 42 O4a events covered in this paper, this occurred for four events, namely GW230628\_231200, GW231028\_153006, GW231110\_040320, and GW231123, which showed some deviations. The last three of these produced results with GR outside the 90% credible interval for the MDR test, though for GW231028\_153006 this is due

to priors, as discussed in Appendix B. The deviations for GW231110\_040320 are only slight, and the Bayes factors still favor GR, while the deviations for GW231123 can be attributed to waveform systematics, as discussed in Appendix C, though alternative explanations such as wave-optics lensing have also been raised (Abac et al. 2025j). TIGER also finds deviations for GW231028\_153006 for most post-inspiral coefficients but the Bayes factors still favor GR (FTI does not analyze this event), while both FTI and TIGER find deviations for GW231110\_040320. Both FTI and TIGER find GR outside the 90% credible interval for GW230628\_231200.

For events before O4, the tests in this paper find GR inside the 90% credible interval for all but GW190814 (Abbott et al. 2020b), where the TIGER and PCA analyses find GR to be outside the 90% credible interval for some parameters. FTI also finds minor shifts away from zero for some parameters (though GR is still in the 90% credible interval), which studies in Mehta et al. (2023) attribute to properties of the noise around the time of the event. Inclusion of GW190814 in the PCA combined results for TIGER also leads to shifts away from zero for some parameters, with the largest shift in the fifth PCA parameter, with a 98% GR quantile, while there are no notable shifts for any PCA parameters if GW190814 is excluded from the combined results.

All other events and tests are consistent with GR for the entire GWTC-4.0 catalog, though the SIM analyses find that GR is slightly outside the 90% credible interval in the combined results, due to correlations with the effective inspiral spin. The few events that met the criteria for the LOSA test are consistent with zero LOSA. In summary, almost all events analysed were found to be consistent with the expectations of GR. In those few cases where the results were not seen to be consistent, likely causes of the inconsistency were identified which are likely sufficient to explain these apparent deviations, given the large number of events analysed, without requiring violations of GR. Continued improvement in waveform modeling and detector sensitivities as well as the analysis of additional events will further clarify the situation.

We thus expect to place even better constraints on deviations from GR with the analysis of additional events from the remainder of the fourth observing run and from future observing runs (Abbott et al. 2020a).<sup>1</sup> Additionally, improvements in analyses will also lead to better constraints, particularly performing tests for specific alternative theories, where waveform models have started to be developed and applied to data (Julié et al. 2025).

All strain data analyzed in this paper are available from the Gravitational Wave Open Science Center (Abac et al. 2025k). The data and scripts used to prepare the figures and tables are available at LIGO Scientific, Virgo, and KAGRA Collaboration (2026).

## ACKNOWLEDGEMENTS

<sup>1</sup> LVK observing run plans <https://observing.docs.ligo.org/plan>

1291 This material is based upon work supported by NSF’s LIGO  
 1292 Laboratory, which is a major facility fully funded by the Na-  
 1293 tional Science Foundation. The authors also gratefully ac-  
 1294 knowledge the support of the Science and Technology Facili-  
 1295 ties Council (STFC) of the United Kingdom, the Max-Planck-  
 1296 Society (MPS), and the State of Niedersachsen/Germany for  
 1297 support of the construction of Advanced LIGO and construc-  
 1298 tion and operation of the GEO 600 detector. Additional sup-  
 1299 port for Advanced LIGO was provided by the Australian Re-  
 1300 search Council. The authors gratefully acknowledge the Ital-  
 1301 ian Istituto Nazionale di Fisica Nucleare (INFN), the French  
 1302 Centre National de la Recherche Scientifique (CNRS) and the  
 1303 Netherlands Organization for Scientific Research (NWO) for  
 1304 the construction and operation of the Virgo detector and the  
 1305 creation and support of the EGO consortium. The authors also  
 1306 gratefully acknowledge research support from these agencies  
 1307 as well as by the Council of Scientific and Industrial Research  
 1308 of India, the Department of Science and Technology, India,  
 1309 the Science & Engineering Research Board (SERB), India, the  
 1310 Ministry of Human Resource Development, India, the Spanish  
 1311 Agencia Estatal de Investigación (AEI), the Spanish Minis-  
 1312 terio de Ciencia, Innovación y Universidades, the European  
 1313 Union NextGenerationEU/PRTR (PRTR-C17.11), the ICSC -  
 1314 CentroNazionale di Ricerca in High Performance Computing,  
 1315 Big Data and Quantum Computing, funded by the European  
 1316 Union NextGenerationEU, the Comunitat Autònoma de les  
 1317 Illes Balears through the Conselleria d’Educació i Univer-  
 1318 sitats, the Conselleria d’Innovació, Universitats, Ciència i  
 1319 Societat Digital de la Generalitat Valenciana and the CERCA  
 1320 Programme Generalitat de Catalunya, Spain, the Polish Na-  
 1321 tional Agency for Academic Exchange, the National Science  
 1322 Centre of Poland and the European Union - European Re-  
 1323 gional Development Fund; the Foundation for Polish Science  
 1324 (FNP), the Polish Ministry of Science and Higher Education,  
 1325 the Swiss National Science Foundation (SNSF), the Russian  
 1326 Science Foundation, the European Commission, the European  
 1327 Social Funds (ESF), the European Regional Development  
 1328 Funds (ERDF), the Royal Society, the Scottish Funding Coun-  
 1329 cil, the Scottish Universities Physics Alliance, the Hungarian  
 1330 Scientific Research Fund (OTKA), the French Lyon Institute  
 1331 of Origins (LIO), the Belgian Fonds de la Recherche Scien-  
 1332 tifique (FRS-FNRS), Actions de Recherche Concertées (ARC)  
 1333 and Fonds Wetenschappelijk Onderzoek - Vlaanderen (FWO),  
 1334 Belgium, the Paris Île-de-France Region, the National Re-  
 1335 search, Development and Innovation Office of Hungary (NK-  
 1336 FIH), the National Research Foundation of Korea, the Nat-  
 1337 ural Sciences and Engineering Research Council of Canada  
 1338 (NSERC), the Canadian Foundation for Innovation (CFI), the  
 1339 Brazilian Ministry of Science, Technology, and Innovations,  
 1340 the International Center for Theoretical Physics South Ameri-  
 1341 can Institute for Fundamental Research (ICTP-SAIFR), the  
 1342 Research Grants Council of Hong Kong, the National Natural  
 1343 Science Foundation of China (NSFC), the Israel Science Foun-  
 1344 dation (ISF), the US-Israel Binational Science Fund (BSF),  
 1345 the Leverhulme Trust, the Research Corporation, the National  
 1346 Science and Technology Council (NSTC), Taiwan, the United  
 1347 States Department of Energy, and the Kavli Foundation. The

1348 authors gratefully acknowledge the support of the NSF, STFC,  
 1349 INFN and CNRS for provision of computational resources.  
 1350 This work was supported by MEXT, the JSPS Leading-  
 1351 edge Research Infrastructure Program, JSPS Grant-in-Aid  
 1352 for Specially Promoted Research 26000005, JSPS Grant-  
 1353 in-Aid for Scientific Research on Innovative Areas 2402:  
 1354 24103006, 24103005, and 2905: JP17H06358, JP17H06361  
 1355 and JP17H06364, JSPS Core-to-Core Program A. Advanced  
 1356 Research Networks, JSPS Grants-in-Aid for Scientific Re-  
 1357 search (S) 17H06133 and 20H05639, JSPS Grant-in-Aid for  
 1358 Transformative Research Areas (A) 20A203: JP20H05854,  
 1359 the joint research program of the Institute for Cosmic Ray  
 1360 Research, University of Tokyo, the National Research Foun-  
 1361 dation (NRF), the Computing Infrastructure Project of the  
 1362 Global Science experimental Data hub Center (GSDC) at  
 1363 KISTI, the Korea Astronomy and Space Science Institute  
 1364 (KASI), the Ministry of Science and ICT (MSIT) in Korea,  
 1365 Academia Sinica (AS), the AS Grid Center (ASGC) and the  
 1366 National Science and Technology Council (NSTC) in Taiwan  
 1367 under grants including the Science Vanguard Research Pro-  
 1368 gram, the Advanced Technology Center (ATC) of NAOJ, and  
 1369 the Mechanical Engineering Center of KEK.  
 1370 Additional acknowledgements for support of individual  
 1371 authors may be found in the following document:  
 1372 <https://dcc.ligo.org/LIGO-M2300033/public>.  
 1373 For the purpose of open access, the authors have applied  
 1374 a Creative Commons Attribution (CC BY) license to any  
 1375 Author Accepted Manuscript version arising. We request that  
 1376 citations to this article use ‘A. G. Abac *et al.* (LIGO-Virgo-  
 1377 KAGRA Collaboration), ...’ or similar phrasing, depending  
 1378 on journal convention.  
 1379 *The following open-source software has been used:*  
 1380 Calibration of the Laser Interferometer Gravitational-Wave  
 1381 Observatory (LIGO) strain data was performed with a GST-  
 1382 LAL-based calibration software pipeline (Viets *et al.* 2018).  
 1383 Calibration of the Virgo strain data is performed with C-  
 1384 based software (Acernese *et al.* 2022). Data-quality prod-  
 1385 ucts and event-validation results were computed using the  
 1386 DMT (Zweizig, J. 2006), DQR (LIGO Scientific Collabora-  
 1387 tion and Virgo Collaboration 2018), DQSEGDB (Fisher  
 1388 *et al.* 2021), GWDETCAR (Urban *et al.* 2021), HVETO (Smith  
 1389 *et al.* 2011), IDQ (Essick *et al.* 2020), OMICRON (Robinet  
 1390 *et al.* 2020) and PYTHONVIRGOTOOLS (Virgo Collabora-  
 1391 tion 2021) software packages and contributing software tools.  
 1392 Analyses in this catalog relied upon the LALSUITE software  
 1393 library (LIGO Scientific, Virgo, and KAGRA Collaboration  
 1394 2025; Wette 2020). The detection of the signals and subse-  
 1395 quent significance evaluations in this catalog were performed  
 1396 with the GSTLAL-based inspiral software pipeline (Messick  
 1397 *et al.* 2017; Sachdev *et al.* 2019; Hanna *et al.* 2020; Cannon  
 1398 *et al.* 2021), with the MBTA pipeline (Adams *et al.* 2016;  
 1399 Aubin *et al.* 2021), and with the PYCBC (Usman *et al.* 2016;  
 1400 Nitz *et al.* 2017; Davies *et al.* 2020) and the cWB (Klimenko  
 1401 *et al.* 2004, 2011, 2016) packages. Estimates of the noise spec-  
 1402 tra and glitch models were obtained using BAYESWAVE (Cor-  
 1403 nish & Littenberg 2015; Littenberg *et al.* 2016; Cornish *et al.*  
 1404 2021; Gupta & Cornish 2024). Noise subtraction for one

1405 candidate was also performed with GWSUBTRACT (Davis  
1406 et al. 2022). Source-parameter estimation was performed  
1407 with the BILBY and PARALLELILBY libraries (Ashton et al.  
1408 2019; Romero-Shaw et al. 2020; Smith et al. 2020) using the  
1409 DYNESTY nested sampling package (Speagle 2020). FTI,  
1410 TIGER, SIM, LOSA, MDR, and SSB waveforms used for  
1411 testing GR were generated using BILBYTGR (Ashton et al.  
1412 2025b). PESUMMARY was used to postprocess and col-

1413 late parameter-estimation results (Hoy & Raymond 2021).  
1414 The various stages of the parameter-estimation analysis were  
1415 managed with the ASIMOV library (Williams et al. 2023) to-  
1416 gether with CBCFLOW (Ashton et al. 2025a). Plots were pre-  
1417 pared with MATPLOTLIB (Hunter 2007), SEABORN (Waskom  
1418 2021), and GWPY (Macleod et al. 2021). NUMPY (Har-  
1419 ris et al. 2020), SCIKIT-LEARN (Pedregosa et al. 2011), and  
1420 SCIPY (Virtanen et al. 2020) were used in the preparation of  
1421 the manuscript.

1422

## APPENDIX

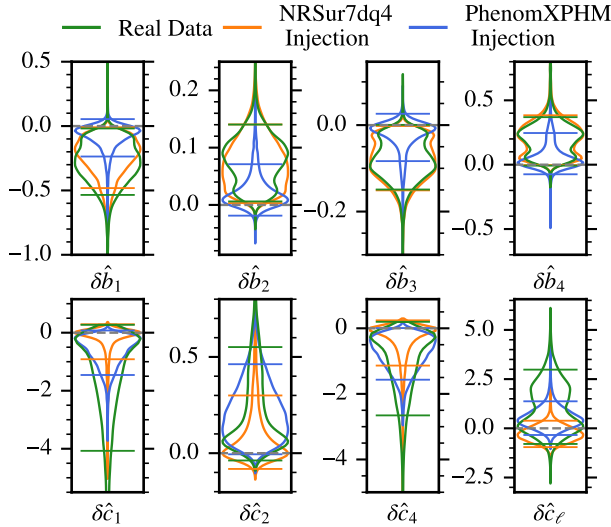


**Figure 13.** Results from the TIGER test on the intermediate and merger-ringdown portion of the signal GW231028\_153006, including the real data and two zero-noise injection studies, one with NRSUR7DQ4 and one with IMRPHENOMXPHM, both based on the maximum-likelihood sample from the GR analysis. All TIGER analyses were carried out using the IMRPHENOMXPHM waveform model as the baseline.

1423 In these Appendices, we discuss GR deviations and sys-  
1424 tematic errors from waveform modeling for the events  
1425 GW231028\_153006 for the TIGER and MDR analyses  
1426 (Appendices A and B) and GW231123 for the MDR anal-  
1427 ysis (Appendix C). See Abac et al. (2025j) for studies of  
1428 waveform-driven systematic uncertainties in standard param-  
1429 eter estimation for GW231123.

1430

1431

## A. TIGER AND GW231028\_153006

1432 As the GR analysis of GW231028\_153006 found poten-  
1433 tial waveform systematic uncertainties (Abac et al. 2025b),  
1434 we highlight the TIGER results for this event. This event  
1435 only passes the criteria for TIGER analysis with post-inspiral  
1436 parameters. For all intermediate parameters and two merger-  
1437 ringdown parameters, the GR value lies at the edge of the  
1438 90% credible interval, as shown in the orange violin plot in  
1439 Figure 13. However, the Bayes factor in favor of the beyond-

1440 GR model against the GR model is negative for all deviation  
1441 parameters; specifically, all  $\log_{10}$  Bayes factor values are less  
1442 than  $-1.2$ .

1443 To investigate whether the apparent tension with GR is  
1444 driven by waveform uncertainties, we perform a zero-noise  
1445 injection analysis (i.e., analyzing simulated observations with  
1446 no noise added) using the NRSUR7DQ4 model (Varma et al.  
1447 2019), which directly interpolates numerical-relativity simu-  
1448 lations, avoiding the approximations used to construct IMR-  
1449 PHENOMXPHM. The injection waveform is generated from  
1450 the maximum-likelihood sample of the NRSUR7DQ4 GR  
1451 analysis for this event (Abac et al. 2025b). The same injection  
1452 study for the MDR analysis is presented in Appendix B. As  
1453 shown in Figure 13, the posteriors of the deviation param-  
1454 eters from the injection analysis are consistent with those from  
1455 the real data. In particular, the GR value for the posterior of  
1456 intermediate parameters is also found at the edge of the 90%  
1457 credible interval. Since the TIGER baseline model is IMR-  
1458 PHENOMXPHM, the apparent tension may be driven by the  
1459 choice of waveform model used in the injection simulations.

1460 To further investigate the degeneracy between the deviation  
1461 parameter and the GR parameters, we performed a zero-noise  
1462 injection study using the maximum-likelihood sample from  
1463 the IMRPHENOMXPHM GR analysis of this event. This  
1464 approach avoids systematics arising from the choice of wave-  
1465 form models. The blue violin plots in Figure 13 show the  
1466 posterior distributions of the deviation parameters. For the in-  
1467 termediate parameters, the GR values are recovered within the  
1468 90% credible intervals. However, for the merger-ringdown  
1469 parameters, the GR values lie at the edge of the intervals. We  
1470 find that the masses and spins are strongly correlated with the  
1471 deviation parameter. In particular, the spin magnitude of the  
1472 injection parameters is nearly unity, while the recovery with  
1473 the TIGER model shows reduced consistency at high spin  
1474 values for some deviation parameters. Moreover, the poster-  
1475 iors of the mass-related parameters differ significantly from  
1476 those obtained with the GR model. Therefore, we conclude  
1477 that while the shifts away from GR seen in the intermediate  
1478 coefficients are primarily due to waveform uncertainties, the  
1479 results for the merger-ringdown parameters are partly due to  
1480 a strong degeneracy between the deviation parameter and the  
1481 GR parameters, not by physics beyond GR.

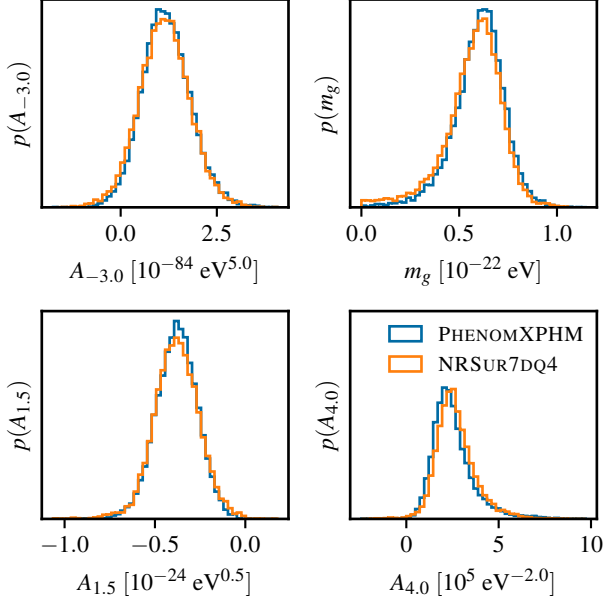


**Figure 14.** Representative posteriors for the MDR amplitude parameters  $A_\alpha$  and the graviton mass  $m_g$  for GW231028\_153006. Inference using both the IMRPHENOMXPHM and NRSUR7DQ4 waveform models does not show any significant systematic uncertainties. We instead find that this shift away from GR is due to a prior effect.

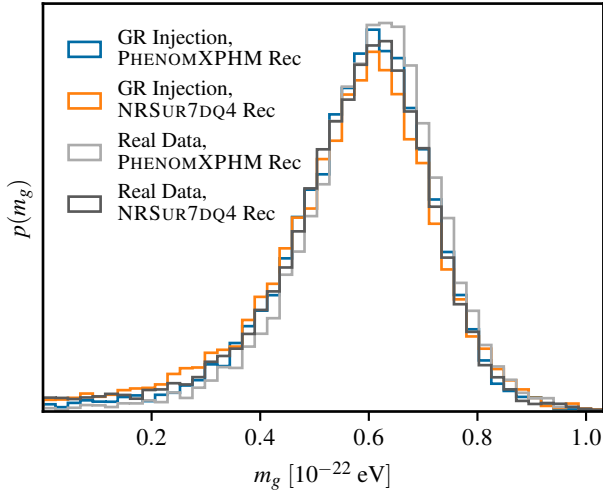


**Figure 15.** Graviton-mass posterior for GW231028\_153006 both for real data and NRSUR7DQ4 injections into zero noise based on the maximum-likelihood sample from GR analysis. Both are analyzed with IMRPHENOMXPHM and NRSUR7DQ4 waveform models. We thus find that this shift away from GR is due to a prior effect.

## B. MDR AND GW231028\_153006

1482

1483 Of the 40 new events contributing to the improved bounds  
1484 on the dispersion amplitudes  $A_\alpha$ , GW231028\_153006 is the  
1485 least consistent with GR. Since the GR analysis identified  
1486 potential waveform systematic uncertainties for this event,  
1487 we performed an additional analysis using the more accurate  
1488 NRSUR7DQ4 waveform model. Representative posteriors  
1489 are shown in Figure 14. The posteriors are consistent across  
1490 waveform models, indicating that our initial analysis with  
1491 IMRPHENOMXPHM is reliable.

1492 To better understand the apparent tension with GR, we  
1493 analyzed a NRSUR7DQ4 injection into zero noise, based on  
1494 the maximum-likelihood sample from the GR analysis of this  
1495 event. In Figure 15, we show the inferred posterior distribution  
1496 of the graviton mass  $m_g$  for this injection, compared to the  
1497 result from the analysis of the actual data. The posteriors  
1498 agree and both exhibit a peak in  $m_g$  away from zero, even  
1499 though the injected signal is consistent with GR.

1500 This can be attributed to a degeneracy between  $m_g$  and other  
1501 binary parameters: the inferred parameters differ from those of  
1502 the injection, yet the corresponding waveforms remain similar.  
1503 We quantify this similarity using the mismatch between two  
1504 templates  $h_1$  and  $h_2$ , defined as (Cutler & Flanagan 1994):

$$1505 \quad \text{MM} = 1 - \left| \frac{\langle h_1 | h_2 \rangle}{\sqrt{\langle h_1 | h_1 \rangle \langle h_2 | h_2 \rangle}} \right|, \quad (\text{B1})$$

1506 where  $\langle \cdot | \cdot \rangle$  denotes the noise-weighted inner product and a  
1507 mismatch of 0 corresponds to identical templates. Comparing  
1508 the injected signal with the waveform corresponding to  
1509 the maximum-posterior sample, we find a low mismatch of  
1510  $\text{MM} = 0.0054$ . While the likelihood near both the injection  
1511 point and the maximum-posterior sample is similar, the prior  
1512 density at the maximum-posterior location is higher by a fac-  
1513 tor of  $3.31 \times 10^5$ . Consequently, samples near the maximum-  
1514 posterior point dominate, and GR-consistent solutions lie at  
1515 the edge of the posterior distribution.

## C. MDR AND GW231123

1516

1517 While GW231123 passed the MDR selection criteria, this  
1518 event shows significant issues with waveform systematic un-  
1519 certainties (Abac et al. 2025j). As the MDR analysis with  
1520 IMRPHENOMXPHM showed an apparent GR violation, we  
1521 reanalyzed the data with the NRSUR7DQ4 waveform model  
1522 to check if waveform uncertainties are responsible. NR-  
1523 SUR7DQ4 is a surrogate model that shows better agreement  
1524 than IMRPHENOMXPHM with numerical-relativity simulations  
1525 for systems with similar total mass to GW231123 (Abac  
1526 et al. 2025j). The results show significant discrepancies in the  
1527 inferred posteriors of the amplitude parameters  $A_\alpha$  and the  
1528 graviton mass  $m_g$ ; we show a few examples in Figure 16. The  
1529 use of the NRSUR7DQ4 waveform model shifts the posteriors  
1530 so that the GR value of 0 is included in the posterior mass.  
1531 For  $\alpha \leq 0$ , the posteriors are unimodal and centered near  
1532 zero. For  $\alpha \in \{0.5, 1.5, 2.5\}$ , the posteriors have multiple  
1533 peaks but still show consistency with GR. For  $\alpha \geq 3$ , the

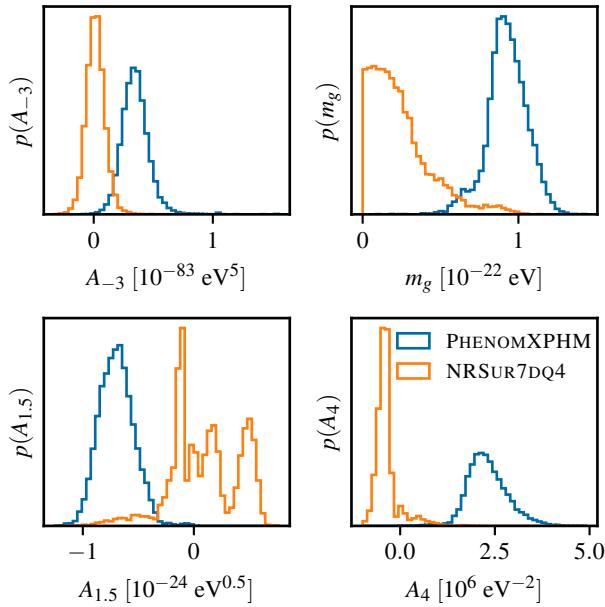


**Figure 16.** Representative posteriors for the MDR amplitude parameters  $A_\alpha$  and the graviton mass  $m_g$  for GW231123. We find a large discrepancy in the results between those obtained using IMRPHENOMXPHM and NRSUR7DQ4.

posterior are almost unimodal, with a small peak near 0 and a larger peak further away. The inferred amplitude parameter  $A_\alpha$  is closer to 0 and with the opposite sign compared to the IMRPHENOMXPHM results.

In Table 7, we compare how the Bayes factors  $\mathcal{B}_{\text{GR}}^{\text{MDR}}$  in favor of MDR over GR vary depending on the waveform used. For IMRPHENOMXPHM, the Bayes factor shows a preference for MDR for  $\alpha > -2$ , despite its larger prior

volume compared to GR (due to one additional parameter and an expanded prior range for the chirp mass to avoid railing). In the NRSUR7DQ4 analysis, GR is generally preferred over MDR, except for the  $\alpha = 4$  case, where there is a small preference for MDR, though the uncertainty on the Bayes factors has a standard deviation of  $\sim 0.2$ .

**Table 7.**  $\mathcal{B}_{\text{GR}}^{\text{MDR}}$  comparison for GW231123

	XPHM $\log_{10} \mathcal{B}_{\text{GR}}^{\text{MDR}}$	NRSUR $\log_{10} \mathcal{B}_{\text{GR}}^{\text{MDR}}$
$\alpha = -3.0$	-0.5	-2.5
$\alpha = -2.0$	-0.3	-2.5
$\alpha = -1.0$	0.1	-2.5
$m_g$	1.0	-1.3
$\alpha = 0.0$	0.2	-2.4
$\alpha = 0.5$	0.3	-2.2
$\alpha = 1.5$	0.8	-1.2
$\alpha = 2.5$	1.0	-0.6
$\alpha = 3.0$	1.0	-0.5
$\alpha = 3.5$	1.1	-0.2
$\alpha = 4.0$	1.8	0.1

NOTE—We give the values of the log Bayes factor  $\mathcal{B}_{\text{GR}}^{\text{MDR}}$  in favor of MDR over GR for GW231123 analyzed with the IMRPHENOMXPHM and NRSUR7DQ4 waveform models and consider a selection of different dispersion models (different values of  $\alpha$ ). The  $m_g$  row denotes the analysis with a prior uniform in the graviton mass. Each entry compares analyses performed with the same waveform model.

Due to these issues with the waveform systematic uncertainties, we have excluded GW231123 from the combined bounds on GW dispersion.

## REFERENCES

- Abac, A. G., et al. 2025a, *Astrophys. J. Lett.*, 995, L18, doi: [10.3847/2041-8213/ae0c06](https://doi.org/10.3847/2041-8213/ae0c06)
- , 2025b. <https://arxiv.org/abs/2508.18082>
- , 2025c. <https://dcc.ligo.org/LIGO-P2500065/public>
- , 2025d. <https://dcc.ligo.org/LIGO-P2500067/public>
- , 2025e. <https://arxiv.org/abs/2509.07348>
- , 2025f, *Phys. Rev. Lett.*, 135, 111403, doi: [10.1103/kw5g-d732](https://doi.org/10.1103/kw5g-d732)
- , 2025g, *Astrophys. J. Lett.*, 993, L21, doi: [10.3847/2041-8213/ae0d54](https://doi.org/10.3847/2041-8213/ae0d54)
- , 2025h. <https://arxiv.org/abs/2508.18083>
- , 2025i. <https://arxiv.org/abs/2509.04348>
- , 2025j, *Astrophys. J. Lett.*, 993, L25, doi: [10.3847/2041-8213/ae0c9c](https://doi.org/10.3847/2041-8213/ae0c9c)
- , 2025k. <https://arxiv.org/abs/2508.18079>
- , 2026, *Phys. Rev. Lett.*, 136, 041403, doi: [10.1103/6c61-fm1n](https://doi.org/10.1103/6c61-fm1n)
- Abbott, B. P., et al. 2016a, *Phys. Rev. X*, 6, 041015, doi: [10.1103/PhysRevX.6.041015](https://doi.org/10.1103/PhysRevX.6.041015)
- , 2016b, *Phys. Rev. Lett.*, 116, 221101, doi: [10.1103/PhysRevLett.116.221101](https://doi.org/10.1103/PhysRevLett.116.221101)
- , 2017, *Phys. Rev. Lett.*, 118, 221101, doi: [10.1103/PhysRevLett.118.221101](https://doi.org/10.1103/PhysRevLett.118.221101)
- , 2019a, *Phys. Rev. X*, 9, 031040, doi: [10.1103/PhysRevX.9.031040](https://doi.org/10.1103/PhysRevX.9.031040)
- , 2019b, *Phys. Rev. Lett.*, 123, 011102, doi: [10.1103/PhysRevLett.123.011102](https://doi.org/10.1103/PhysRevLett.123.011102)
- , 2019c, *Phys. Rev. D*, 100, 104036, doi: [10.1103/PhysRevD.100.104036](https://doi.org/10.1103/PhysRevD.100.104036)
- , 2020a, *Living Rev. Relativity*, 23, 3, doi: [10.1007/s41114-020-00026-9](https://doi.org/10.1007/s41114-020-00026-9)

- 1580 Abbott, R., et al. 2020b, *Astrophys. J. Lett.*, 896, L44,  
 1581 doi: [10.3847/2041-8213/ab960f](https://doi.org/10.3847/2041-8213/ab960f)
- 1582 —. 2021a, *Phys. Rev. X*, 11, 021053,  
 1583 doi: [10.1103/PhysRevX.11.021053](https://doi.org/10.1103/PhysRevX.11.021053)
- 1584 —. 2021b, *Phys. Rev. D*, 103, 122002,  
 1585 doi: [10.1103/PhysRevD.103.122002](https://doi.org/10.1103/PhysRevD.103.122002)
- 1586 —. 2023, *Phys. Rev. X*, 13, 041039,  
 1587 doi: [10.1103/PhysRevX.13.041039](https://doi.org/10.1103/PhysRevX.13.041039)
- 1588 —. 2024, *Phys. Rev. D*, 109, 022001,  
 1589 doi: [10.1103/PhysRevD.109.022001](https://doi.org/10.1103/PhysRevD.109.022001)
- 1590 —. 2025, *Phys. Rev. D*, 112, 084080,  
 1591 doi: [10.1103/PhysRevD.112.084080](https://doi.org/10.1103/PhysRevD.112.084080)
- 1592 Acernese, F., et al. 2022, *Class. Quantum Grav.*, 39, 045006,  
 1593 doi: [10.1088/1361-6382/ac3c8e](https://doi.org/10.1088/1361-6382/ac3c8e)
- 1594 Adams, T., Buskulic, D., Germain, V., et al. 2016, *Class. Quantum*  
 1595 *Grav.*, 33, 175012, doi: [10.1088/0264-9381/33/17/175012](https://doi.org/10.1088/0264-9381/33/17/175012)
- 1596 Agathos, M., Del Pozzo, W., Li, T. G. F., et al. 2014, *Phys. Rev. D*,  
 1597 89, 082001, doi: [10.1103/PhysRevD.89.082001](https://doi.org/10.1103/PhysRevD.89.082001)
- 1598 Alexander, S., & Yunes, N. 2009, *Phys. Rept.*, 480, 1,  
 1599 doi: [10.1016/j.physrep.2009.07.002](https://doi.org/10.1016/j.physrep.2009.07.002)
- 1600 Amelino-Camelia, G. 2002, *Nature (London)*, 418, 34,  
 1601 doi: [10.1038/418034a](https://doi.org/10.1038/418034a)
- 1602 Arun, K. G., Buonanno, A., Faye, G., & Ochsner, E. 2009, *Phys.*  
 1603 *Rev. D*, 79, 104023, doi: [10.1103/PhysRevD.79.104023](https://doi.org/10.1103/PhysRevD.79.104023)
- 1604 Arun, K. G., Iyer, B. R., Qusailah, M. S. S., & Sathyaprakash, B. S.  
 1605 2006a, *Phys. Rev. D*, 74, 024006,  
 1606 doi: [10.1103/PhysRevD.74.024006](https://doi.org/10.1103/PhysRevD.74.024006)
- 1607 —. 2006b, *Class. Quantum Grav.*, 23, L37,  
 1608 doi: [10.1088/0264-9381/23/9/L01](https://doi.org/10.1088/0264-9381/23/9/L01)
- 1609 Arun, K. G., & Pai, A. 2013, *Int. J. Mod. Phys. D*, 22, 1341012,  
 1610 doi: [10.1142/S0218271813410125](https://doi.org/10.1142/S0218271813410125)
- 1611 Ashton, G., Udall, R., & Yarbrough, Z. 2025a, *CBC Workflow*.  
 1612 <https://github.com/Rhiannon-Udall/cbcflow>
- 1613 Ashton, G., et al. 2019, *Astrophys. J. Suppl. Ser.*, 241, 27,  
 1614 doi: [10.3847/1538-4365/ab06fc](https://doi.org/10.3847/1538-4365/ab06fc)
- 1615 Ashton, G., Talbot, C., Roy, S., et al. 2025b, *Bilby TGR*, v0.2,  
 1616 *Zenodo*, doi: [10.5281/zenodo.15676285](https://doi.org/10.5281/zenodo.15676285)
- 1617 Aubin, F., et al. 2021, *Class. Quantum Grav.*, 38, 095004,  
 1618 doi: [10.1088/1361-6382/abe913](https://doi.org/10.1088/1361-6382/abe913)
- 1619 Baka, T., Cirok, B., Haris, K., Noller, J., & Krishnendu, N. V. 2025.  
 1620 <https://arxiv.org/abs/2511.00497>
- 1621 Baker, T., et al. 2022, *JCAP*, 08, 031,  
 1622 doi: [10.1088/1475-7516/2022/08/031](https://doi.org/10.1088/1475-7516/2022/08/031)
- 1623 Beltrán Jiménez, J., Ezquiaga, J. M., & Heisenberg, L. 2020, *JCAP*,  
 1624 04, 027, doi: [10.1088/1475-7516/2020/04/027](https://doi.org/10.1088/1475-7516/2020/04/027)
- 1625 Bernard, L., Blanchet, L., & Trestini, D. 2022, *JCAP*, 08, 008,  
 1626 doi: [10.1088/1475-7516/2022/08/008](https://doi.org/10.1088/1475-7516/2022/08/008)
- 1627 Blanchet, L. 2024, *Living Rev. Relativity*, 27, 4,  
 1628 doi: [10.1007/s41114-024-00050-z](https://doi.org/10.1007/s41114-024-00050-z)
- 1629 Blanchet, L., Faye, G., Henry, Q., Larrouturou, F., & Trestini, D.  
 1630 2023, *Phys. Rev. Lett.*, 131, 121402,  
 1631 doi: [10.1103/PhysRevLett.131.121402](https://doi.org/10.1103/PhysRevLett.131.121402)
- 1632 Blanchet, L., & Sathyaprakash, B. S. 1994, *Class. Quantum Grav.*,  
 1633 11, 2807, doi: [10.1088/0264-9381/11/11/020](https://doi.org/10.1088/0264-9381/11/11/020)
- 1634 —. 1995, *Phys. Rev. Lett.*, 74, 1067,  
 1635 doi: [10.1103/PhysRevLett.74.1067](https://doi.org/10.1103/PhysRevLett.74.1067)
- 1636 Bohé, A., Hannam, M., Husa, S., et al. 2016, *PhenomPv2 -*  
 1637 *Technical Notes for LAL Implementation*, Tech. Rep.  
 1638 LIGO-T1500602, LIGO Project.  
 1639 <https://dcc.ligo.org/LIGO-T1500602/public>
- 1640 Bohé, A., et al. 2017, *Phys. Rev. D*, 95, 044028,  
 1641 doi: [10.1103/PhysRevD.95.044028](https://doi.org/10.1103/PhysRevD.95.044028)
- 1642 Buonanno, A., Iyer, B. R., Ochsner, E., Pan, Y., & Sathyaprakash,  
 1643 B. S. 2009, *Phys. Rev. D*, 80, 084043,  
 1644 doi: [10.1103/PhysRevD.80.084043](https://doi.org/10.1103/PhysRevD.80.084043)
- 1645 Cabero, M., Nielsen, A. B., Lundgren, A. P., & Capano, C. D. 2017,  
 1646 *Phys. Rev. D*, 95, 064016, doi: [10.1103/PhysRevD.95.064016](https://doi.org/10.1103/PhysRevD.95.064016)
- 1647 Calcagni, G. 2010, *Phys. Rev. Lett.*, 104, 251301,  
 1648 doi: [10.1103/PhysRevLett.104.251301](https://doi.org/10.1103/PhysRevLett.104.251301)
- 1649 Cannon, K., Caudill, S., Chan, C., et al. 2021, *SoftwareX*, 14,  
 1650 100680, doi: [10.1016/j.softx.2021.100680](https://doi.org/10.1016/j.softx.2021.100680)
- 1651 Cardoso, V., Franzin, E., Maselli, A., Pani, P., & Raposo, G. 2017,  
 1652 *Phys. Rev. D*, 95, 084014, doi: [10.1103/PhysRevD.95.084014](https://doi.org/10.1103/PhysRevD.95.084014)
- 1653 Carter, B. 1971, *Phys. Rev. Lett.*, 26, 331,  
 1654 doi: [10.1103/PhysRevLett.26.331](https://doi.org/10.1103/PhysRevLett.26.331)
- 1655 Caspar, G., Schonenbach, T., Hess, P. O., Schafer, M., & Greiner, W.  
 1656 2012, *Int. J. Mod. Phys. E*, 21, 1250015,  
 1657 doi: [10.1142/S0218301312500152](https://doi.org/10.1142/S0218301312500152)
- 1658 Chandrasekhar, S. 1965, *Astrophys. J.*, 142, 1488,  
 1659 doi: [10.1086/148432](https://doi.org/10.1086/148432)
- 1660 Chia, H. S., Zhou, Z., & Ivanov, M. M. 2025, *Phys. Rev. D*, 111,  
 1661 063002, doi: [10.1103/PhysRevD.111.063002](https://doi.org/10.1103/PhysRevD.111.063002)
- 1662 Colladay, D., & Kostelecký, V. A. 1998, *Phys. Rev. D*, 58, 116002,  
 1663 doi: [10.1103/PhysRevD.58.116002](https://doi.org/10.1103/PhysRevD.58.116002)
- 1664 Colleoni, M., Ramis Vidal, F. A., Johnson-McDaniel, N. K., et al.  
 1665 2025a, *Phys. Rev. D*, 111, 064025,  
 1666 doi: [10.1103/PhysRevD.111.064025](https://doi.org/10.1103/PhysRevD.111.064025)
- 1667 Colleoni, M., Vidal, F. A. R., García-Quirós, C., Akçay, S., & Bera,  
 1668 S. 2025b, *Phys. Rev. D*, 111, 104019,  
 1669 doi: [10.1103/PhysRevD.111.104019](https://doi.org/10.1103/PhysRevD.111.104019)
- 1670 Cornish, N., Sampson, L., Yunes, N., & Pretorius, F. 2011, *PhRvD*,  
 1671 84, 062003, doi: [10.1103/PhysRevD.84.062003](https://doi.org/10.1103/PhysRevD.84.062003)
- 1672 Cornish, N. J., & Littenberg, T. B. 2015, *Class. Quantum Grav.*, 32,  
 1673 135012, doi: [10.1088/0264-9381/32/13/135012](https://doi.org/10.1088/0264-9381/32/13/135012)
- 1674 Cornish, N. J., Littenberg, T. B., Bécsy, B., et al. 2021, *Phys. Rev. D*,  
 1675 103, 044006, doi: [10.1103/PhysRevD.103.044006](https://doi.org/10.1103/PhysRevD.103.044006)
- 1676 Cotesta, R., Marsat, S., & Pürrer, M. 2020, *Phys. Rev. D*, 101,  
 1677 124040, doi: [10.1103/PhysRevD.101.124040](https://doi.org/10.1103/PhysRevD.101.124040)

- 1678 Cutler, C., & Flanagan, É. É. 1994, *Phys. Rev. D*, 49, 2658,  
1679 doi: [10.1103/PhysRevD.49.2658](https://doi.org/10.1103/PhysRevD.49.2658)
- 1680 Datta, S., & Bose, S. 2019, *Phys. Rev. D*, 99, 084001,  
1681 doi: [10.1103/PhysRevD.99.084001](https://doi.org/10.1103/PhysRevD.99.084001)
- 1682 Datta, S., Brito, R., Bose, S., Pani, P., & Hughes, S. A. 2020, *Phys.*  
1683 *Rev. D*, 101, 044004, doi: [10.1103/PhysRevD.101.044004](https://doi.org/10.1103/PhysRevD.101.044004)
- 1684 Datta, S., Gupta, A., Kastha, S., Arun, K. G., & Sathyaprakash, B. S.  
1685 2021, *Phys. Rev. D*, 103, 024036,  
1686 doi: [10.1103/PhysRevD.103.024036](https://doi.org/10.1103/PhysRevD.103.024036)
- 1687 Datta, S., Saleem, M., Arun, K. G., & Sathyaprakash, B. S. 2024,  
1688 *Phys. Rev. D*, 109, 044036, doi: [10.1103/PhysRevD.109.044036](https://doi.org/10.1103/PhysRevD.109.044036)
- 1689 Davies, G. S., Dent, T., Tápai, M., et al. 2020, *Phys. Rev. D*, 102,  
1690 022004, doi: [10.1103/PhysRevD.102.022004](https://doi.org/10.1103/PhysRevD.102.022004)
- 1691 Davis, D., Littenberg, T. B., Romero-Shaw, I. M., et al. 2022, *Class.*  
1692 *Quantum Grav.*, 39, 245013, doi: [10.1088/1361-6382/aca238](https://doi.org/10.1088/1361-6382/aca238)
- 1693 de Rham, C., & Melville, S. 2018, *Phys. Rev. Lett.*, 121, 221101,  
1694 doi: [10.1103/PhysRevLett.121.221101](https://doi.org/10.1103/PhysRevLett.121.221101)
- 1695 Dietrich, T., Samajdar, A., Khan, S., et al. 2019, *Phys. Rev. D*, 100,  
1696 044003, doi: [10.1103/PhysRevD.100.044003](https://doi.org/10.1103/PhysRevD.100.044003)
- 1697 Divyajyoti, Krishnendu, N. V., Saleem, M., et al. 2024, *Phys. Rev.*  
1698 *D*, 109, 023016, doi: [10.1103/PhysRevD.109.023016](https://doi.org/10.1103/PhysRevD.109.023016)
- 1699 Einstein, A., Infeld, L., & Hoffmann, B. 1938, *Ann. Math.*, 39, 65,  
1700 doi: [10.2307/1968714](https://doi.org/10.2307/1968714)
- 1701 Essick, R., Farr, W. M., Fishbach, M., Holz, D. E., & Katsavounidis,  
1702 E. 2023, *Phys. Rev. D*, 107, 043016,  
1703 doi: [10.1103/PhysRevD.107.043016](https://doi.org/10.1103/PhysRevD.107.043016)
- 1704 Essick, R., Godwin, P., Hanna, C., Blackburn, L., & Katsavounidis,  
1705 E. 2020, *Mach. Learn. Sci. Technol.*, 2, 015004,  
1706 doi: [10.1088/2632-2153/abab5f](https://doi.org/10.1088/2632-2153/abab5f)
- 1707 Ezquiaga, J. M., Hu, W., Lagos, M., Lin, M.-X., & Xu, F. 2022,  
1708 *JCAP*, 08, 016, doi: [10.1088/1475-7516/2022/08/016](https://doi.org/10.1088/1475-7516/2022/08/016)
- 1709 Fisher, R. P., Hemming, G., Bizouard, M.-A., et al. 2021,  
1710 *SoftwareX*, 14, 100677, doi: [10.1016/j.softx.2021.100677](https://doi.org/10.1016/j.softx.2021.100677)
- 1711 Gao, B., Tang, S.-P., Wang, H.-T., Yan, J., & Fan, Y.-Z. 2024, *Phys.*  
1712 *Rev. D*, 110, 044022, doi: [10.1103/PhysRevD.110.044022](https://doi.org/10.1103/PhysRevD.110.044022)
- 1713 Gross, D. J., & Sloan, J. H. 1987, *Nucl. Phys. B*, 291, 41,  
1714 doi: [10.1016/0550-3213\(87\)90465-2](https://doi.org/10.1016/0550-3213(87)90465-2)
- 1715 Gupta, A., Datta, S., Kastha, S., et al. 2020, *Phys. Rev. Lett.*, 125,  
1716 201101, doi: [10.1103/PhysRevLett.125.201101](https://doi.org/10.1103/PhysRevLett.125.201101)
- 1717 Gupta, T., & Cornish, N. J. 2024, *Phys. Rev. D*, 109, 064040,  
1718 doi: [10.1103/PhysRevD.109.064040](https://doi.org/10.1103/PhysRevD.109.064040)
- 1719 Haegel, L., O'Neal-Ault, K., Bailey, Q. G., et al. 2023, *Phys. Rev. D*,  
1720 107, 064031, doi: [10.1103/PhysRevD.107.064031](https://doi.org/10.1103/PhysRevD.107.064031)
- 1721 Hanna, C., et al. 2020, *Phys. Rev. D*, 101, 022003,  
1722 doi: [10.1103/PhysRevD.101.022003](https://doi.org/10.1103/PhysRevD.101.022003)
- 1723 Hannam, M., Schmidt, P., Bohé, A., et al. 2014, *Phys. Rev. Lett.*,  
1724 113, 151101, doi: [10.1103/PhysRevLett.113.151101](https://doi.org/10.1103/PhysRevLett.113.151101)
- 1725 Hansen, R. O. 1974, *J. Math. Phys.*, 15, 46, doi: [10.1063/1.1666501](https://doi.org/10.1063/1.1666501)
- 1726 Harris, C. R., et al. 2020, *Nature*, 585, 357,  
1727 doi: [10.1038/s41586-020-2649-2](https://doi.org/10.1038/s41586-020-2649-2)
- 1728 Harry, I., & Hinderer, T. 2018, *Class. Quantum Grav.*, 35, 145010,  
1729 doi: [10.1088/1361-6382/aac7e3](https://doi.org/10.1088/1361-6382/aac7e3)
- 1730 Harry, I., & Noller, J. 2022, *Gen. Rel. Grav.*, 54, 133,  
1731 doi: [10.1007/s10714-022-03016-0](https://doi.org/10.1007/s10714-022-03016-0)
- 1732 Hess, P. O. 2016, *Mon. Not. R. Astron. Soc.*, 462, 3026,  
1733 doi: [10.1093/mnras/stw1919](https://doi.org/10.1093/mnras/stw1919)
- 1734 Hess, P. O., & Greiner, W. 2009, *Int. J. Mod. Phys. E*, 18, 51,  
1735 doi: [10.1142/S0218301309012045](https://doi.org/10.1142/S0218301309012045)
- 1736 Hořava, P. 2009, *Phys. Rev. D*, 79, 084008,  
1737 doi: [10.1103/PhysRevD.79.084008](https://doi.org/10.1103/PhysRevD.79.084008)
- 1738 Horbatsch, M. W., & Burgess, C. P. 2012, *JCAP*, 05, 010,  
1739 doi: [10.1088/1475-7516/2012/05/010](https://doi.org/10.1088/1475-7516/2012/05/010)
- 1740 Hoy, C., & Raymond, V. 2021, *SoftwareX*, 15, 100765,  
1741 doi: [10.1016/j.softx.2021.100765](https://doi.org/10.1016/j.softx.2021.100765)
- 1742 Hunter, J. D. 2007, *Comput. Sci. Eng.*, 9, 90,  
1743 doi: [10.1109/MCSE.2007.55](https://doi.org/10.1109/MCSE.2007.55)
- 1744 Husa, S., Khan, S., Hannam, M., et al. 2016, *Phys. Rev. D*, 93,  
1745 044006, doi: [10.1103/PhysRevD.93.044006](https://doi.org/10.1103/PhysRevD.93.044006)
- 1746 Jacobson, T. 1999, *Phys. Rev. Lett.*, 83, 2699,  
1747 doi: [10.1103/PhysRevLett.83.2699](https://doi.org/10.1103/PhysRevLett.83.2699)
- 1748 Johnson-McDaniel, N. K., Ghosh, A., Ghonge, S., et al. 2022, *Phys.*  
1749 *Rev. D*, 105, 044020, doi: [10.1103/PhysRevD.105.044020](https://doi.org/10.1103/PhysRevD.105.044020)
- 1750 Johnson-McDaniel, N. K., Mukherjee, A., Kashyap, R., et al. 2020,  
1751 *Phys. Rev. D*, 102, 123010, doi: [10.1103/PhysRevD.102.123010](https://doi.org/10.1103/PhysRevD.102.123010)
- 1752 Julié, F.-L., Pompili, L., & Buonanno, A. 2025, *Phys. Rev. D*, 111,  
1753 024016, doi: [10.1103/PhysRevD.111.024016](https://doi.org/10.1103/PhysRevD.111.024016)
- 1754 Julié, F.-L. 2018, *J. Cosmol. Astropart. Phys.*, 10, 033,  
1755 doi: [10.1088/1475-7516/2018/10/033](https://doi.org/10.1088/1475-7516/2018/10/033)
- 1756 Kanti, P., Mavromatos, N. E., Rizos, J., Tamvakis, K., & Winstanley,  
1757 E. 1996, *Phys. Rev. D*, 54, 5049, doi: [10.1103/PhysRevD.54.5049](https://doi.org/10.1103/PhysRevD.54.5049)
- 1758 Kastha, S., Gupta, A., Arun, K. G., Sathyaprakash, B. S., & Van  
1759 Den Broeck, C. 2018, *Phys. Rev. D*, 98, 124033,  
1760 doi: [10.1103/PhysRevD.98.124033](https://doi.org/10.1103/PhysRevD.98.124033)
- 1761 —. 2019, *Phys. Rev. D*, 100, 044007,  
1762 doi: [10.1103/PhysRevD.100.044007](https://doi.org/10.1103/PhysRevD.100.044007)
- 1763 Khalil, M., Sennett, N., Steinhoff, J., & Buonanno, A. 2019, *Phys.*  
1764 *Rev. D*, 100, 124013, doi: [10.1103/PhysRevD.100.124013](https://doi.org/10.1103/PhysRevD.100.124013)
- 1765 Khalil, M., Sennett, N., Steinhoff, J., Vines, J., & Buonanno, A.  
1766 2018, *Phys. Rev. D*, 98, 104010,  
1767 doi: [10.1103/PhysRevD.98.104010](https://doi.org/10.1103/PhysRevD.98.104010)
- 1768 Khan, S., Chatziioannou, K., Hannam, M., & Ohme, F. 2019, *Phys.*  
1769 *Rev. D*, 100, 024059, doi: [10.1103/PhysRevD.100.024059](https://doi.org/10.1103/PhysRevD.100.024059)
- 1770 Khan, S., Husa, S., Hannam, M., et al. 2016, *Phys. Rev. D*, 93,  
1771 044007, doi: [10.1103/PhysRevD.93.044007](https://doi.org/10.1103/PhysRevD.93.044007)
- 1772 Khan, S., Ohme, F., Chatziioannou, K., & Hannam, M. 2020, *Phys.*  
1773 *Rev. D*, 101, 024056, doi: [10.1103/PhysRevD.101.024056](https://doi.org/10.1103/PhysRevD.101.024056)
- 1774 Klimenko, S., Yakushin, I., Rakhmanov, M., & Mitselmakher, G.  
1775 2004, *Class. Quantum Grav.*, 21, S1685,  
1776 doi: [10.1088/0264-9381/21/20/011](https://doi.org/10.1088/0264-9381/21/20/011)

- 1777 Klimentenko, S., Vedovato, G., Drago, M., et al. 2011, *Phys. Rev. D*,  
1778 83, 102001, doi: [10.1103/PhysRevD.83.102001](https://doi.org/10.1103/PhysRevD.83.102001)
- 1779 Klimentenko, S., et al. 2016, *Phys. Rev. D*, 93, 042004,  
1780 doi: [10.1103/PhysRevD.93.042004](https://doi.org/10.1103/PhysRevD.93.042004)
- 1781 Kostecký, V. A. 2004, *Phys. Rev. D*, 69, 105009,  
1782 doi: [10.1103/PhysRevD.69.105009](https://doi.org/10.1103/PhysRevD.69.105009)
- 1783 Kostecký, V. A., & Mewes, M. 2016, *Phys. Lett.*, B757, 510,  
1784 doi: [10.1016/j.physletb.2016.04.040](https://doi.org/10.1016/j.physletb.2016.04.040)
- 1785 Kostecký, V. A., & Russell, N. 2026,  
1786 <https://arxiv.org/abs/0801.0287v19>
- 1787 Kramer, M., et al. 2021, *Phys. Rev. X*, 11, 041050,  
1788 doi: [10.1103/PhysRevX.11.041050](https://doi.org/10.1103/PhysRevX.11.041050)
- 1789 Krishnendu, N. V., Arun, K. G., & Mishra, C. K. 2017, *Phys. Rev.*  
1790 *Lett.*, 119, 091101, doi: [10.1103/PhysRevLett.119.091101](https://doi.org/10.1103/PhysRevLett.119.091101)
- 1791 Krishnendu, N. V., Mishra, C. K., & Arun, K. G. 2019a, *Phys. Rev.*  
1792 *D*, 99, 064008, doi: [10.1103/PhysRevD.99.064008](https://doi.org/10.1103/PhysRevD.99.064008)
- 1793 Krishnendu, N. V., Saleem, M., Samajdar, A., et al. 2019b, *Phys.*  
1794 *Rev. D*, 100, 104019, doi: [10.1103/PhysRevD.100.104019](https://doi.org/10.1103/PhysRevD.100.104019)
- 1795 Lang, R. N. 2014, *Phys. Rev. D*, 89, 084014,  
1796 doi: [10.1103/PhysRevD.89.084014](https://doi.org/10.1103/PhysRevD.89.084014)
- 1797 —. 2015, *Phys. Rev. D*, 91, 084027,  
1798 doi: [10.1103/PhysRevD.91.084027](https://doi.org/10.1103/PhysRevD.91.084027)
- 1799 Li, T. G. F., Del Pozzo, W., Vitale, S., et al. 2012a, *Phys. Rev. D*, 85,  
1800 082003, doi: [10.1103/PhysRevD.85.082003](https://doi.org/10.1103/PhysRevD.85.082003)
- 1801 —. 2012b, *J. Phys. Conf. Ser.*, 363, 012028,  
1802 doi: [10.1088/1742-6596/363/1/012028](https://doi.org/10.1088/1742-6596/363/1/012028)
- 1803 LIGO Scientific Collaboration and Virgo Collaboration. 2018, Data  
1804 quality report user documentation,  
1805 [docs.ligo.org/detchar/data-quality-report/](https://docs.ligo.org/detchar/data-quality-report/)
- 1806 LIGO Scientific, Virgo, and KAGRA Collaboration. 2025, LVK  
1807 Algorithm Library - LALSuite, doi: [10.7935/GT1W-FZ16](https://doi.org/10.7935/GT1W-FZ16)
- 1808 —. 2026, Data release for GWTC-4.0: Tests of General Relativity. II.  
1809 Parameterized Tests. <https://dcc.ligo.org/P2600128/public>
- 1810 Lin, J. 1991, *IEEE Trans. Info. Theor.*, 37, 145,  
1811 doi: [10.1109/18.61115](https://doi.org/10.1109/18.61115)
- 1812 Littenberg, T. B., Kanner, J. B., Cornish, N. J., & Millhouse, M.  
1813 2016, *Phys. Rev. D*, 94, 044050,  
1814 doi: [10.1103/PhysRevD.94.044050](https://doi.org/10.1103/PhysRevD.94.044050)
- 1815 Macleod, D., et al. 2021, gwpy/gwpy, Zenodo,  
1816 doi: [10.5281/zenodo.597016](https://doi.org/10.5281/zenodo.597016)
- 1817 Maggiore, M. 2007, *Gravitational Waves. Vol. 1: Theory and*  
1818 *Experiments* (Oxford University Press),  
1819 doi: [10.1093/acprof:oso/9780198570745.001.0001](https://doi.org/10.1093/acprof:oso/9780198570745.001.0001)
- 1820 Mahapatra, P. 2024, *Phys. Rev. D*, 109, 024050,  
1821 doi: [10.1103/PhysRevD.109.024050](https://doi.org/10.1103/PhysRevD.109.024050)
- 1822 Mahapatra, P., & Kastha, S. 2024, *Phys. Rev. D*, 109, 084069,  
1823 doi: [10.1103/PhysRevD.109.084069](https://doi.org/10.1103/PhysRevD.109.084069)
- 1824 Mahapatra, P., Kastha, S., Gupta, A., Sathyaprakash, B. S., & Arun,  
1825 K. G. 2024, *Phys. Rev. D*, 109, 064036,  
1826 doi: [10.1103/PhysRevD.109.064036](https://doi.org/10.1103/PhysRevD.109.064036)
- 1827 Mahapatra, P., et al. 2025, *Phys. Rev. D*, 112, 104007,  
1828 doi: [10.1103/c1sj-jc4v](https://doi.org/10.1103/c1sj-jc4v)
- 1829 Maimon, Y. I., Nielsen, A. B., & Birnholtz, O. 2025, *Class. Quant.*  
1830 *Grav.*, 42, 185011, doi: [10.1088/1361-6382/ae008a](https://doi.org/10.1088/1361-6382/ae008a)
- 1831 Mariani, V., Fienga, A., Minazzoli, O., Gastineau, M., & Laskar, J.  
1832 2023, *Phys. Rev. D*, 108, 024047,  
1833 doi: [10.1103/PhysRevD.108.024047](https://doi.org/10.1103/PhysRevD.108.024047)
- 1834 Marsat, S. 2015, *Class. Quant. Grav.*, 32, 085008,  
1835 doi: [10.1088/0264-9381/32/8/085008](https://doi.org/10.1088/0264-9381/32/8/085008)
- 1836 Maselli, A., Pani, P., Cardoso, V., et al. 2018, *Phys. Rev. Lett.*, 120,  
1837 081101, doi: [10.1103/PhysRevLett.120.081101](https://doi.org/10.1103/PhysRevLett.120.081101)
- 1838 Matas, A., et al. 2020, *Phys. Rev. D*, 102, 043023,  
1839 doi: [10.1103/PhysRevD.102.043023](https://doi.org/10.1103/PhysRevD.102.043023)
- 1840 Mehta, A. K., Buonanno, A., Costeta, R., et al. 2023, *Phys. Rev. D*,  
1841 107, 044020, doi: [10.1103/PhysRevD.107.044020](https://doi.org/10.1103/PhysRevD.107.044020)
- 1842 Meidam, J., et al. 2018, *Phys. Rev. D*, 97, 044033,  
1843 doi: [10.1103/PhysRevD.97.044033](https://doi.org/10.1103/PhysRevD.97.044033)
- 1844 Messick, C., et al. 2017, *Phys. Rev. D*, 95, 042001,  
1845 doi: [10.1103/PhysRevD.95.042001](https://doi.org/10.1103/PhysRevD.95.042001)
- 1846 Mewes, M. 2019, *Phys. Rev. D*, 99, 104062,  
1847 doi: [10.1103/PhysRevD.99.104062](https://doi.org/10.1103/PhysRevD.99.104062)
- 1848 Mirshekari, S., & Will, C. M. 2013, *Phys. Rev. D*, 87, 084070,  
1849 doi: [10.1103/PhysRevD.87.084070](https://doi.org/10.1103/PhysRevD.87.084070)
- 1850 Mirshekari, S., Yunes, N., & Will, C. M. 2012, *Phys. Rev. D*, 85,  
1851 024041, doi: [10.1103/PhysRevD.85.024041](https://doi.org/10.1103/PhysRevD.85.024041)
- 1852 Mishra, C. K., Arun, K. G., Iyer, B. R., & Sathyaprakash, B. S. 2010,  
1853 *Phys. Rev. D*, 82, 064010, doi: [10.1103/PhysRevD.82.064010](https://doi.org/10.1103/PhysRevD.82.064010)
- 1854 Mishra, C. K., Kela, A., Arun, K. G., & Faye, G. 2016, *Phys. Rev. D*,  
1855 93, 084054, doi: [10.1103/PhysRevD.93.084054](https://doi.org/10.1103/PhysRevD.93.084054)
- 1856 Narikawa, T., Uchikata, N., & Tanaka, T. 2021, *Phys. Rev. D*, 104,  
1857 084056, doi: [10.1103/PhysRevD.104.084056](https://doi.org/10.1103/PhysRevD.104.084056)
- 1858 Nielsen, A. B., & Birnholtz, O. 2018, *Astron. Nachr.*, 339, 298,  
1859 doi: [10.1002/asna.201813473](https://doi.org/10.1002/asna.201813473)
- 1860 Nitz, A. H., Dent, T., Dal Canton, T., Fairhurst, S., & Brown, D. A.  
1861 2017, *Astrophys. J.*, 849, 118, doi: [10.3847/1538-4357/aa8f50](https://doi.org/10.3847/1538-4357/aa8f50)
- 1862 O'Neal-Ault, K., Bailey, Q. G., Dumerchat, T., Haegel, L., &  
1863 Tasson, J. 2021, *Universe*, 7, 380, doi: [10.3390/universe7100380](https://doi.org/10.3390/universe7100380)
- 1864 Pacilio, C., Vaglio, M., Maselli, A., & Pani, P. 2020, *Phys. Rev. D*,  
1865 102, 083002, doi: [10.1103/PhysRevD.102.083002](https://doi.org/10.1103/PhysRevD.102.083002)
- 1866 Pai, A., & Arun, K. G. 2013, *Class. Quantum Grav.*, 30, 025011,  
1867 doi: [10.1088/0264-9381/30/2/025011](https://doi.org/10.1088/0264-9381/30/2/025011)
- 1868 Pappas, G., & Apostolatos, T. A. 2012a,  
1869 <https://arxiv.org/abs/1211.6299>
- 1870 —. 2012b, *Phys. Rev. Lett.*, 108, 231104,  
1871 doi: [10.1103/PhysRevLett.108.231104](https://doi.org/10.1103/PhysRevLett.108.231104)
- 1872 Pedregosa, F., et al. 2011, *J. Machine Learning Res.*, 12, 2825
- 1873 Perkins, S., & Yunes, N. 2022, *Phys. Rev. D*, 105, 124047,  
1874 doi: [10.1103/PhysRevD.105.124047](https://doi.org/10.1103/PhysRevD.105.124047)
- 1875 Poisson, E., & Will, C. M. 2014, *Gravity* (Cambridge, UK:  
1876 Cambridge University Press), doi: [10.1017/CBO9781139507486](https://doi.org/10.1017/CBO9781139507486)

- 1877 Pompili, L., et al. 2023, *Phys. Rev. D*, 108, 124035,  
1878 doi: [10.1103/PhysRevD.108.124035](https://doi.org/10.1103/PhysRevD.108.124035)
- 1879 Pratten, G., Husa, S., Garcia-Quiros, C., et al. 2020, *Phys. Rev. D*,  
1880 102, 064001, doi: [10.1103/PhysRevD.102.064001](https://doi.org/10.1103/PhysRevD.102.064001)
- 1881 Pratten, G., et al. 2021, *Phys. Rev. D*, 103, 104056,  
1882 doi: [10.1103/PhysRevD.103.104056](https://doi.org/10.1103/PhysRevD.103.104056)
- 1883 Robinet, F., Arnaud, N., Leroy, N., et al. 2020, *SoftwareX*, 12,  
1884 100620, doi: [10.1016/j.softx.2020.100620](https://doi.org/10.1016/j.softx.2020.100620)
- 1885 Romero-Shaw, I. M., et al. 2020, *Mon. Not. R. Astron. Soc.*, 499,  
1886 3295, doi: [10.1093/mnras/staa2850](https://doi.org/10.1093/mnras/staa2850)
- 1887 Roy, S., Haney, M., Pratten, G., Pang, P. T. H., & Van Den Broeck,  
1888 C. 2026, *Phys. Rev. D*, 113, 024016, doi: [10.1103/855k-sys5](https://doi.org/10.1103/855k-sys5)
- 1889 Ryan, F. D. 1997, *Phys. Rev. D*, 55, 6081,  
1890 doi: [10.1103/PhysRevD.55.6081](https://doi.org/10.1103/PhysRevD.55.6081)
- 1891 Sachdev, S., et al. 2019. <https://arxiv.org/abs/1901.08580>
- 1892 Saleem, M., Datta, S., Arun, K. G., & Sathyaprakash, B. S. 2022,  
1893 *Phys. Rev. D*, 105, 084062, doi: [10.1103/PhysRevD.105.084062](https://doi.org/10.1103/PhysRevD.105.084062)
- 1894 Sampson, L., Cornish, N., & Yunes, N. 2013, *Phys. Rev. D*, 87,  
1895 102001, doi: [10.1103/PhysRevD.87.102001](https://doi.org/10.1103/PhysRevD.87.102001)
- 1896 —. 2014, *Phys. Rev. D*, 89, 064037,  
1897 doi: [10.1103/PhysRevD.89.064037](https://doi.org/10.1103/PhysRevD.89.064037)
- 1898 Sanger, E. M., et al. 2024. <https://arxiv.org/abs/2406.03568>
- 1899 Sathyaprakash, B. S., & Dhurandhar, S. V. 1991, *Phys. Rev. D*, 44,  
1900 3819, doi: [10.1103/PhysRevD.44.3819](https://doi.org/10.1103/PhysRevD.44.3819)
- 1901 Sefiedgar, A. S., Nozari, K., & Sepangi, H. R. 2011, *Phys. Lett.*,  
1902 B696, 119, doi: [10.1016/j.physletb.2010.11.067](https://doi.org/10.1016/j.physletb.2010.11.067)
- 1903 Sennett, N., Hinderer, T., Steinhoff, J., Buonanno, A., & Ossokine,  
1904 S. 2017, *Phys. Rev. D*, 96, 024002,  
1905 doi: [10.1103/PhysRevD.96.024002](https://doi.org/10.1103/PhysRevD.96.024002)
- 1906 Shiralilou, B., Hinderer, T., Nissanke, S. M., Ortiz, N., & Witek, H.  
1907 2022, *Class. Quantum Grav.*, 39, 035002,  
1908 doi: [10.1088/1361-6382/ac4196](https://doi.org/10.1088/1361-6382/ac4196)
- 1909 Shoom, A. A., Gupta, P. K., Krishnan, B., Nielsen, A. B., & Capano,  
1910 C. D. 2023, *Gen. Rel. Grav.*, 55, 55,  
1911 doi: [10.1007/s10714-023-03100-z](https://doi.org/10.1007/s10714-023-03100-z)
- 1912 Silva, H. O., Holgado, A. M., Cardenas-Avenda˜no, A., & Yunes, N.  
1913 2021, *Phys. Rev. Lett.*, 126, 181101,  
1914 doi: [10.1103/PhysRevLett.126.181101](https://doi.org/10.1103/PhysRevLett.126.181101)
- 1915 Smith, J. R., Abbott, T., Hirose, E., et al. 2011, *Class. Quantum*  
1916 *Grav.*, 28, 235005, doi: [10.1088/0264-9381/28/23/235005](https://doi.org/10.1088/0264-9381/28/23/235005)
- 1917 Smith, R., Ashton, G., Vajpeyi, A., & Talbot, C. 2020, *Mon. Not. R.*  
1918 *Astron. Soc.*, 498, 4492, doi: [10.1093/mnras/staa2483](https://doi.org/10.1093/mnras/staa2483)
- 1919 Sotiriou, T. P., & Barausse, E. 2007, *Phys. Rev. D*, 75, 084007,  
1920 doi: [10.1103/PhysRevD.75.084007](https://doi.org/10.1103/PhysRevD.75.084007)
- 1921 Speagle, J. S. 2020, *Mon. Not. R. Astron. Soc.*, 493, 3132,  
1922 doi: [10.1093/mnras/staa278](https://doi.org/10.1093/mnras/staa278)
- 1923 Tahura, S., & Yagi, K. 2018, *Phys. Rev. D*, 98, 084042,  
1924 doi: [10.1103/PhysRevD.98.084042](https://doi.org/10.1103/PhysRevD.98.084042)
- 1925 Taylor, J. H., & Weisberg, J. M. 1982, *Astrophys. J.*, 253, 908,  
1926 doi: [10.1086/159690](https://doi.org/10.1086/159690)
- 1927 —. 1989, *Astrophys. J.*, 345, 434, doi: [10.1086/167917](https://doi.org/10.1086/167917)
- 1928 Thompson, J. E., Fauchon-Jones, E., Khan, S., et al. 2020, *Phys.*  
1929 *Rev. D*, 101, 124059, doi: [10.1103/PhysRevD.101.124059](https://doi.org/10.1103/PhysRevD.101.124059)
- 1930 Thorne, K. S. 1980, *Rev. Mod. Phys.*, 52, 299,  
1931 doi: [10.1103/RevModPhys.52.299](https://doi.org/10.1103/RevModPhys.52.299)
- 1932 Tiwari, A., Vijaykumar, A., Kapadia, S. J., Ghosh, S., & Nielsen,  
1933 A. B. 2025. <https://arxiv.org/abs/2506.22272>
- 1934 Uchikata, N., & Yoshida, S. 2016, *Class. Quantum Grav.*, 33,  
1935 025005, doi: [10.1088/0264-9381/33/2/025005](https://doi.org/10.1088/0264-9381/33/2/025005)
- 1936 Urban, A. L., et al. 2021, *gwdetchar/gwdetchar*, Zenodo,  
1937 doi: [10.5281/zenodo.597016](https://doi.org/10.5281/zenodo.597016)
- 1938 Usman, S. A., et al. 2016, *Class. Quantum Grav.*, 33, 215004,  
1939 doi: [10.1088/0264-9381/33/21/215004](https://doi.org/10.1088/0264-9381/33/21/215004)
- 1940 Varma, V., Field, S. E., Scheel, M. A., et al. 2019, *Phys. Rev.*  
1941 *Research.*, 1, 033015, doi: [10.1103/PhysRevResearch.1.033015](https://doi.org/10.1103/PhysRevResearch.1.033015)
- 1942 Viets, A., et al. 2018, *Class. Quantum Grav.*, 35, 095015,  
1943 doi: [10.1088/1361-6382/aab658](https://doi.org/10.1088/1361-6382/aab658)
- 1944 Vijaykumar, A., Tiwari, A., Kapadia, S. J., Arun, K. G., & Ajith, P.  
1945 2023, *Astrophys. J.*, 954, 105, doi: [10.3847/1538-4357/acd77d](https://doi.org/10.3847/1538-4357/acd77d)
- 1946 Virgo Collaboration. 2021, *PythonVirgoTools*, v5.1.1,  
1947 [git.ligo.org/virgo/virgoapp/PythonVirgoTools](https://git.ligo.org/virgo/virgoapp/PythonVirgoTools)
- 1948 Virtanen, P., et al. 2020, *Nat. Meth.*, 17, 261,  
1949 doi: [10.1038/s41592-019-0686-2](https://doi.org/10.1038/s41592-019-0686-2)
- 1950 Waskom, M. L. 2021, *J. Open Source Softw.*, 6, 3021,  
1951 doi: [10.21105/joss.03021](https://doi.org/10.21105/joss.03021)
- 1952 Wette, K. 2020, *SoftwareX*, 12, 100634,  
1953 doi: [10.1016/j.softx.2020.100634](https://doi.org/10.1016/j.softx.2020.100634)
- 1954 Will, C. M. 1998, *Phys. Rev. D*, 57, 2061,  
1955 doi: [10.1103/PhysRevD.57.2061](https://doi.org/10.1103/PhysRevD.57.2061)
- 1956 —. 2014, *Living Rev. Relativity*, 17, 4, doi: [10.12942/lrr-2014-4](https://doi.org/10.12942/lrr-2014-4)
- 1957 Will, C. M. 2018, *Theory and Experiment in Gravitational Physics*,  
1958 2nd edn. (Cambridge, UK: Cambridge University Press),  
1959 doi: [10.1017/9781316338612](https://doi.org/10.1017/9781316338612)
- 1960 Williams, D., Veitch, J., Chiofalo, M. L., et al. 2023, *J. Open Source*  
1961 *Softw.*, 8, 4170, doi: [10.21105/joss.04170](https://doi.org/10.21105/joss.04170)
- 1962 Yagi, K., Stein, L. C., Yunes, N., & Tanaka, T. 2012, *Phys. Rev. D*,  
1963 85, 064022, doi: [10.1103/PhysRevD.85.064022](https://doi.org/10.1103/PhysRevD.85.064022)
- 1964 Yunes, N., & Hughes, S. A. 2010, *Phys. Rev. D*, 82, 082002,  
1965 doi: [10.1103/PhysRevD.82.082002](https://doi.org/10.1103/PhysRevD.82.082002)
- 1966 Yunes, N., & Pretorius, F. 2009, *Phys. Rev. D*, 80, 122003,  
1967 doi: [10.1103/PhysRevD.80.122003](https://doi.org/10.1103/PhysRevD.80.122003)
- 1968 Zweizig, J. 2006, *The Data Monitor Tool Project*,  
1969 [labcit.ligo.caltech.edu/~jzweizig/DMT-Project.html](https://labcit.ligo.caltech.edu/~jzweizig/DMT-Project.html)

1970 THE LIGO SCIENTIFIC COLLABORATION, THE VIRGO COLLABORATION, AND THE KAGRA COLLABORATION, A. G. ABAC,<sup>1</sup>  
 1971 I. ABOUELFETTOUH,<sup>2</sup> F. ACERNESE,<sup>3,4</sup> K. ACKLEY,<sup>5</sup> C. ADAMCEWICZ,<sup>6</sup> S. ADHICARY,<sup>7</sup> D. ADHIKARI,<sup>8,9</sup> N. ADHIKARI,<sup>10</sup>  
 1972 R. X. ADHIKARI,<sup>11</sup> V. K. ADKINS,<sup>12</sup> S. AFROZ,<sup>13</sup> A. AGAPITO,<sup>14</sup> D. AGARWAL,<sup>15</sup> M. AGATHOS,<sup>16</sup> N. AGGARWAL,<sup>17</sup> S. AGGARWAL,<sup>18</sup>  
 1973 O. D. AGUIAR,<sup>19</sup> I.-L. AHREND,<sup>20</sup> L. AIELLO,<sup>21,22</sup> A. AIN,<sup>23</sup> P. AJITH,<sup>24</sup> T. AKUTSU,<sup>25,26</sup> S. ALBANESI,<sup>27,28</sup> W. ALI,<sup>29,30</sup>  
 1974 S. AL-KERSHI,<sup>8,9</sup> C. ALLÉNÉ,<sup>31</sup> A. ALLOCCA,<sup>32,4</sup> S. AL-SHAMMARI,<sup>33</sup> P. A. ALTIN,<sup>34</sup> S. ALVAREZ-LOPEZ,<sup>35</sup> W. AMAR,<sup>31</sup>  
 1975 O. AMARASINGHE,<sup>33</sup> A. AMATO,<sup>36,37</sup> F. AMICUCCI,<sup>38,39</sup> C. AMRA,<sup>40</sup> A. ANANYEVA,<sup>11</sup> S. B. ANDERSON,<sup>11</sup> W. G. ANDERSON,<sup>11</sup>  
 1976 M. ANDIA,<sup>41</sup> M. ANDO,<sup>42</sup> M. ANDRÉS-CARCASONA,<sup>43</sup> T. ANDRIĆ,<sup>44,45,8,9</sup> J. ANGLIN,<sup>46</sup> S. ANSOLDI,<sup>47,48</sup> J. M. ANTELIS,<sup>49</sup>  
 1977 S. ANTIER,<sup>41</sup> M. AOUMI,<sup>50</sup> E. Z. APPAVURAVTHER,<sup>51,52</sup> S. APPERT,<sup>11</sup> S. K. APPLE,<sup>53</sup> K. ARAI,<sup>11</sup> A. ARAYA,<sup>42</sup> M. C. ARAYA,<sup>11</sup>  
 1978 M. ARCA SEDDA,<sup>44,45</sup> J. S. AREEDA,<sup>54</sup> N. ARITOMI,<sup>2</sup> F. ARMATO,<sup>29,30</sup> S. ARMSTRONG,<sup>55</sup> N. ARNAUD,<sup>56</sup> M. AROGETI,<sup>57</sup>  
 1979 S. M. ARONSON,<sup>12</sup> K. G. ARUN,<sup>58</sup> G. ASHTON,<sup>59</sup> Y. ASO,<sup>25,60</sup> L. ASPREA,<sup>28</sup> M. ASSIDUO,<sup>61,62</sup> S. ASSIS DE SOUZA MELO,<sup>63</sup>  
 1980 S. M. ASTON,<sup>64</sup> P. ASTONE,<sup>38</sup> F. ATTADIO,<sup>39,38</sup> F. AUBIN,<sup>65</sup> K. AULTONEAL,<sup>66</sup> G. AVALONE,<sup>67</sup> E. A. AVILA,<sup>49</sup> S. BABAK,<sup>20</sup>  
 1981 C. BADGER,<sup>68</sup> S. BAE,<sup>69</sup> S. BAGNASCO,<sup>28</sup> L. BAIOTTI,<sup>70</sup> R. BAJPAI,<sup>71</sup> T. BAKA,<sup>72,37</sup> A. M. BAKER,<sup>6</sup> K. A. BAKER,<sup>73</sup> T. BAKER,<sup>74</sup>  
 1982 G. BALDI,<sup>75,76</sup> N. BALDICCHI,<sup>77,51</sup> M. BALL,<sup>78</sup> G. BALLARDIN,<sup>63</sup> S. W. BALLMER,<sup>79</sup> S. BANAGIRI,<sup>6</sup> B. BANERJEE,<sup>44</sup> D. BANKAR,<sup>80</sup>  
 1983 T. M. BAPTISTE,<sup>12</sup> P. BARAL,<sup>10</sup> M. BARATTI,<sup>81,82</sup> J. C. BARAYOGA,<sup>11</sup> B. C. BARISH,<sup>11</sup> D. BARKER,<sup>2</sup> N. BARMAN,<sup>80</sup>  
 1984 P. BARNEO,<sup>83,84,85</sup> F. BARONE,<sup>86,4</sup> B. BARR,<sup>87</sup> L. BARSOTTI,<sup>35</sup> M. BARSUGLIA,<sup>20</sup> D. BARTA,<sup>88</sup> A. M. BARTOLETTI,<sup>89</sup>  
 1985 M. A. BARTON,<sup>87</sup> I. BARTOS,<sup>46</sup> A. BASALAEV,<sup>8,9</sup> R. BASSIRI,<sup>90</sup> A. BASTI,<sup>82,81</sup> M. BAWAJ,<sup>77,51</sup> P. BAXI,<sup>91</sup> J. C. BAYLEY,<sup>87</sup>  
 1986 A. C. BAYLOR,<sup>10</sup> P. A. BAYNARD II,<sup>57</sup> M. BAZZAN,<sup>92,93</sup> V. M. BEDAKIHALE,<sup>94</sup> F. BEIRNAERT,<sup>95</sup> M. BEJGER,<sup>96</sup> D. BELARDINELLI,<sup>22</sup>  
 1987 A. S. BELL,<sup>87</sup> D. S. BELLIE,<sup>97</sup> L. BELLIZZI,<sup>81,82</sup> W. BENOIT,<sup>18</sup> I. BENTARA,<sup>56</sup> J. D. BENTLEY,<sup>98</sup> M. BEN YAALA,<sup>55</sup> S. BERA,<sup>99,100</sup>  
 1988 F. BERGAMIN,<sup>33</sup> B. K. BERGER,<sup>90</sup> S. BERNUZZI,<sup>27</sup> M. BEROIZ,<sup>11</sup> C. P. L. BERRY,<sup>87</sup> D. BERSANETTI,<sup>29</sup> T. BERTHEAS,<sup>101</sup>  
 1989 A. BERTOLINI,<sup>37,36</sup> J. BETZWIESER,<sup>64</sup> D. BEVERIDGE,<sup>73</sup> G. BEVILACQUA,<sup>102</sup> N. BEVINS,<sup>103</sup> S. BHAGWAT,<sup>104</sup> R. BHANDARE,<sup>105</sup>  
 1990 S. A. BHAT,<sup>80</sup> R. BHATT,<sup>11</sup> D. BHATTACHARJEE,<sup>106,107</sup> S. BHATTACHARYYA,<sup>108</sup> S. BHAUMIK,<sup>46</sup> V. BIANCALANA,<sup>102</sup>  
 1991 A. BIANCHI,<sup>37,109</sup> I. A. BILENKO,<sup>110</sup> G. BILLINGSLEY,<sup>11</sup> A. BINETTI,<sup>111</sup> S. BINI,<sup>11,75,76</sup> C. BINU,<sup>112</sup> S. BIOT,<sup>113</sup> O. BIRNHOLTZ,<sup>114</sup>  
 1992 S. BISCOVEANU,<sup>97</sup> A. BISHT,<sup>9</sup> M. BITOSI,<sup>63,81</sup> M.-A. BIZOUARD,<sup>115</sup> S. BLABER,<sup>116</sup> J. K. BLACKBURN,<sup>11</sup> L. A. BLAGG,<sup>78</sup>  
 1993 C. D. BLAIR,<sup>73,64</sup> D. G. BLAIR,<sup>73</sup> N. BODE,<sup>8,9</sup> N. BOETTNER,<sup>98</sup> G. BOILEAU,<sup>115</sup> M. BOLDRINI,<sup>38</sup> G. N. BOLINGBROKE,<sup>117</sup>  
 1994 A. BOLLIAND,<sup>118,40</sup> L. D. BONAVENTA,<sup>46</sup> R. BONDARESCU,<sup>83</sup> F. BONDU,<sup>119</sup> E. BONILLA,<sup>90</sup> M. S. BONILLA,<sup>54</sup> A. BONINO,<sup>104</sup>  
 1995 R. BONNAND,<sup>31,118</sup> A. BORCHERS,<sup>8,9</sup> V. BOSCHI,<sup>81</sup> S. BOSE,<sup>120</sup> V. BOSSILKOV,<sup>64</sup> Y. BOTHRA,<sup>37,109</sup> A. BOUDON,<sup>56</sup> L. BOURG,<sup>57</sup>  
 1996 M. BOYLE,<sup>121</sup> A. BOZZI,<sup>63</sup> C. BRADASCHIA,<sup>81</sup> P. R. BRADY,<sup>10</sup> A. BRANCH,<sup>64</sup> M. BRANCHESI,<sup>44,45</sup> I. BRAUN,<sup>106</sup> T. BRIANT,<sup>122</sup>  
 1997 A. BRILLET,<sup>115</sup> M. BRINKMANN,<sup>8,9</sup> P. BROCKILL,<sup>10</sup> E. BROCKMUELLER,<sup>8,9</sup> A. F. BROOKS,<sup>11</sup> B. C. BROWN,<sup>46</sup> D. D. BROWN,<sup>117</sup>  
 1998 M. L. BROZZETTI,<sup>77,51</sup> S. BRUNETT,<sup>11</sup> G. BRUNO,<sup>15</sup> R. BRUNTZ,<sup>123</sup> J. BRYANT,<sup>104</sup> Y. BU,<sup>124</sup> F. BUCCI,<sup>62</sup> J. BUCHANAN,<sup>123</sup>  
 1999 O. BULASHENKO,<sup>83,84</sup> T. BULIK,<sup>125</sup> H. J. BULTEN,<sup>37</sup> A. BUONANNO,<sup>126,1</sup> K. BURTYNYK,<sup>2</sup> R. BUSCICCHIO,<sup>127,128</sup> D. BUSKULIC,<sup>31</sup>  
 2000 C. BUY,<sup>101</sup> R. L. BYER,<sup>90</sup> G. S. CABOURN DAVIES,<sup>74</sup> R. CABRITA,<sup>15</sup> V. CÁ CERES-BARBOSA,<sup>7</sup> L. CADONATI,<sup>57</sup> G. CAGNOLI,<sup>129</sup>  
 2001 C. CAHILLANE,<sup>79</sup> A. CALAFAT,<sup>99</sup> T. A. CALLISTER,<sup>130</sup> E. CALLONI,<sup>32,4</sup> S. R. CALLOS,<sup>78</sup> M. CANEPA,<sup>30,29</sup> G. CANEVA SANTORO,<sup>43</sup>  
 2002 K. C. CANNON,<sup>42</sup> H. CAO,<sup>35</sup> L. A. CAPISTRAN,<sup>131</sup> E. CAPOCASA,<sup>20</sup> E. CAPOTE,<sup>2,11</sup> G. CAPURRI,<sup>82,81</sup> G. CARAPELLA,<sup>67,132</sup>  
 2003 F. CARBOGNANI,<sup>63</sup> M. CARLASSARA,<sup>8,9</sup> J. B. CARLIN,<sup>124</sup> T. K. CARLSON,<sup>133</sup> M. F. CARNEY,<sup>106</sup> M. CARPINELLI,<sup>127,63</sup>  
 2004 G. CARRILLO,<sup>78</sup> J. J. CARTER,<sup>8,9</sup> G. CARULLO,<sup>104,134</sup> A. CASALLAS-LAGOS,<sup>135</sup> J. CASANUEVA DIAZ,<sup>63</sup> C. CASENTINI,<sup>136,22</sup>  
 2005 S. Y. CASTRO-LUCAS,<sup>137</sup> S. CAUDILL,<sup>133</sup> M. CAVAGLIÀ,<sup>107</sup> R. CAVALIERI,<sup>63</sup> A. CEJA,<sup>54</sup> G. CELLA,<sup>81</sup> P. CERDÁ-DURÁN,<sup>138,139</sup>  
 2006 E. CESARINI,<sup>22</sup> N. CHABBRA,<sup>34</sup> W. CHAIBI,<sup>115</sup> A. CHAKRABORTY,<sup>13</sup> P. CHAKRABORTY,<sup>8,9</sup> S. CHAKRABORTY,<sup>105</sup>  
 2007 S. CHALATHADKA SUBRAHMANYA,<sup>98</sup> J. C. L. CHAN,<sup>140</sup> M. CHAN,<sup>116</sup> K. CHANG,<sup>141</sup> S. CHAO,<sup>142,141</sup> P. CHARLTON,<sup>143</sup>  
 2008 E. CHASSANDE-MOTTIN,<sup>20</sup> C. CHATTERJEE,<sup>144</sup> DEBARATI CHATTERJEE,<sup>80</sup> DEEP CHATTERJEE,<sup>35</sup> M. CHATURVEDI,<sup>105</sup> S. CHATY,<sup>20</sup>  
 2009 K. CHATZIOANNOS,<sup>11</sup> A. CHEN,<sup>145</sup> A. H.-Y. CHEN,<sup>146</sup> D. CHEN,<sup>147</sup> H. CHEN,<sup>142</sup> H. Y. CHEN,<sup>148</sup> S. CHEN,<sup>144</sup> YANBEI CHEN,<sup>149</sup>  
 2010 YITIAN CHEN,<sup>121</sup> H. P. CHENG,<sup>150</sup> P. CHESSA,<sup>77,51</sup> H. T. CHEUNG,<sup>91</sup> S. Y. CHEUNG,<sup>6</sup> F. CHIADINI,<sup>151,132</sup> G. CHIARINI,<sup>8,9,93</sup>  
 2011 A. CHIBA,<sup>152</sup> A. CHINCARINI,<sup>29</sup> M. L. CHIOFALO,<sup>82,81</sup> A. CHIUMMO,<sup>4,63</sup> C. CHOU,<sup>146</sup> S. CHOUDHARY,<sup>73</sup> N. CHRISTENSEN,<sup>115,153</sup>  
 2012 S. S. Y. CHUA,<sup>34</sup> G. CIANI,<sup>75,76</sup> P. CIECIELAG,<sup>96</sup> M. CIEŚLAR,<sup>125</sup> M. CIFALDI,<sup>22</sup> B. CIROK,<sup>154</sup> F. CLARA,<sup>2</sup> J. A. CLARK,<sup>11,57</sup>  
 2013 T. A. CLARKE,<sup>6</sup> P. CLEARWATER,<sup>155</sup> S. CLESSE,<sup>113</sup> F. CLEVA,<sup>115,118</sup> E. COCCIA,<sup>44,45,43</sup> E. CODAZZO,<sup>156,157</sup> P.-F. COHADON,<sup>122</sup>  
 2014 S. COLACE,<sup>30</sup> E. COLANGELI,<sup>74</sup> M. COLLEONI,<sup>99</sup> C. G. COLLETTE,<sup>158</sup> J. COLLINS,<sup>64</sup> S. COLLOMS,<sup>87</sup> A. COLOMBO,<sup>159,128</sup>  
 2015 C. M. COMPTON,<sup>2</sup> G. CONNOLLY,<sup>78</sup> L. CONTI,<sup>93</sup> T. R. CORBITT,<sup>12</sup> I. CORDERO-CARRIÓN,<sup>160</sup> S. COREZZI,<sup>77,51</sup> M. CORMAN,<sup>1</sup>  
 2016 N. J. CORNISH,<sup>161</sup> I. CORONADO,<sup>162</sup> A. CORSI,<sup>163</sup> R. COTTINGHAM,<sup>64</sup> M. W. COUGHLIN,<sup>18</sup> A. COUINEAUX,<sup>38</sup> P. COUVARES,<sup>11,57</sup>  
 2017 D. M. COWARD,<sup>73</sup> R. COYNE,<sup>164</sup> A. COZZUMBO,<sup>44</sup> J. D. E. CREIGHTON,<sup>10</sup> T. D. CREIGHTON,<sup>165</sup> P. CREMONESE,<sup>99</sup> S. CROOK,<sup>64</sup>  
 2018 R. CROUCH,<sup>2</sup> J. CSIZMAZIA,<sup>2</sup> J. R. CUDELL,<sup>166</sup> T. J. CULLEN,<sup>11</sup> A. CUMMING,<sup>87</sup> E. CUOCO,<sup>167,168</sup> M. CUSINATO,<sup>138</sup>  
 2019 L. V. DA CONCEIÇÃO,<sup>169</sup> T. DAL CANTON,<sup>41</sup> S. DAL PRA,<sup>170</sup> G. DÁLYA,<sup>101</sup> O. DAN,<sup>114</sup> B. D'ANGELO,<sup>29</sup> S. DANILISHIN,<sup>36,37</sup>  
 2020 S. D'ANTONIO,<sup>38</sup> K. DANZMANN,<sup>9,8,9</sup> K. E. DARROCH,<sup>123</sup> L. P. DARTEZ,<sup>64</sup> R. DAS,<sup>108</sup> A. DASGUPTA,<sup>94</sup> V. DATTILO,<sup>63</sup> A. DAUMAS,<sup>20</sup>  
 2021 N. DAVARI,<sup>171,172</sup> I. DAVE,<sup>105</sup> A. DAVENPORT,<sup>137</sup> M. DAVIER,<sup>41</sup> T. F. DAVIES,<sup>73</sup> D. DAVIS,<sup>11</sup> L. DAVIS,<sup>73</sup> M. C. DAVIS,<sup>18</sup>  
 2022 P. DAVIS,<sup>173,174</sup> E. J. DAW,<sup>175</sup> M. DAX,<sup>1</sup> J. DE BOLLE,<sup>95</sup> M. DEENADAYALAN,<sup>80</sup> J. DEGALLAIX,<sup>176</sup> M. DE LAURENTIS,<sup>32,4</sup>  
 2023 F. DE LILLO,<sup>23</sup> S. DELLA TORRE,<sup>128</sup> W. DEL POZZO,<sup>82,81</sup> A. DEMAGNY,<sup>31</sup> F. DE MARCO,<sup>39,38</sup> G. DEMASI,<sup>177,62</sup> F. DE MATTEIS,<sup>21,22</sup>  
 2024 N. DEMOS,<sup>35</sup> T. DENT,<sup>178</sup> A. DEPASSE,<sup>15</sup> N. DEPERGOLA,<sup>103</sup> R. DE PIETRI,<sup>179,180</sup> R. DE ROSA,<sup>32,4</sup> C. DE ROSSI,<sup>63</sup> M. DESAI,<sup>35</sup>  
 2025 R. DESALVO,<sup>181</sup> A. DESIMONE,<sup>182</sup> R. DE SIMONE,<sup>151,132</sup> A. DHANI,<sup>1</sup> R. DIAB,<sup>46</sup> M. C. DÍAZ,<sup>165</sup> M. DI CESARE,<sup>32,4</sup> G. DIDERON,<sup>183</sup>  
 2026 T. DIETRICH,<sup>1</sup> L. DI FIORE,<sup>4</sup> C. DI FRONZO,<sup>73</sup> M. DI GIOVANNI,<sup>39,38</sup> T. DI GIROLAMO,<sup>32,4</sup> D. DIKSHA,<sup>37,36</sup> J. DING,<sup>20,184</sup>  
 2027 S. DI PACE,<sup>39,38</sup> I. DI PALMA,<sup>39,38</sup> D. DI PIERO,<sup>185,48</sup> F. DI RENZO,<sup>56</sup> DIVYAJYOTI,<sup>33</sup> A. DMITRIEV,<sup>104</sup> J. P. DOCHERTY,<sup>87</sup>  
 2028 Z. DOCTOR,<sup>97</sup> N. DOERKSEN,<sup>169</sup> E. DOHMEN,<sup>2</sup> A. DOKE,<sup>133</sup> A. DOMICIANO DE SOUZA,<sup>186</sup> L. D'ONOFRIO,<sup>38</sup> F. DONOVAN,<sup>35</sup>  
 2029 K. L. DOOLEY,<sup>33</sup> T. DOONEY,<sup>72</sup> S. DORAVARI,<sup>80</sup> O. DOROSH,<sup>187</sup> W. J. D. DOYLE,<sup>123</sup> M. DRAGO,<sup>39,38</sup> J. C. DRIGGERS,<sup>2</sup> L. DUNN,<sup>124</sup>  
 2030 U. DUPLETSA,<sup>44</sup> P.-A. DUVERNE,<sup>20</sup> D. D'URSO,<sup>171,156</sup> P. DUTTA ROY,<sup>46</sup> H. DUVAL,<sup>188</sup> S. E. DWYER,<sup>2</sup> C. EASSA,<sup>2</sup> W. EAST,<sup>183</sup>  
 2031 M. EBERSOLD,<sup>189,31</sup> T. ECKHARDT,<sup>98</sup> G. EDDOLLS,<sup>79</sup> A. EFFLER,<sup>64</sup> J. EICHHOLZ,<sup>34</sup> H. EINSLE,<sup>115</sup> M. EISENMANN,<sup>25</sup> M. EMMA,<sup>59</sup>  
 2032 K. ENDO,<sup>152</sup> R. ENFICIAUD,<sup>1</sup> L. ERRICO,<sup>32,4</sup> R. ESPINOSA,<sup>165</sup> M. ESPOSITO,<sup>4,32</sup> R. C. ESSICK,<sup>190</sup> H. ESTELLÉS,<sup>1</sup> T. ETZEL,<sup>11</sup>  
 2033 M. EVANS,<sup>35</sup> T. EVSTAFYEVA,<sup>183</sup> B. E. EWING,<sup>7</sup> J. M. EZQUIAGA,<sup>140</sup> F. FABRIZI,<sup>61,62</sup> V. FAFONE,<sup>21,22</sup> S. FAIRHURST,<sup>33</sup>

- 2034 A. M. FARAH,<sup>130</sup> B. FARR,<sup>78</sup> W. M. FARR,<sup>191,192</sup> G. FAVARO,<sup>92</sup> M. FAVATA,<sup>193</sup> M. FAYS,<sup>166</sup> M. FAZIO,<sup>55</sup> J. FEICHT,<sup>11</sup> M. M. FEJER,<sup>90</sup>  
 2035 R. FELICETTI,<sup>185,48</sup> E. FENYVESI,<sup>88,194</sup> J. FERNANDES,<sup>195</sup> T. FERNANDES,<sup>196,138</sup> D. FERNANDO,<sup>112</sup> S. FERRAIUOLO,<sup>197,39,38</sup>  
 2036 T. A. FERREIRA,<sup>12</sup> F. FIDECARO,<sup>82,81</sup> A. FIENGA,<sup>115</sup> P. FIGURA,<sup>96</sup> A. FIORI,<sup>81,82</sup> I. FIORI,<sup>63</sup> M. FISHBACH,<sup>190</sup> R. P. FISHER,<sup>123</sup>  
 2037 R. FITTIPALDI,<sup>198,132</sup> V. FIUMARA,<sup>199,132</sup> R. FLAMINIO,<sup>31</sup> S. M. FLEISCHER,<sup>200</sup> L. S. FLEMING,<sup>201</sup> E. FLODEN,<sup>18</sup> H. FONG,<sup>116</sup>  
 2038 J. A. FONT,<sup>138,139</sup> F. FONTINELE-NUNES,<sup>18</sup> C. FOO,<sup>1</sup> B. FORNAL,<sup>202</sup> K. FRANCESCHETTI,<sup>179</sup> F. FRAPPEZ,<sup>31</sup> S. FRASCA,<sup>39,38</sup>  
 2039 F. FRASCONI,<sup>81</sup> J. P. FREED,<sup>66</sup> Z. FREI,<sup>203</sup> A. FREISE,<sup>37,109</sup> O. FREITAS,<sup>196,138</sup> R. FREY,<sup>78</sup> W. FRISCHHERTZ,<sup>64</sup> P. FRITSCHEL,<sup>35</sup>  
 2040 V. V. FROLOV,<sup>64</sup> G. G. FRONZÉ,<sup>28</sup> M. FUENTES-GARCIA,<sup>11</sup> S. FUJII,<sup>204</sup> T. FUJIMORI,<sup>205</sup> P. FULDA,<sup>46</sup> M. FYFFE,<sup>64</sup> B. GADRE,<sup>72</sup>  
 2041 J. R. GAIR,<sup>1</sup> S. GALAUDAGE,<sup>186</sup> V. GALDI,<sup>206</sup> R. GAMBA,<sup>7</sup> A. GAMBOA,<sup>1</sup> S. GAMOJI,<sup>181</sup> D. GANAPATHY,<sup>207</sup> A. GANGULY,<sup>80</sup>  
 2042 B. GARAVENTA,<sup>29</sup> J. GARCÍA-BELLIDO,<sup>208</sup> C. GARCÍA-QUIRÓS,<sup>189</sup> J. W. GARDNER,<sup>34</sup> K. A. GARDNER,<sup>116</sup> S. GARG,<sup>42</sup>  
 2043 J. GARGIULO,<sup>63</sup> X. GARRIDO,<sup>41</sup> A. GARRON,<sup>99</sup> F. GARUFI,<sup>32,4</sup> P. A. GARVER,<sup>90</sup> C. GASBARRA,<sup>21,22</sup> B. GATELEY,<sup>2</sup> F. GAUTIER,<sup>209</sup>  
 2044 V. GAYATHRI,<sup>10</sup> T. GAYER,<sup>79</sup> G. GEMME,<sup>29</sup> A. GENNAI,<sup>81</sup> V. GENNARI,<sup>101</sup> J. GEORGE,<sup>105</sup> R. GEORGE,<sup>148</sup> O. GERBERDING,<sup>98</sup>  
 2045 L. GERGELY,<sup>154</sup> ARCHISMAN GHOSH,<sup>95</sup> SAYANTAN GHOSH,<sup>195</sup> SHAON GHOSH,<sup>193</sup> SHROBANA GHOSH,<sup>8,9</sup> SUPROVO GHOSH,<sup>210</sup>  
 2046 TATHAGATA GHOSH,<sup>80</sup> J. A. GIAIME,<sup>12,64</sup> K. D. GIARDINA,<sup>64</sup> D. R. GIBSON,<sup>201</sup> C. GIER,<sup>55</sup> S. GKAITATZIS,<sup>82,81</sup> J. GLANZER,<sup>11</sup>  
 2047 F. GLOTIN,<sup>41</sup> J. GODFREY,<sup>78</sup> R. V. GODLEY,<sup>8,9</sup> P. GODWIN,<sup>11</sup> A. S. GOETTEL,<sup>33</sup> E. GOETZ,<sup>116</sup> J. GOLOMB,<sup>11</sup> S. GOMEZ LOPEZ,<sup>39,38</sup>  
 2048 B. GONCHAROV,<sup>44</sup> G. GONZÁLEZ,<sup>12</sup> P. GOODARZI,<sup>211</sup> S. GOODE,<sup>15</sup> A. W. GOODWIN-JONES,<sup>15</sup> M. GOSELIN,<sup>63</sup> R. GOUATY,<sup>31</sup>  
 2049 D. W. GOULD,<sup>34</sup> K. GOVORKOVA,<sup>35</sup> A. GRADO,<sup>77,51</sup> V. GRAHAM,<sup>87</sup> A. E. GRANADOS,<sup>18</sup> M. GRANATA,<sup>176</sup> V. GRANATA,<sup>212,132</sup>  
 2050 S. GRAS,<sup>35</sup> P. GRASSIA,<sup>11</sup> J. GRAVES,<sup>57</sup> C. GRAY,<sup>2</sup> R. GRAY,<sup>87</sup> G. GRECO,<sup>51</sup> A. C. GREEN,<sup>37,109</sup> L. GREEN,<sup>213</sup> S. M. GREEN,<sup>74</sup>  
 2051 S. R. GREEN,<sup>214</sup> C. GREENBERG,<sup>133</sup> A. M. GRETARSSON,<sup>66</sup> H. K. GRIFFIN,<sup>18</sup> D. GRIFFITH,<sup>11</sup> H. L. GRIGGS,<sup>57</sup> G. GRIGNANI,<sup>77,51</sup>  
 2052 C. GRIMAUD,<sup>31</sup> H. GROTE,<sup>33</sup> S. GRUNEWALD,<sup>1</sup> D. GUERRA,<sup>138</sup> D. GUETTA,<sup>215</sup> G. M. GUIDI,<sup>61,62</sup> A. R. GUIMARAES,<sup>12</sup>  
 2053 H. K. GULATI,<sup>94</sup> F. GULMINELLI,<sup>173,174</sup> H. GUO,<sup>145</sup> W. GUO,<sup>73</sup> Y. GUO,<sup>37,36</sup> ANURADHA GUPTA,<sup>216</sup> I. GUPTA,<sup>7</sup> N. C. GUPTA,<sup>94</sup>  
 2054 S. K. GUPTA,<sup>46</sup> V. GUPTA,<sup>18</sup> N. GUPTA,<sup>1</sup> J. GURS,<sup>98</sup> N. GUTIERREZ,<sup>176</sup> N. GUTTMAN,<sup>6</sup> F. GUZMAN,<sup>131</sup> D. HABA,<sup>217</sup>  
 2055 M. HABERLAND,<sup>1</sup> S. HAINO,<sup>218</sup> E. D. HALL,<sup>35</sup> E. Z. HAMILTON,<sup>99</sup> G. HAMMOND,<sup>87</sup> M. HANEY,<sup>37</sup> J. HANKS,<sup>2</sup> C. HANNA,<sup>7</sup>  
 2056 M. D. HANNAM,<sup>33</sup> O. A. HANNUKSELA,<sup>219</sup> A. G. HANSELMAN,<sup>130</sup> H. HANSEN,<sup>2</sup> J. HANSON,<sup>64</sup> S. HANUMASAGAR,<sup>57</sup> R. HARADA,<sup>42</sup>  
 2057 A. R. HARDISON,<sup>182</sup> S. HARIKUMAR,<sup>187</sup> K. HARIS,<sup>37,72</sup> I. HARLEY-TROCHIMCZYK,<sup>131</sup> T. HARMARK,<sup>134</sup> J. HARMS,<sup>44,45</sup>  
 2058 G. M. HARRY,<sup>220</sup> I. W. HARRY,<sup>74</sup> J. HART,<sup>106</sup> B. HASKELL,<sup>96,221,222</sup> C.-J. HASTER,<sup>213</sup> K. HAUGHIAN,<sup>87</sup> H. HAYAKAWA,<sup>50</sup>  
 2059 K. HAYAMA,<sup>223</sup> M. C. HEINTZE,<sup>64</sup> J. HEINZE,<sup>104</sup> J. HEINZEL,<sup>35</sup> H. HEITMANN,<sup>115</sup> F. HELLMAN,<sup>207</sup> A. F. HELMLING-CORNELL,<sup>78</sup>  
 2060 G. HEMMING,<sup>63</sup> O. HENDERSON-SAPIR,<sup>117</sup> M. HENDRY,<sup>87</sup> I. S. HENG,<sup>87</sup> M. H. HENNIG,<sup>87</sup> C. HENSHAW,<sup>57</sup> M. HEURS,<sup>8,9</sup>  
 2061 A. L. HEWITT,<sup>224,225</sup> J. HEYNEN,<sup>15</sup> J. HEYNS,<sup>35</sup> S. HIGGINBOTHAM,<sup>33</sup> S. HILD,<sup>36,37</sup> S. HILL,<sup>87</sup> Y. HIMEMOTO,<sup>226</sup> N. HIRATA,<sup>25</sup>  
 2062 C. HIROSE,<sup>227</sup> D. HOFMAN,<sup>176</sup> B. E. HOGAN,<sup>66</sup> N. A. HOLLAND,<sup>37,109</sup> K. HOLLEY-BOCKELMANN,<sup>144</sup> I. J. HOLLOWES,<sup>175</sup>  
 2063 D. E. HOLZ,<sup>130</sup> L. HONET,<sup>113</sup> D. J. HORTON-BAILEY,<sup>207</sup> J. HOUGH,<sup>87</sup> S. HOURIHANE,<sup>11</sup> N. T. HOWARD,<sup>144</sup> E. J. HOWELL,<sup>73</sup>  
 2064 C. G. HOY,<sup>74</sup> C. A. HRISHIKESH,<sup>21</sup> P. HSI,<sup>35</sup> H.-F. HSIEH,<sup>142</sup> H.-Y. HSIEH,<sup>142</sup> C. HSIUNG,<sup>228</sup> S.-H. HSU,<sup>146</sup> W.-F. HSU,<sup>111</sup> Q. HU,<sup>87</sup>  
 2065 H. Y. HUANG,<sup>141</sup> Y. HUANG,<sup>7</sup> Y. T. HUANG,<sup>79</sup> A. D. HUDDART,<sup>229</sup> B. HUGHEY,<sup>66</sup> V. HUI,<sup>31</sup> S. HUSA,<sup>99</sup> R. HUXFORD,<sup>7</sup>  
 2066 L. IAMPIERI,<sup>39,38</sup> G. A. IANDOLO,<sup>36</sup> M. IANNI,<sup>22,21</sup> G. IANNONE,<sup>132</sup> J. IASCAU,<sup>78</sup> K. IDE,<sup>230</sup> R. IDEN,<sup>217</sup> A. IERARDI,<sup>44,45</sup>  
 2067 S. IKEDA,<sup>147</sup> H. IMAFUKU,<sup>42</sup> Y. INOUE,<sup>141</sup> G. IORIO,<sup>92</sup> P. IOSIF,<sup>185,48</sup> M. H. IQBAL,<sup>34</sup> J. IRWIN,<sup>87</sup> R. ISHIKAWA,<sup>230</sup> M. ISI,<sup>191,192</sup>  
 2068 K. S. ISLEIF,<sup>231</sup> Y. ITOH,<sup>205,232</sup> M. IWAYA,<sup>204</sup> B. R. IYER,<sup>24</sup> C. JACQUET,<sup>101</sup> P.-E. JACQUET,<sup>122</sup> T. JACQUOT,<sup>41</sup> S. J. JADHAV,<sup>233</sup>  
 2069 S. P. JADHAV,<sup>155</sup> M. JAIN,<sup>133</sup> T. JAIN,<sup>224</sup> A. L. JAMES,<sup>11</sup> K. JANI,<sup>144</sup> J. JANQUART,<sup>15</sup> N. N. JANTHALUR,<sup>233</sup> S. JARABA,<sup>234</sup>  
 2070 P. JARANOWSKI,<sup>235</sup> R. JAUME,<sup>99</sup> W. JAVED,<sup>33</sup> A. JENNINGS,<sup>2</sup> M. JENSEN,<sup>2</sup> W. JIA,<sup>35</sup> J. JIANG,<sup>150</sup> H.-B. JIN,<sup>236,237</sup> G. R. JOHNS,<sup>123</sup>  
 2071 N. A. JOHNSON,<sup>46</sup> N. K. JOHNSON-MCDANIEL,<sup>216</sup> M. C. JOHNSTON,<sup>213</sup> R. JOHNSTON,<sup>87</sup> N. JOHNY,<sup>8,9</sup> D. H. JONES,<sup>34</sup> D. I. JONES,<sup>210</sup>  
 2072 R. JONES,<sup>87</sup> H. E. JOSE,<sup>78</sup> P. JOSHI,<sup>7</sup> S. K. JOSHI,<sup>80</sup> G. JOUBERT,<sup>56</sup> J. JU,<sup>238</sup> L. JU,<sup>73</sup> K. JUNG,<sup>239</sup> J. JUNKER,<sup>34</sup> V. JUSTE,<sup>113</sup>  
 2073 H. B. KABAGOSY,<sup>64,35</sup> T. KAJITA,<sup>240</sup> I. KAKU,<sup>205</sup> V. KALOGERA,<sup>97</sup> M. KALOMENPOULOS,<sup>213</sup> M. KAMIIZUMI,<sup>50</sup> N. KANDA,<sup>232,205</sup>  
 2074 S. KANDHASAMY,<sup>80</sup> G. KANG,<sup>241</sup> N. C. KANNACHEL,<sup>6</sup> J. B. KANNER,<sup>11</sup> S. A. KANTI MAHANTY,<sup>18</sup> S. J. KAPADIA,<sup>80</sup> D. P. KAPASI,<sup>54</sup>  
 2075 M. KARTHIKEYAN,<sup>133</sup> M. KASPRZACK,<sup>11</sup> H. KATO,<sup>152</sup> T. KATO,<sup>204</sup> E. KATSAVOUNIDIS,<sup>35</sup> W. KATZMAN,<sup>64</sup> R. KAUSHIK,<sup>105</sup>  
 2076 K. KAWABE,<sup>2</sup> R. KAWAMOTO,<sup>205</sup> D. KEITEL,<sup>99</sup> L. J. KEMPERMAN,<sup>117</sup> J. KENNINGTON,<sup>7</sup> F. A. KERKOW,<sup>18</sup> R. KESHARWANI,<sup>80</sup>  
 2077 J. S. KEY,<sup>242</sup> R. KHADELA,<sup>8,9</sup> S. KHADKA,<sup>90</sup> S. S. KHADKIKAR,<sup>7</sup> F. Y. KHALILI,<sup>110</sup> F. KHAN,<sup>8,9</sup> T. KHANAM,<sup>163</sup> M. KHURSHEED,<sup>105</sup>  
 2078 N. M. KHUSID,<sup>191,192</sup> W. KIENDREBEOGO,<sup>115,243</sup> N. KIJUNCHOO,<sup>117</sup> C. KIM,<sup>244</sup> J. C. KIM,<sup>245</sup> K. KIM,<sup>246</sup> M. H. KIM,<sup>238</sup> S. KIM,<sup>247</sup>  
 2079 Y.-M. KIM,<sup>246</sup> C. KIMBALL,<sup>97</sup> K. KIMES,<sup>54</sup> M. KINNEAR,<sup>33</sup> J. S. KISSEL,<sup>2</sup> S. KLIMENKO,<sup>46</sup> A. M. KNEE,<sup>116</sup> E. J. KNOX,<sup>78</sup>  
 2080 N. KNUST,<sup>8,9</sup> K. KOBAYASHI,<sup>204</sup> S. M. KOEHLNBECK,<sup>90</sup> G. KOEKOEK,<sup>37,36</sup> K. KOHRI,<sup>248,249</sup> K. KOKEYAMA,<sup>33,250</sup> S. KOLEY,<sup>44,166</sup>  
 2081 P. KOLITSIDOU,<sup>104</sup> A. E. KOLONIARI,<sup>251</sup> K. KOMORI,<sup>42</sup> A. K. H. KONG,<sup>142</sup> A. KONTOS,<sup>252</sup> L. M. KOPONEN,<sup>104</sup> M. KOROBKO,<sup>98</sup>  
 2082 X. KOU,<sup>18</sup> A. KOUSHIK,<sup>23</sup> N. KOUVATOS,<sup>68</sup> M. KOVALAM,<sup>73</sup> T. KOYAMA,<sup>152</sup> D. B. KOZAK,<sup>11</sup> S. L. KRANZHOF, <sup>36,37</sup> V. KRINGEL,<sup>8,9</sup>  
 2083 N. V. KRISHNENDU,<sup>104</sup> S. KROKER,<sup>253</sup> A. KRÓLAK,<sup>254,187</sup> K. KRUSKA,<sup>8,9</sup> J. KUBISZ,<sup>255</sup> G. KUEHN,<sup>8,9</sup> S. KULKARNI,<sup>216</sup>  
 2084 A. KULUR RAMAMOHAN,<sup>34</sup> ACHAL KUMAR,<sup>46</sup> ANIL KUMAR,<sup>233</sup> PRAVEEN KUMAR,<sup>178</sup> PRAYUSH KUMAR,<sup>24</sup> RAHUL KUMAR,<sup>2</sup>  
 2085 RAKESH KUMAR,<sup>94</sup> J. KUME,<sup>256,257,42</sup> K. KUNS,<sup>35</sup> N. KUNTIMADDI,<sup>33</sup> S. KUROYANAGI,<sup>208,258</sup> S. KUWAHARA,<sup>42</sup> K. KWAK,<sup>239</sup>  
 2086 K. KWAN,<sup>34</sup> S. KWON,<sup>42</sup> G. LACAILLE,<sup>87</sup> D. LAGHI,<sup>189,101</sup> A. H. LAITY,<sup>164</sup> E. LALANDE,<sup>259</sup> M. LALLEMAN,<sup>23</sup> P. C. LALREMUATI,<sup>260</sup>  
 2087 M. LANDRY,<sup>2</sup> B. B. LANE,<sup>35</sup> R. N. LANG,<sup>35</sup> J. LANGE,<sup>148</sup> R. LANGGIN,<sup>213</sup> B. LANTZ,<sup>90</sup> I. LA ROSA,<sup>99</sup> J. LARSEN,<sup>200</sup>  
 2088 A. LARTAUD-VOLLARD,<sup>41</sup> P. D. LASKY,<sup>6</sup> J. LAWRENCE,<sup>165</sup> M. LAXEN,<sup>64</sup> C. LAZARTE,<sup>138</sup> A. LAZZARINI,<sup>11</sup> C. LAZZARO,<sup>157,156</sup>  
 2089 P. LEACI,<sup>39,38</sup> L. LEALI,<sup>18</sup> Y. K. LECOEUCE,<sup>116</sup> H. M. LEE,<sup>261</sup> H. W. LEE,<sup>262</sup> J. LEE,<sup>79</sup> K. LEE,<sup>238</sup> R.-K. LEE,<sup>142</sup> R. LEE,<sup>35</sup>  
 2090 SUNGHO LEE,<sup>246</sup> SUNJAE LEE,<sup>238</sup> Y. LEE,<sup>141</sup> I. N. LEGRED,<sup>11</sup> J. LEHMANN,<sup>8,9</sup> L. LEHNER,<sup>183</sup> M. LE JEAN,<sup>176,118</sup> A. LEMAÎTRE,<sup>263</sup>  
 2091 M. LENTI,<sup>62,177</sup> M. LEONARDI,<sup>75,76,264</sup> M. LEQUIME,<sup>40</sup> N. LEROY,<sup>41</sup> M. LESOVSKY,<sup>11</sup> N. LETENDRE,<sup>31</sup> M. LETHUILLIER,<sup>56</sup>  
 2092 Y. LEVIN,<sup>6</sup> K. LEYDE,<sup>74</sup> A. K. Y. LI,<sup>11</sup> K. L. LI,<sup>265</sup> T. G. F. LI,<sup>111</sup> X. LI,<sup>149</sup> Y. LI,<sup>97</sup> Z. LI,<sup>87</sup> A. LIHOS,<sup>123</sup> E. T. LIN,<sup>142</sup> F. LIN,<sup>141</sup>  
 2093 L. C.-C. LIN,<sup>265</sup> Y.-C. LIN,<sup>142</sup> C. LINDSAY,<sup>201</sup> S. D. LINKER,<sup>181</sup> A. LIU,<sup>219</sup> G. C. LIU,<sup>228</sup> JIAN LIU,<sup>73</sup> F. LLAMAS VILLARREAL,<sup>165</sup>  
 2094 J. LLOBERA-QUEROL,<sup>99</sup> R. K. L. LO,<sup>140</sup> J.-P. LOCQUET,<sup>111</sup> S. C. G. LOGGINS,<sup>266</sup> M. R. LOIZOU,<sup>133</sup> L. T. LONDON,<sup>68</sup> A. LONGO,<sup>61,62</sup>  
 2095 D. LOPEZ,<sup>166</sup> M. LOPEZ PORTILLA,<sup>72</sup> M. LORENZINI,<sup>21,22</sup> A. LORENZO-MEDINA,<sup>178</sup> V. LORIETTE,<sup>41</sup> M. LORMAND,<sup>64</sup>  
 2096 G. LOSURDO,<sup>267,81</sup> E. LOTTI,<sup>133</sup> T. P. LOTT IV,<sup>57</sup> J. D. LOUGH,<sup>8,9</sup> H. A. LOUGHLIN,<sup>35</sup> C. O. LOUSTO,<sup>112</sup> N. LOW,<sup>124</sup> N. LU,<sup>34</sup>  
 2097 L. LUCCHESI,<sup>81</sup> H. LÜCK,<sup>9,8,9</sup> D. LUMACA,<sup>22</sup> A. P. LUNDGREN,<sup>268,269</sup> A. W. LUSSIER,<sup>259</sup> R. MACAS,<sup>74</sup> M. MACINNIS,<sup>35</sup>

- 2098 D. M. MACLEOD,<sup>33</sup> I. A. O. MACMILLAN,<sup>11</sup> A. MACQUET,<sup>41</sup> K. MAEDA,<sup>152</sup> S. MAENAUT,<sup>111</sup> S. S. MAGARE,<sup>80</sup> R. M. MAGEE,<sup>11</sup>  
2099 E. MAGGIO,<sup>1</sup> R. MAGGIORE,<sup>37,109</sup> M. MAGNOZZI,<sup>29,30</sup> P. MAHAPATRA,<sup>33</sup> M. MAHESH,<sup>98</sup> Y. MAIMON,<sup>114</sup> M. MAINI,<sup>164</sup> S. MAJHI,<sup>80</sup>  
2100 E. MAJORANA,<sup>39,38</sup> C. N. MAKAREM,<sup>11</sup> D. MALAKAR,<sup>107</sup> J. A. MALAQUIAS-REIS,<sup>19</sup> U. MALI,<sup>190</sup> S. MALIAKAL,<sup>11</sup> A. MALIK,<sup>105</sup>  
2101 L. MALLICK,<sup>169,190</sup> A.-K. MALZ,<sup>59</sup> N. MAN,<sup>115</sup> M. MANCARELLA,<sup>100</sup> V. MANDIC,<sup>18</sup> V. MANGANO,<sup>171,156</sup> B. MANNIX,<sup>78</sup>  
2102 G. L. MANSELL,<sup>79</sup> M. MANSKE,<sup>10</sup> M. MANTOVANI,<sup>63</sup> M. MAPELLI,<sup>92,93,270</sup> C. MARINELLI,<sup>102</sup> F. MARION,<sup>31</sup> A. S. MARKOSYAN,<sup>90</sup>  
2103 A. MARKOWITZ,<sup>11</sup> E. MAROS,<sup>11</sup> S. MARSAT,<sup>101</sup> F. MARTELLI,<sup>61,62</sup> I. W. MARTIN,<sup>87</sup> R. M. MARTIN,<sup>193</sup> B. B. MARTINEZ,<sup>131</sup>  
2104 D. A. MARTINEZ,<sup>54</sup> M. MARTINEZ,<sup>43,271</sup> V. MARTINEZ,<sup>129</sup> A. MARTINI,<sup>75,76</sup> J. C. MARTINS,<sup>19</sup> D. V. MARTYNOV,<sup>104</sup> E. J. MARX,<sup>35</sup>  
2105 L. MASSARO,<sup>36,37</sup> A. MASSEROT,<sup>31</sup> M. MASSO-REID,<sup>87</sup> S. MASTROGIOVANNI,<sup>38</sup> T. MATCOVICH,<sup>51</sup> M. MATIUSHECHKINA,<sup>8,9</sup>  
2106 L. MAURIN,<sup>209</sup> N. MAVALVALA,<sup>35</sup> N. MAXWELL,<sup>2</sup> G. MCCARROL,<sup>64</sup> R. MCCARTHY,<sup>2</sup> D. E. MCCLELLAND,<sup>34</sup> S. MCCORMICK,<sup>64</sup>  
2107 L. MCCULLER,<sup>11</sup> S. MCEACHIN,<sup>123</sup> C. MCELHENNY,<sup>123</sup> G. I. MCGHEE,<sup>87</sup> K. B. M. MCGOWAN,<sup>144</sup> J. MCIVER,<sup>116</sup> A. MCLEOD,<sup>73</sup>  
2108 I. MCMAHON,<sup>189</sup> T. MCRAE,<sup>34</sup> R. MCTEAGUE,<sup>87</sup> D. MEACHER,<sup>10</sup> B. N. MEAGHER,<sup>79</sup> R. MECHUM,<sup>112</sup> Q. MEIJER,<sup>72</sup> A. MELATOS,<sup>124</sup>  
2109 C. S. MENONI,<sup>137</sup> F. MERA,<sup>2</sup> R. A. MERCER,<sup>10</sup> L. MERENI,<sup>176</sup> K. MERFELD,<sup>163</sup> E. L. MERILH,<sup>64</sup> J. R. MÉROU,<sup>99</sup> J. D. MERRITT,<sup>78</sup>  
2110 M. MERZOUGUI,<sup>115</sup> C. MESSICK,<sup>10</sup> B. MESTICHELLI,<sup>44</sup> M. MEYER-CONDE,<sup>272</sup> F. MEYLAHN,<sup>8,9</sup> A. MHASKE,<sup>80</sup> A. MIANI,<sup>75,76</sup>  
2111 H. MIAO,<sup>273</sup> C. MICHEL,<sup>176</sup> Y. MICHIMURA,<sup>42</sup> H. MIDDLETON,<sup>104</sup> D. P. MIHAYLOV,<sup>106</sup> S. J. MILLER,<sup>11</sup> M. MILLHOUSE,<sup>57</sup>  
2112 E. MILOTTI,<sup>185,48</sup> V. MILOTTI,<sup>92</sup> Y. MINENKOV,<sup>22</sup> E. M. MINIHAN,<sup>66</sup> L. M. MIR,<sup>43</sup> L. MIRASOLA,<sup>156,157</sup> M. MIRAVET-TENÉS,<sup>138</sup>  
2113 C.-A. MIRITESCU,<sup>43</sup> A. MISHRA,<sup>24</sup> C. MISHRA,<sup>108</sup> T. MISHRA,<sup>46</sup> A. L. MITCHELL,<sup>37,109</sup> J. G. MITCHELL,<sup>66</sup> S. MITRA,<sup>80</sup>  
2114 V. P. MITROFANOV,<sup>110</sup> K. MITSUHASHI,<sup>25</sup> R. MITTLEMAN,<sup>35</sup> O. MIYAKAWA,<sup>50</sup> S. MIYOKI,<sup>50</sup> A. MIYOKO,<sup>66</sup> G. MO,<sup>35</sup>  
2115 L. MOBILIA,<sup>61,62</sup> S. MOHAN S.,<sup>274</sup> S. R. P. MOHAPATRA,<sup>11</sup> S. R. MOHITE,<sup>7</sup> M. MOLINA-RUIZ,<sup>207</sup> M. MONDIN,<sup>181</sup> M. MONTANI,<sup>61,62</sup>  
2116 C. J. MOORE,<sup>224</sup> D. MORARU,<sup>2</sup> A. MORE,<sup>80</sup> S. MORE,<sup>80</sup> C. MORENO,<sup>135</sup> E. A. MORENO,<sup>35</sup> G. MORENO,<sup>2</sup> A. MORESO SERRA,<sup>83</sup>  
2117 S. MORISAKI,<sup>42,204</sup> Y. MORIWAKI,<sup>152</sup> G. MORRAS,<sup>208</sup> A. MOSCATELLO,<sup>92</sup> M. MOULD,<sup>35</sup> B. MOURS,<sup>65</sup> C. M. MOW-LOWRY,<sup>37,109</sup>  
2118 L. MUCCILLO,<sup>177,62</sup> F. MUCIACCA,<sup>39,38</sup> D. MUKHERJEE,<sup>104</sup> SAMANWAYA MUKHERJEE,<sup>24</sup> SOMA MUKHERJEE,<sup>165</sup>  
2119 SUBROTO MUKHERJEE,<sup>94</sup> SUVODIP MUKHERJEE,<sup>13</sup> N. MUKUND,<sup>35</sup> A. MULLAVEY,<sup>64</sup> H. MULLOCK,<sup>116</sup> J. MUNDI,<sup>220</sup>  
2120 C. L. MUNGIOLI,<sup>73</sup> M. MURAKOSHI,<sup>230</sup> P. G. MURRAY,<sup>87</sup> D. NABARI,<sup>75,76</sup> S. L. NADJI,<sup>8,9</sup> A. NAGAR,<sup>28,275</sup> N. NAGARAJAN,<sup>87</sup>  
2121 K. NAKAGAKI,<sup>50</sup> K. NAKAMURA,<sup>25</sup> H. NAKANO,<sup>276</sup> M. NAKANO,<sup>11</sup> D. NANADOUNGAR-LACROZE,<sup>43</sup> D. NANDI,<sup>12</sup> V. NAPOLANO,<sup>63</sup>  
2122 P. NARAYAN,<sup>216</sup> I. NARDECCHIA,<sup>22</sup> T. NARIKAWA,<sup>204</sup> H. NAROLA,<sup>72</sup> L. NATICCHIONI,<sup>38</sup> R. K. NAYAK,<sup>260</sup> L. NEGRI,<sup>72</sup> A. NELA,<sup>87</sup>  
2123 C. NELLE,<sup>78</sup> A. NELSON,<sup>131</sup> T. J. N. NELSON,<sup>64</sup> M. NERY,<sup>8,9</sup> A. NEUNZERT,<sup>2</sup> S. NG,<sup>54</sup> L. NGUYEN QUYNH,<sup>277</sup> S. A. NICHOLS,<sup>12</sup>  
2124 A. B. NIELSEN,<sup>278</sup> Y. NISHINO,<sup>25,42</sup> A. NISHIZAWA,<sup>279</sup> S. NISSANKE,<sup>280,37</sup> W. NIU,<sup>7</sup> F. NOCERA,<sup>63</sup> J. NOLLER,<sup>281</sup> M. NORMAN,<sup>33</sup>  
2125 C. NORTH,<sup>33</sup> J. NOVAK,<sup>118,234,282</sup> R. NOWICKI,<sup>144</sup> J. F. NUÑO SILES,<sup>208</sup> L. K. NUTTALL,<sup>74</sup> K. OBAYASHI,<sup>230</sup> J. OBERLING,<sup>2</sup>  
2126 J. O'DELL,<sup>229</sup> E. OELKER,<sup>35</sup> M. OERTEL,<sup>234,118,283,282</sup> G. OGANESYAN,<sup>44,45</sup> T. O'HANLON,<sup>64</sup> M. OHASHI,<sup>50</sup> F. OHME,<sup>8,9</sup>  
2127 R. OLIVERI,<sup>118,283,282</sup> R. OMER,<sup>18</sup> B. O'NEAL,<sup>123</sup> M. ONISHI,<sup>152</sup> K. OOHARA,<sup>284</sup> B. O'REILLY,<sup>64</sup> M. ORSELLI,<sup>51,77</sup>  
2128 R. O'SHAUGHNESSY,<sup>112</sup> S. O'SHEA,<sup>87</sup> S. OSHINO,<sup>50</sup> C. OSTHELDER,<sup>11</sup> I. OTA,<sup>12</sup> D. J. OTTAWAY,<sup>117</sup> A. OUZRIAT,<sup>56</sup> H. OVERMIER,<sup>64</sup>  
2129 B. J. OWEN,<sup>285</sup> R. OZAKI,<sup>230</sup> A. E. PACE,<sup>7</sup> R. PAGANO,<sup>12</sup> M. A. PAGE,<sup>25</sup> A. PAI,<sup>195</sup> L. PAIELLA,<sup>44</sup> A. PAL,<sup>286</sup> S. PAL,<sup>260</sup>  
2130 M. A. PALAIA,<sup>81,82</sup> M. PÁLFI,<sup>203</sup> P. P. PALMA,<sup>39,21,22</sup> C. PALOMBA,<sup>38</sup> P. PALUD,<sup>20</sup> H. PAN,<sup>142</sup> J. PAN,<sup>73</sup> K. C. PAN,<sup>142</sup> P. K. PANDA,<sup>233</sup>  
2131 SHIKSHA PANDEY,<sup>7</sup> SWADHA PANDEY,<sup>35</sup> P. T. H. PANG,<sup>37,72</sup> F. PANNARALE,<sup>39,38</sup> K. A. PANNONE,<sup>54</sup> B. C. PANT,<sup>105</sup> F. H. PANTHER,<sup>73</sup>  
2132 M. PANZERI,<sup>61,62</sup> F. PAOLETTI,<sup>81</sup> A. PAOLONE,<sup>38,287</sup> A. PAPADOPOULOS,<sup>87</sup> E. E. PAPALEXAKIS,<sup>211</sup> L. PAPALINI,<sup>81,82</sup>  
2133 G. PAPIGIOTIS,<sup>251</sup> A. PAQUIS,<sup>41</sup> A. PARISI,<sup>77,51</sup> B.-J. PARK,<sup>246</sup> J. PARK,<sup>288</sup> W. PARKER,<sup>64</sup> G. PASCALE,<sup>8,9</sup> D. PASCUCCI,<sup>95</sup>  
2134 A. PASQUALETTI,<sup>63</sup> R. PASSAQUIETI,<sup>82,81</sup> L. PASSENGER,<sup>6</sup> D. PASSUELLO,<sup>81</sup> O. PATANE,<sup>2</sup> A. V. PATEL,<sup>141</sup> D. PATHAK,<sup>80</sup> A. PATRA,<sup>33</sup>  
2135 B. PATRICELLI,<sup>82,81</sup> B. G. PATTERSON,<sup>33</sup> K. PAUL,<sup>108</sup> S. PAUL,<sup>78</sup> E. PAYNE,<sup>11</sup> T. PEARCE,<sup>33</sup> M. PEDRAZA,<sup>11</sup> A. PELE,<sup>11</sup>  
2136 F. E. PEÑA ARELLANO,<sup>289</sup> X. PENG,<sup>104</sup> Y. PENG,<sup>57</sup> S. PENN,<sup>290</sup> M. D. PENULIAR,<sup>54</sup> A. PEREGO,<sup>75,76</sup> Z. PEREIRA,<sup>133</sup>  
2137 C. PÉRIGOS,<sup>291,93,92</sup> G. PERNA,<sup>92</sup> A. PERRECA,<sup>39,76,44</sup> J. PERRET,<sup>20</sup> S. PERRIÉS,<sup>56</sup> J. W. PERRY,<sup>37,109</sup> D. PESIOS,<sup>251</sup> S. PETERS,<sup>166</sup>  
2138 S. PETRACCA,<sup>206</sup> C. PETRILLO,<sup>77</sup> H. P. PFEIFFER,<sup>1</sup> H. PHAM,<sup>64</sup> K. A. PHAM,<sup>18</sup> K. S. PHUKON,<sup>104</sup> H. PHURAILATPAM,<sup>219</sup>  
2139 M. PIARULLI,<sup>101</sup> L. PICCARI,<sup>39,38</sup> O. J. PICCINI,<sup>34</sup> M. PICHOT,<sup>115</sup> M. PIENDIBENE,<sup>82,81</sup> F. PIERGIOVANNI,<sup>61,62</sup> L. PIERINI,<sup>38</sup>  
2140 G. PIERRA,<sup>38</sup> V. PIERRO,<sup>292,132</sup> M. PIETRZAK,<sup>96</sup> M. PILLAS,<sup>166</sup> F. PILO,<sup>81</sup> L. PINARD,<sup>176</sup> I. M. PINTO,<sup>292,132,293,32</sup> M. PINTO,<sup>63</sup>  
2141 B. J. PIOTRZKOWSKI,<sup>10</sup> M. PIRELLO,<sup>2</sup> M. D. PITKIN,<sup>224,87</sup> A. PLACIDI,<sup>51</sup> E. PLACIDI,<sup>39,38</sup> M. L. PLANAS,<sup>99</sup> W. PLASTINO,<sup>212,22</sup>  
2142 C. PLUNKETT,<sup>35</sup> R. POGGIANI,<sup>82,81</sup> E. POLINI,<sup>35</sup> J. POMPER,<sup>81,82</sup> L. POMPILI,<sup>1</sup> J. POON,<sup>219</sup> E. PORCELLI,<sup>37</sup> E. K. PORTER,<sup>20</sup>  
2143 C. POSNANSKY,<sup>7</sup> R. POULTON,<sup>63</sup> J. POWELL,<sup>155</sup> G. S. PRABHU,<sup>80</sup> M. PRACCHIA,<sup>166</sup> B. K. PRADHAN,<sup>80</sup> T. PRADIER,<sup>65</sup>  
2144 A. K. PRAJAPATI,<sup>94</sup> K. PRAJAI,<sup>294</sup> R. PRASANNA,<sup>233</sup> P. PRASIA,<sup>80</sup> G. PRATTEN,<sup>104</sup> G. PRINCIPE,<sup>185,48</sup> G. A. PRODI,<sup>75,76</sup>  
2145 P. PROSPERI,<sup>81</sup> P. PROSPITO,<sup>21,22</sup> A. C. PROVIDENCE,<sup>66</sup> A. PUECHER,<sup>1</sup> J. PULLIN,<sup>12</sup> P. PUPPO,<sup>38</sup> M. PÜRREER,<sup>164</sup> H. QI,<sup>16</sup> J. QIN,<sup>34</sup>  
2146 G. QUÉMÉNER,<sup>174,118</sup> V. QUETSCHKE,<sup>165</sup> P. J. QUINONEZ,<sup>66</sup> N. QUTOB,<sup>57</sup> R. RADING,<sup>231</sup> I. RAINHO,<sup>138</sup> S. RAJA,<sup>105</sup> C. RAJAN,<sup>105</sup>  
2147 B. RAJBHANDARI,<sup>112</sup> K. E. RAMIREZ,<sup>64</sup> F. A. RAMIS VIDAL,<sup>99</sup> M. RAMOS AREVALO,<sup>165</sup> A. RAMOS-BUADES,<sup>99,37</sup> S. RANJAN,<sup>57</sup>  
2148 K. RANSOM,<sup>64</sup> P. RAPAGNANI,<sup>39,38</sup> B. RATTO,<sup>66</sup> A. RAVICHANDRAN,<sup>133</sup> A. RAY,<sup>97</sup> V. RAYMOND,<sup>33</sup> M. RAZZANO,<sup>82,81</sup> J. READ,<sup>54</sup>  
2149 T. REGIMBAU,<sup>31</sup> S. REID,<sup>55</sup> C. REISSEL,<sup>35</sup> D. H. REITZE,<sup>11</sup> A. I. RENZINI,<sup>127,11</sup> B. REVENU,<sup>295,41</sup> A. REVILLA PEÑA,<sup>83</sup> R. REYES,<sup>181</sup>  
2150 L. RICCA,<sup>15</sup> F. RICCI,<sup>39,38</sup> M. RICCI,<sup>38,39</sup> A. RICCIARDONE,<sup>82,81</sup> J. RICE,<sup>79</sup> J. W. RICHARDSON,<sup>211</sup> M. L. RICHARDSON,<sup>117</sup>  
2151 A. RIJAL,<sup>66</sup> K. RILES,<sup>91</sup> H. K. RILEY,<sup>33</sup> S. RINALDI,<sup>270</sup> J. RITTMAYER,<sup>98</sup> C. ROBERTSON,<sup>229</sup> F. ROBINET,<sup>41</sup> M. ROBINSON,<sup>2</sup>  
2152 A. ROCCHI,<sup>22</sup> L. ROLLAND,<sup>31</sup> J. G. ROLLINS,<sup>11</sup> A. E. ROMANO,<sup>296</sup> R. ROMANO,<sup>3,4</sup> A. ROMERO,<sup>31</sup> I. M. ROMERO-SHAW,<sup>224</sup>  
2153 J. H. ROMIE,<sup>64</sup> S. RONCHINI,<sup>7</sup> T. J. ROOCKE,<sup>117</sup> L. ROSA,<sup>4,32</sup> T. J. ROSAUER,<sup>211</sup> C. A. ROSE,<sup>57</sup> D. ROSIŃSKA,<sup>125</sup> M. P. ROSS,<sup>53</sup>  
2154 M. ROSSELLO-SASTRE,<sup>99</sup> S. ROWAN,<sup>87</sup> S. K. ROY,<sup>191,192</sup> S. ROY,<sup>15</sup> D. ROZZA,<sup>127,128</sup> P. RUGGI,<sup>63</sup> N. RUHAMA,<sup>239</sup>  
2155 E. RUIZ MORALES,<sup>297,208</sup> K. RUIZ-ROCHA,<sup>144</sup> S. SACHDEV,<sup>57</sup> T. SADECKI,<sup>2</sup> P. SAFFARIEH,<sup>37,109</sup> S. SAFI-HARB,<sup>169</sup> M. R. SAH,<sup>13</sup>  
2156 S. SAHA,<sup>142</sup> T. SAINRAT,<sup>65</sup> S. SAJJITH MENON,<sup>215,39,38</sup> K. SAKAI,<sup>298</sup> Y. SAKAI,<sup>272</sup> M. SAKELLARIADOU,<sup>68</sup> S. SAKON,<sup>7</sup>  
2157 O. S. SALAFIA,<sup>159,128,127</sup> F. SALCES-CARCOBA,<sup>11</sup> L. SALCONI,<sup>63</sup> M. SALEEM,<sup>148</sup> F. SALEMI,<sup>39,38</sup> M. SALLÉ,<sup>37</sup> S. U. SALUNKHE,<sup>80</sup>  
2158 S. SALVADOR,<sup>174,173</sup> A. SALVARESE,<sup>148</sup> A. SAMAJDAR,<sup>72,37</sup> A. SANCHEZ,<sup>2</sup> E. J. SANCHEZ,<sup>11</sup> L. E. SANCHEZ,<sup>11</sup> N. SANCHIS-GUAL,<sup>138</sup>  
2159 J. R. SANDERS,<sup>182</sup> E. M. SÄNGER,<sup>1</sup> F. SANTOLÍQUIDO,<sup>44,45</sup> F. SARANDREA,<sup>28</sup> T. R. SARAVANAN,<sup>80</sup> N. SARIN,<sup>6</sup> P. SARKAR,<sup>8,9</sup>  
2160 A. SASLI,<sup>251</sup> P. SASSI,<sup>51,77</sup> B. SASSOLAS,<sup>176</sup> B. S. SATHYAPRAKASH,<sup>7,33</sup> R. SATO,<sup>227</sup> S. SATO,<sup>152</sup> YUKINO SATO,<sup>152</sup> YU SATO,<sup>152</sup>  
2161 O. SAUTER,<sup>46</sup> R. L. SAVAGE,<sup>2</sup> T. SAWADA,<sup>50</sup> H. L. SAWANT,<sup>80</sup> S. SAYAH,<sup>176</sup> V. SCACCO,<sup>21,22</sup> D. SCHAETZL,<sup>11</sup> M. SCHEEL,<sup>149</sup>

2162 A. SCHIEBELBEIN,<sup>190</sup> M. G. SCHIWORSKI,<sup>79</sup> P. SCHMIDT,<sup>104</sup> S. SCHMIDT,<sup>72</sup> R. SCHNABEL,<sup>98</sup> M. SCHNEEWIND,<sup>8,9</sup>  
 2163 R. M. S. SCHOFIELD,<sup>78</sup> K. SCHOUTEDEN,<sup>111</sup> B. W. SCHULTE,<sup>8,9</sup> B. F. SCHUTZ,<sup>33,8,9</sup> E. SCHWARTZ,<sup>299</sup> M. SCIALPI,<sup>300</sup> J. SCOTT,<sup>87</sup>  
 2164 S. M. SCOTT,<sup>34</sup> R. M. SEDAS,<sup>64</sup> T. C. SEETHARAMU,<sup>87</sup> M. SEGLAR-ARROYO,<sup>43</sup> Y. SEKIGUCHI,<sup>301</sup> D. SELLERS,<sup>64</sup> N. SEMBO,<sup>205</sup>  
 2165 A. S. SENGUPTA,<sup>302</sup> E. G. SEO,<sup>87</sup> J. W. SEO,<sup>111</sup> V. SEQUINO,<sup>32,4</sup> M. SERRA,<sup>38</sup> A. SEVRIN,<sup>188</sup> T. SHAFFER,<sup>2</sup> U. S. SHAH,<sup>57</sup>  
 2166 M. A. SHAIKH,<sup>261</sup> L. SHAO,<sup>303</sup> A. K. SHARMA,<sup>99</sup> PREETI SHARMA,<sup>12</sup> PRIANKA SHARMA,<sup>105</sup> RITWIK SHARMA,<sup>18</sup>  
 2167 S. SHARMA CHAUDHARY,<sup>107</sup> P. SHAWHAN,<sup>126</sup> N. S. SHCHEBLANOV,<sup>304,263</sup> E. SHERIDAN,<sup>144</sup> Z.-H. SHI,<sup>142</sup> M. SHIKAUCHI,<sup>42</sup>  
 2168 R. SHIMOMURA,<sup>305</sup> H. SHINKAI,<sup>305</sup> S. SHIRKE,<sup>80</sup> D. H. SHOEMAKER,<sup>35</sup> D. M. SHOEMAKER,<sup>148</sup> R. W. SHORT,<sup>2</sup> S. SHYAMSUNDAR,<sup>105</sup>  
 2169 A. SIDER,<sup>158</sup> H. SIEGEL,<sup>191,192</sup> D. SIGG,<sup>2</sup> L. SILENZI,<sup>36,37</sup> L. SILVESTRI,<sup>39,170</sup> M. SIMMONDS,<sup>117</sup> L. P. SINGER,<sup>306</sup> AMITESH SINGH,<sup>216</sup>  
 2170 ANIKA SINGH,<sup>11</sup> D. SINGH,<sup>207</sup> N. SINGH,<sup>99</sup> S. SINGH,<sup>217,60</sup> A. M. SINTES,<sup>99</sup> V. SIPALA,<sup>171,156</sup> V. SKLIRIS,<sup>33</sup> B. J. J. SLAGMOLEN,<sup>34</sup>  
 2171 D. A. SLATER,<sup>200</sup> T. J. SLAVEN-BLAIR,<sup>73</sup> J. SMETANA,<sup>104</sup> J. R. SMITH,<sup>54</sup> L. SMITH,<sup>87,185,48</sup> R. J. E. SMITH,<sup>6</sup> W. J. SMITH,<sup>144</sup>  
 2172 S. SOARES DE ALBUQUERQUE FILHO,<sup>61</sup> M. SOARES-SANTOS,<sup>189</sup> K. SOMIYA,<sup>217</sup> I. SONG,<sup>142</sup> S. SONI,<sup>35</sup> V. SORDINI,<sup>56</sup>  
 2173 F. SORRENTINO,<sup>29</sup> H. SOTANI,<sup>307</sup> F. SPADA,<sup>81</sup> V. SPAGNUOLO,<sup>37</sup> A. P. SPENCER,<sup>87</sup> P. SPINICELLI,<sup>63</sup> A. K. SRIVASTAVA,<sup>94</sup>  
 2174 F. STACHURSKI,<sup>87</sup> C. J. STARK,<sup>123</sup> D. A. STEER,<sup>308</sup> J. STEINHOFF,<sup>1</sup> N. STEINLE,<sup>169</sup> J. STEINLECHNER,<sup>36,37</sup> S. STEINLECHNER,<sup>36,37</sup>  
 2175 N. STERGIIOULAS,<sup>251</sup> P. STEVENS,<sup>41</sup> M. STPIERRE,<sup>164</sup> M. D. STRONG,<sup>12</sup> A. L. STRUNK,<sup>2</sup> A. L. STUVER,<sup>103,\*</sup> M. SUCHENEK,<sup>96</sup>  
 2176 S. SUDHAGAR,<sup>96</sup> Y. SUDO,<sup>230</sup> N. SUELTSMANN,<sup>98</sup> L. SULEIMAN,<sup>54</sup> K. D. SULLIVAN,<sup>12</sup> J. SUN,<sup>241</sup> L. SUN,<sup>34</sup> S. SUNIL,<sup>94</sup> J. SURESH,<sup>115</sup>  
 2177 B. J. SUTTON,<sup>68</sup> P. J. SUTTON,<sup>33</sup> K. SUZUKI,<sup>217</sup> M. SUZUKI,<sup>204</sup> S. SWAIN,<sup>104</sup> B. L. SWINKELS,<sup>37</sup> A. SYX,<sup>118</sup> M. J. SZCZEPAŃCZYK,<sup>309</sup>  
 2178 P. SZEWCZYK,<sup>125</sup> M. TACCA,<sup>37</sup> H. TAGOSHI,<sup>204</sup> S. C. TAIT,<sup>11</sup> K. TAKADA,<sup>204</sup> H. TAKAHASHI,<sup>272</sup> R. TAKAHASHI,<sup>25</sup> A. TAKAMORI,<sup>42</sup>  
 2179 S. TAKANO,<sup>310</sup> H. TAKEDA,<sup>311,312</sup> K. TAKESHITA,<sup>217</sup> I. TAKIMOTO SCHMIEGELOW,<sup>44,45</sup> M. TAKOU-AYAOH,<sup>79</sup> C. TALBOT,<sup>130</sup>  
 2180 M. TAMAKI,<sup>204</sup> N. TAMANINI,<sup>101</sup> D. TANABE,<sup>141</sup> K. TANAKA,<sup>50</sup> S. J. TANAKA,<sup>230</sup> S. TANIOKA,<sup>33</sup> D. B. TANNER,<sup>46</sup> W. TANNER,<sup>8,9</sup>  
 2181 L. TAO,<sup>211</sup> R. D. TAPIA,<sup>7</sup> E. N. TAPIA SAN MARTÍN,<sup>37</sup> C. TARANTO,<sup>21,22</sup> A. TARUYA,<sup>313</sup> J. D. TASSON,<sup>153</sup> J. G. TAU,<sup>112</sup> D. TELLEZ,<sup>54</sup>  
 2182 R. TENORIO,<sup>99</sup> H. THEMANN,<sup>181</sup> A. THEODOROPOULOS,<sup>138</sup> M. P. THIRUGNANASAMBANDAM,<sup>80</sup> L. M. THOMAS,<sup>11</sup> M. THOMAS,<sup>64</sup>  
 2183 P. THOMAS,<sup>2</sup> J. E. THOMPSON,<sup>210</sup> S. R. THONDAPU,<sup>105</sup> K. A. THORNE,<sup>64</sup> E. THRANE,<sup>6</sup> J. TISSINO,<sup>44,45</sup> A. TIWARI,<sup>80</sup>  
 2184 PAWAN TIWARI,<sup>44</sup> PRAVEER TIWARI,<sup>195</sup> S. TIWARI,<sup>189</sup> V. TIWARI,<sup>104</sup> M. R. TODD,<sup>79</sup> M. TOFFANO,<sup>92</sup> A. M. TOIVONEN,<sup>18</sup>  
 2185 K. TOLAND,<sup>87</sup> A. E. TOLLEY,<sup>74</sup> T. TOMARU,<sup>25</sup> V. TOMMASINI,<sup>11</sup> T. TOMURA,<sup>50</sup> H. TONG,<sup>6</sup> C. TONG-YU,<sup>141</sup>  
 2186 A. TORRES-FORNÉ,<sup>138,139</sup> C. I. TORRIE,<sup>11</sup> I. TOSTA E MELO,<sup>314</sup> E. TOURNEFIER,<sup>31</sup> M. TRAD NERY,<sup>115</sup> K. TRAN,<sup>123</sup>  
 2187 A. TRAPANANTI,<sup>52,51</sup> R. TRAVAGLINI,<sup>168</sup> F. TRAVASSO,<sup>52,51</sup> G. TRAYLOR,<sup>64</sup> M. TREVOR,<sup>126</sup> M. C. TRINGALI,<sup>63</sup> A. TRIPATHEE,<sup>91</sup>  
 2188 G. TROIAN,<sup>185,48</sup> A. TROVATO,<sup>185,48</sup> L. TROZZO,<sup>4</sup> R. J. TRUDEAU,<sup>11</sup> T. TSANG,<sup>33</sup> S. TSUCHIDA,<sup>315</sup> L. TSUKADA,<sup>213</sup>  
 2189 K. TURBANG,<sup>188,23</sup> M. TURCONI,<sup>115</sup> C. TURSCHI,<sup>95</sup> H. UBACH,<sup>83,84</sup> N. UCHIKATA,<sup>204</sup> T. UCHIYAMA,<sup>50</sup> R. P. UDALL,<sup>11</sup> T. UEHARA,<sup>316</sup>  
 2190 K. UENO,<sup>42</sup> V. UNDHEIM,<sup>278</sup> L. E. URONEN,<sup>219</sup> T. USHIBA,<sup>50</sup> M. VACATELLO,<sup>81,82</sup> H. VAHLBRUCH,<sup>8,9</sup> N. VAIDYA,<sup>11</sup> G. VAJENTE,<sup>11</sup>  
 2191 A. VAJPEYI,<sup>6</sup> J. VALENCIA,<sup>99</sup> M. VALENTINI,<sup>109,37</sup> S. A. VALLEJO-PEÑA,<sup>296</sup> S. VALLERO,<sup>28</sup> V. VALSAN,<sup>10</sup> M. VAN DAEL,<sup>37,317</sup>  
 2192 E. VAN DEN BOSSCHE,<sup>188</sup> J. F. J. VAN DEN BRAND,<sup>36,109,37</sup> C. VAN DEN BROECK,<sup>72,37</sup> M. VAN DER SLUYS,<sup>37,72</sup> A. VAN DE WALLE,<sup>41</sup>  
 2193 J. VAN DONGEN,<sup>37,109</sup> K. VANDRA,<sup>103</sup> M. VANDYKE,<sup>120</sup> H. VAN HAEVERMAET,<sup>23</sup> J. V. VAN HEIJNINGEN,<sup>37,109</sup> P. VAN HOVE,<sup>65</sup>  
 2194 J. VANIER,<sup>259</sup> M. VANKEUREN,<sup>106</sup> J. VANOSKY,<sup>2</sup> N. VAN REMORTEL,<sup>23</sup> M. VARDARO,<sup>36,37</sup> A. F. VARGAS,<sup>124</sup> V. VARMA,<sup>133</sup>  
 2195 A. N. VAZQUEZ,<sup>90</sup> A. VECCHIO,<sup>104</sup> G. VEDOVATO,<sup>93</sup> J. VEITCH,<sup>87</sup> P. J. VEITCH,<sup>117</sup> S. VENIKOUDIS,<sup>15</sup> R. C. VENTEREA,<sup>18</sup>  
 2196 P. VERDIER,<sup>56</sup> M. VERECKEN,<sup>15</sup> D. VERKINDT,<sup>31</sup> B. VERMA,<sup>133</sup> Y. VERMA,<sup>105</sup> S. M. VERMEULEN,<sup>11</sup> F. VETRANO,<sup>61</sup>  
 2197 A. VEUTRO,<sup>38,39</sup> A. VICERÉ,<sup>61,62</sup> S. VIDYANT,<sup>79</sup> A. D. VIETS,<sup>89</sup> A. VIJAYKUMAR,<sup>190</sup> A. VILKHA,<sup>112</sup> N. VILLANUEVA ESPINOSA,<sup>138</sup>  
 2198 V. VILLA-ORTEGA,<sup>178</sup> E. T. VINCENT,<sup>57</sup> J.-Y. VINET,<sup>115</sup> S. VIRET,<sup>56</sup> S. VITALE,<sup>35</sup> H. VOCCA,<sup>77,51</sup> D. VOIGT,<sup>98</sup> E. R. G. VON REIS,<sup>2</sup>  
 2199 J. S. A. VON WRANGEL,<sup>8,9</sup> W. E. VOSSIUS,<sup>231</sup> L. VUJEVA,<sup>140</sup> S. P. VYATCHANIN,<sup>110</sup> J. WACK,<sup>11</sup> L. E. WADE,<sup>106</sup> M. WADE,<sup>106</sup>  
 2200 K. J. WAGNER,<sup>112</sup> R. M. WALD,<sup>130</sup> L. WALLACE,<sup>11</sup> E. J. WANG,<sup>90</sup> H. WANG,<sup>217</sup> J. Z. WANG,<sup>91</sup> W. H. WANG,<sup>165</sup> Y. F. WANG,<sup>1</sup>  
 2201 G. WARATKAR,<sup>195</sup> J. WARNER,<sup>2</sup> M. WAS,<sup>31</sup> T. WASHIMI,<sup>25</sup> N. Y. WASHINGTON,<sup>11</sup> D. WATARAI,<sup>42</sup> B. WEAVER,<sup>2</sup> S. A. WEBSTER,<sup>87</sup>  
 2202 N. L. WEICKHARDT,<sup>98</sup> M. WEINERT,<sup>8,9</sup> A. J. WEINSTEIN,<sup>11</sup> R. WEISS,<sup>35,†</sup> L. WEN,<sup>73</sup> K. WETTE,<sup>34</sup> J. T. WHELAN,<sup>112</sup>  
 2203 B. F. WHITING,<sup>46</sup> C. WHITTLE,<sup>11</sup> E. G. WICKENS,<sup>74</sup> D. WILKEN,<sup>8,9,9</sup> A. T. WILKIN,<sup>211</sup> B. M. WILLIAMS,<sup>120</sup> D. WILLIAMS,<sup>87</sup>  
 2204 M. J. WILLIAMS,<sup>74</sup> N. S. WILLIAMS,<sup>1</sup> J. L. WILLIS,<sup>11</sup> B. WILLKE,<sup>9,8,9</sup> M. WILS,<sup>111</sup> L. WILSON,<sup>106</sup> C. W. WINBORN,<sup>107</sup>  
 2205 J. WINTERFLOOD,<sup>73</sup> C. C. WIPF,<sup>11</sup> G. WOAN,<sup>87</sup> J. WOEHLE,<sup>36,37</sup> N. E. WOLFE,<sup>35</sup> H. T. WONG,<sup>141</sup> I. C. F. WONG,<sup>219,111</sup>  
 2206 K. WONG,<sup>190</sup> T. WOUTERS,<sup>72,37</sup> J. L. WRIGHT,<sup>2</sup> M. WRIGHT,<sup>87,72</sup> B. WU,<sup>79</sup> C. WU,<sup>142</sup> D. S. WU,<sup>8,9</sup> H. WU,<sup>142</sup> K. WU,<sup>120</sup> Q. WU,<sup>53</sup>  
 2207 Y. WU,<sup>97</sup> Z. WU,<sup>101</sup> E. WUCHNER,<sup>54</sup> D. M. WYSOCKI,<sup>10</sup> V. A. XU,<sup>207</sup> Y. XU,<sup>99</sup> N. YADAV,<sup>28</sup> H. YAMAMOTO,<sup>11</sup> K. YAMAMOTO,<sup>152</sup>  
 2208 T. S. YAMAMOTO,<sup>42</sup> T. YAMAMOTO,<sup>50</sup> R. YAMAZAKI,<sup>230</sup> T. YAN,<sup>104</sup> K. Z. YANG,<sup>18</sup> Y. YANG,<sup>146</sup> Z. YARBROUGH,<sup>12</sup> J. YEBANA,<sup>99</sup>  
 2209 S.-W. YEH,<sup>142</sup> A. B. YELIKAR,<sup>144</sup> X. YIN,<sup>35</sup> J. YOKOYAMA,<sup>318,42</sup> T. YOKOZAWA,<sup>50</sup> S. YUAN,<sup>73</sup> H. YUZURIHARA,<sup>50</sup> M. ZANOLIN,<sup>66</sup>  
 2210 M. ZEESHAN,<sup>112</sup> T. ZELENKOVA,<sup>63</sup> J.-P. ZENDRI,<sup>93</sup> M. ZEOLI,<sup>15</sup> M. ZERRAD,<sup>40</sup> M. ZEVIN,<sup>97</sup> L. ZHANG,<sup>11</sup> N. ZHANG,<sup>57</sup> R. ZHANG,<sup>150</sup>  
 2211 T. ZHANG,<sup>104</sup> C. ZHAO,<sup>73</sup> J. ZHAO,<sup>319</sup> YUE ZHAO,<sup>162</sup> YUHANG ZHAO,<sup>20</sup> Z.-C. ZHAO,<sup>319</sup> Y. ZHENG,<sup>107</sup> H. ZHONG,<sup>18</sup> H. ZHOU,<sup>79</sup>  
 2212 H. O. ZHU,<sup>73</sup> Z.-H. ZHU,<sup>319,320</sup> A. B. ZIMMERMAN,<sup>148</sup> L. ZIMMERMANN,<sup>56</sup> M. E. ZUCKER,<sup>35,11</sup> AND J. ZWEIZIG<sup>11</sup>

<sup>1</sup>Max Planck Institute for Gravitational Physics (Albert Einstein Institute), D-14476 Potsdam, Germany

<sup>2</sup>LIGO Hanford Observatory, Richland, WA 99352, USA

<sup>3</sup>Dipartimento di Farmacia, Università di Salerno, I-84084 Fisciano, Salerno, Italy

<sup>4</sup>INFN, Sezione di Napoli, I-80126 Napoli, Italy

<sup>5</sup>University of Warwick, Coventry CV4 7AL, United Kingdom

<sup>6</sup>OzGrav, School of Physics & Astronomy, Monash University, Clayton 3800, Victoria, Australia

<sup>7</sup>The Pennsylvania State University, University Park, PA 16802, USA

<sup>8</sup>Max Planck Institute for Gravitational Physics (Albert Einstein Institute), D-30167 Hannover, Germany

<sup>9</sup>Leibniz Universität Hannover, D-30167 Hannover, Germany

<sup>10</sup>University of Wisconsin-Milwaukee, Milwaukee, WI 53201, USA

<sup>11</sup>LIGO Laboratory, California Institute of Technology, Pasadena, CA 91125, USA

- 2224 <sup>12</sup>Louisiana State University, Baton Rouge, LA 70803, USA
- 2225 <sup>13</sup>Tata Institute of Fundamental Research, Mumbai 400005, India
- 2226 <sup>14</sup>Centre de Physique Théorique, Aix-Marseille Université, Campus de Luminy, 163 Av. de Luminy, 13009 Marseille, France
- 2227 <sup>15</sup>Université catholique de Louvain, B-1348 Louvain-la-Neuve, Belgium
- 2228 <sup>16</sup>Queen Mary University of London, London E1 4NS, United Kingdom
- 2229 <sup>17</sup>University of California, Davis, Davis, CA 95616, USA
- 2230 <sup>18</sup>University of Minnesota, Minneapolis, MN 55455, USA
- 2231 <sup>19</sup>Instituto Nacional de Pesquisas Espaciais, 12227-010 São José dos Campos, São Paulo, Brazil
- 2232 <sup>20</sup>Université Paris Cité, CNRS, Astroparticule et Cosmologie, F-75013 Paris, France
- 2233 <sup>21</sup>Università di Roma Tor Vergata, I-00133 Roma, Italy
- 2234 <sup>22</sup>INFN, Sezione di Roma Tor Vergata, I-00133 Roma, Italy
- 2235 <sup>23</sup>Universiteit Antwerpen, 2000 Antwerpen, Belgium
- 2236 <sup>24</sup>International Centre for Theoretical Sciences, Tata Institute of Fundamental Research, Bengaluru 560089, India
- 2237 <sup>25</sup>Gravitational Wave Science Project, National Astronomical Observatory of Japan, 2-21-1 Osawa, Mitaka City, Tokyo 181-8588, Japan
- 2238 <sup>26</sup>Advanced Technology Center, National Astronomical Observatory of Japan, 2-21-1 Osawa, Mitaka City, Tokyo 181-8588, Japan
- 2239 <sup>27</sup>Theoretisch-Physikalisches Institut, Friedrich-Schiller-Universität Jena, D-07743 Jena, Germany
- 2240 <sup>28</sup>INFN Sezione di Torino, I-10125 Torino, Italy
- 2241 <sup>29</sup>INFN, Sezione di Genova, I-16146 Genova, Italy
- 2242 <sup>30</sup>Dipartimento di Fisica, Università degli Studi di Genova, I-16146 Genova, Italy
- 2243 <sup>31</sup>Univ. Savoie Mont Blanc, CNRS, Laboratoire d'Annecy de Physique des Particules - IN2P3, F-74000 Annecy, France
- 2244 <sup>32</sup>Università di Napoli "Federico II", I-80126 Napoli, Italy
- 2245 <sup>33</sup>Cardiff University, Cardiff CF24 3AA, United Kingdom
- 2246 <sup>34</sup>OzGrav, Australian National University, Canberra, Australian Capital Territory 0200, Australia
- 2247 <sup>35</sup>LIGO Laboratory, Massachusetts Institute of Technology, Cambridge, MA 02139, USA
- 2248 <sup>36</sup>Maastricht University, 6200 MD Maastricht, Netherlands
- 2249 <sup>37</sup>Nikhef, 1098 XG Amsterdam, Netherlands
- 2250 <sup>38</sup>INFN, Sezione di Roma, I-00185 Roma, Italy
- 2251 <sup>39</sup>Università di Roma "La Sapienza", I-00185 Roma, Italy
- 2252 <sup>40</sup>Aix Marseille Univ, CNRS, Centrale Med, Institut Fresnel, F-13013 Marseille, France
- 2253 <sup>41</sup>Université Paris-Saclay, CNRS/IN2P3, IJCLab, 91405 Orsay, France
- 2254 <sup>42</sup>University of Tokyo, Tokyo, 113-0033, Japan
- 2255 <sup>43</sup>Institut de Física d'Altes Energies (IFAE), The Barcelona Institute of Science and Technology, Campus UAB, E-08193 Bellaterra (Barcelona), Spain
- 2256 <sup>44</sup>Gran Sasso Science Institute (GSSI), I-67100 L'Aquila, Italy
- 2257 <sup>45</sup>INFN, Laboratori Nazionali del Gran Sasso, I-67100 Assergi, Italy
- 2258 <sup>46</sup>University of Florida, Gainesville, FL 32611, USA
- 2259 <sup>47</sup>Dipartimento di Scienze Matematiche, Informatiche e Fisiche, Università di Udine, I-33100 Udine, Italy
- 2260 <sup>48</sup>INFN, Sezione di Trieste, I-34127 Trieste, Italy
- 2261 <sup>49</sup>Tecnologico de Monterrey, Escuela de Ingeniería y Ciencias, 64849 Monterrey, Nuevo León, Mexico
- 2262 <sup>50</sup>Institute for Cosmic Ray Research, KAGRA Observatory, The University of Tokyo, 238 Higashi-Mozumi, Kamioka-cho, Hida City, Gifu 506-1205, Japan
- 2263 <sup>51</sup>INFN, Sezione di Perugia, I-06123 Perugia, Italy
- 2264 <sup>52</sup>Università di Camerino, I-62032 Camerino, Italy
- 2265 <sup>53</sup>University of Washington, Seattle, WA 98195, USA
- 2266 <sup>54</sup>California State University Fullerton, Fullerton, CA 92831, USA
- 2267 <sup>55</sup>SUPA, University of Strathclyde, Glasgow G1 1XQ, United Kingdom
- 2268 <sup>56</sup>Université Claude Bernard Lyon 1, CNRS, IP2I Lyon / IN2P3, UMR 5822, F-69622 Villeurbanne, France
- 2269 <sup>57</sup>Georgia Institute of Technology, Atlanta, GA 30332, USA
- 2270 <sup>58</sup>Chennai Mathematical Institute, Chennai 603103, India
- 2271 <sup>59</sup>Royal Holloway, University of London, London TW20 0EX, United Kingdom
- 2272 <sup>60</sup>Astronomical course, The Graduate University for Advanced Studies (SOKENDAI), 2-21-1 Osawa, Mitaka City, Tokyo 181-8588, Japan
- 2273 <sup>61</sup>Università degli Studi di Urbino "Carlo Bo", I-61029 Urbino, Italy
- 2274 <sup>62</sup>INFN, Sezione di Firenze, I-50019 Sesto Fiorentino, Firenze, Italy
- 2275 <sup>63</sup>European Gravitational Observatory (EGO), I-56021 Cascina, Pisa, Italy
- 2276 <sup>64</sup>LIGO Livingston Observatory, Livingston, LA 70754, USA
- 2277 <sup>65</sup>Université de Strasbourg, CNRS, IPHC UMR 7178, F-67000 Strasbourg, France
- 2278 <sup>66</sup>Embry-Riddle Aeronautical University, Prescott, AZ 86301, USA
- 2279 <sup>67</sup>Dipartimento di Fisica "E.R. Caianiello", Università di Salerno, I-84084 Fisciano, Salerno, Italy
- 2280 <sup>68</sup>King's College London, University of London, London WC2R 2LS, United Kingdom

- 2281 <sup>69</sup>*Korea Institute of Science and Technology Information, Daejeon 34141, Republic of Korea*
- 2282 <sup>70</sup>*International College, Osaka University, 1-1 Machikaneyama-cho, Toyonaka City, Osaka 560-0043, Japan*
- 2283 <sup>71</sup>*Accelerator Laboratory, High Energy Accelerator Research Organization (KEK), 1-1 Oho, Tsukuba City, Ibaraki 305-0801, Japan*
- 2284 <sup>72</sup>*Institute for Gravitational and Subatomic Physics (GRASP), Utrecht University, 3584 CC Utrecht, Netherlands*
- 2285 <sup>73</sup>*OzGrav, University of Western Australia, Crawley, Western Australia 6009, Australia*
- 2286 <sup>74</sup>*University of Portsmouth, Portsmouth, PO1 3FX, United Kingdom*
- 2287 <sup>75</sup>*Università di Trento, Dipartimento di Fisica, I-38123 Povo, Trento, Italy*
- 2288 <sup>76</sup>*INFN, Trento Institute for Fundamental Physics and Applications, I-38123 Povo, Trento, Italy*
- 2289 <sup>77</sup>*Università di Perugia, I-06123 Perugia, Italy*
- 2290 <sup>78</sup>*University of Oregon, Eugene, OR 97403, USA*
- 2291 <sup>79</sup>*Syracuse University, Syracuse, NY 13244, USA*
- 2292 <sup>80</sup>*Inter-University Centre for Astronomy and Astrophysics, Pune 411007, India*
- 2293 <sup>81</sup>*INFN, Sezione di Pisa, I-56127 Pisa, Italy*
- 2294 <sup>82</sup>*Università di Pisa, I-56127 Pisa, Italy*
- 2295 <sup>83</sup>*Institut de Ciències del Cosmos (ICCUB), Universitat de Barcelona (UB), c. Martí i Franqués, 1, 08028 Barcelona, Spain*
- 2296 <sup>84</sup>*Departament de Física Quàntica i Astrofísica (FQA), Universitat de Barcelona (UB), c. Martí i Franqués, 1, 08028 Barcelona, Spain*
- 2297 <sup>85</sup>*Institut d'Estudis Espacials de Catalunya, c. Gran Capità, 2-4, 08034 Barcelona, Spain*
- 2298 <sup>86</sup>*Dipartimento di Medicina, Chirurgia e Odontoiatria "Scuola Medica Salernitana", Università di Salerno, I-84081 Baronissi, Salerno, Italy*
- 2299 <sup>87</sup>*IGR, University of Glasgow, Glasgow G12 8QQ, United Kingdom*
- 2300 <sup>88</sup>*HUN-REN Wigner Research Centre for Physics, H-1121 Budapest, Hungary*
- 2301 <sup>89</sup>*Concordia University Wisconsin, Mequon, WI 53097, USA*
- 2302 <sup>90</sup>*Stanford University, Stanford, CA 94305, USA*
- 2303 <sup>91</sup>*University of Michigan, Ann Arbor, MI 48109, USA*
- 2304 <sup>92</sup>*Università di Padova, Dipartimento di Fisica e Astronomia, I-35131 Padova, Italy*
- 2305 <sup>93</sup>*INFN, Sezione di Padova, I-35131 Padova, Italy*
- 2306 <sup>94</sup>*Institute for Plasma Research, Bhat, Gandhinagar 382428, India*
- 2307 <sup>95</sup>*Universiteit Gent, B-9000 Gent, Belgium*
- 2308 <sup>96</sup>*Nicolaus Copernicus Astronomical Center, Polish Academy of Sciences, 00-716, Warsaw, Poland*
- 2309 <sup>97</sup>*Northwestern University, Evanston, IL 60208, USA*
- 2310 <sup>98</sup>*Universität Hamburg, D-22761 Hamburg, Germany*
- 2311 <sup>99</sup>*IAC3–IEEC, Universitat de les Illes Balears, E-07122 Palma de Mallorca, Spain*
- 2312 <sup>100</sup>*Aix-Marseille Université, Université de Toulon, CNRS, CPT, Marseille, France*
- 2313 <sup>101</sup>*Laboratoire des 2 Infinis - Toulouse (L2IT-IN2P3), F-31062 Toulouse Cedex 9, France*
- 2314 <sup>102</sup>*Università di Siena, Dipartimento di Scienze Fisiche, della Terra e dell'Ambiente, I-53100 Siena, Italy*
- 2315 <sup>103</sup>*Villanova University, Villanova, PA 19085, USA*
- 2316 <sup>104</sup>*University of Birmingham, Birmingham B15 2TT, United Kingdom*
- 2317 <sup>105</sup>*RRCAT, Indore, Madhya Pradesh 452013, India*
- 2318 <sup>106</sup>*Kenyon College, Gambier, OH 43022, USA*
- 2319 <sup>107</sup>*Missouri University of Science and Technology, Rolla, MO 65409, USA*
- 2320 <sup>108</sup>*Indian Institute of Technology Madras, Chennai 600036, India*
- 2321 <sup>109</sup>*Department of Physics and Astronomy, Vrije Universiteit Amsterdam, 1081 HV Amsterdam, Netherlands*
- 2322 <sup>110</sup>*Lomonosov Moscow State University, Moscow 119991, Russia*
- 2323 <sup>111</sup>*Katholieke Universiteit Leuven, Oude Markt 13, 3000 Leuven, Belgium*
- 2324 <sup>112</sup>*Rochester Institute of Technology, Rochester, NY 14623, USA*
- 2325 <sup>113</sup>*Université libre de Bruxelles, 1050 Bruxelles, Belgium*
- 2326 <sup>114</sup>*Bar-Ilan University, Ramat Gan, 5290002, Israel*
- 2327 <sup>115</sup>*Université Côte d'Azur, Observatoire de la Côte d'Azur, CNRS, Artemis, F-06304 Nice, France*
- 2328 <sup>116</sup>*University of British Columbia, Vancouver, BC V6T 1Z4, Canada*
- 2329 <sup>117</sup>*OzGrav, University of Adelaide, Adelaide, South Australia 5005, Australia*
- 2330 <sup>118</sup>*Centre national de la recherche scientifique, 75016 Paris, France*
- 2331 <sup>119</sup>*Univ Rennes, CNRS, Institut FOTON - UMR 6082, F-35000 Rennes, France*
- 2332 <sup>120</sup>*Washington State University, Pullman, WA 99164, USA*
- 2333 <sup>121</sup>*Cornell University, Ithaca, NY 14850, USA*
- 2334 <sup>122</sup>*Laboratoire Kastler Brossel, Sorbonne Université, CNRS, ENS-Université PSL, Collège de France, F-75005 Paris, France*
- 2335 <sup>123</sup>*Christopher Newport University, Newport News, VA 23606, USA*
- 2336 <sup>124</sup>*OzGrav, University of Melbourne, Parkville, Victoria 3010, Australia*
- 2337 <sup>125</sup>*Astronomical Observatory Warsaw University, 00-478 Warsaw, Poland*

- 2338 <sup>126</sup>University of Maryland, College Park, MD 20742, USA
- 2339 <sup>127</sup>Università degli Studi di Milano-Bicocca, I-20126 Milano, Italy
- 2340 <sup>128</sup>INFN, Sezione di Milano-Bicocca, I-20126 Milano, Italy
- 2341 <sup>129</sup>Université de Lyon, Université Claude Bernard Lyon 1, CNRS, Institut Lumière Matière, F-69622 Villeurbanne, France
- 2342 <sup>130</sup>University of Chicago, Chicago, IL 60637, USA
- 2343 <sup>131</sup>University of Arizona, Tucson, AZ 85721, USA
- 2344 <sup>132</sup>INFN, Sezione di Napoli, Gruppo Collegato di Salerno, I-80126 Napoli, Italy
- 2345 <sup>133</sup>University of Massachusetts Dartmouth, North Dartmouth, MA 02747, USA
- 2346 <sup>134</sup>Niels Bohr Institute, Copenhagen University, 2100 København, Denmark
- 2347 <sup>135</sup>Universidad de Guadalajara, 44430 Guadalajara, Jalisco, Mexico
- 2348 <sup>136</sup>Istituto di Astrofisica e Planetologia Spaziali di Roma, 00133 Roma, Italy
- 2349 <sup>137</sup>Colorado State University, Fort Collins, CO 80523, USA
- 2350 <sup>138</sup>Departamento de Astronomía y Astrofísica, Universitat de València, E-46100 Burjassot, València, Spain
- 2351 <sup>139</sup>Observatori Astronòmic, Universitat de València, E-46980 Paterna, València, Spain
- 2352 <sup>140</sup>Niels Bohr Institute, University of Copenhagen, 2100 København, Denmark
- 2353 <sup>141</sup>National Central University, Taoyuan City 320317, Taiwan
- 2354 <sup>142</sup>National Tsing Hua University, Hsinchu City 30013, Taiwan
- 2355 <sup>143</sup>OzGrav, Charles Sturt University, Wagga Wagga, New South Wales 2678, Australia
- 2356 <sup>144</sup>Vanderbilt University, Nashville, TN 37235, USA
- 2357 <sup>145</sup>University of the Chinese Academy of Sciences / International Centre for Theoretical Physics Asia-Pacific, Beijing 100049, China
- 2358 <sup>146</sup>Department of Electrophysics, National Yang Ming Chiao Tung University, 101 Univ. Street, Hsinchu, Taiwan
- 2359 <sup>147</sup>Kamioka Branch, National Astronomical Observatory of Japan, 238 Higashi-Mozumi, Kamioka-cho, Hida City, Gifu 506-1205, Japan
- 2360 <sup>148</sup>University of Texas, Austin, TX 78712, USA
- 2361 <sup>149</sup>CaRT, California Institute of Technology, Pasadena, CA 91125, USA
- 2362 <sup>150</sup>Northeastern University, Boston, MA 02115, USA
- 2363 <sup>151</sup>Dipartimento di Ingegneria Industriale (DIIN), Università di Salerno, I-84084 Fisciano, Salerno, Italy
- 2364 <sup>152</sup>Faculty of Science, University of Toyama, 3190 Gofuku, Toyama City, Toyama 930-8555, Japan
- 2365 <sup>153</sup>Carleton College, Northfield, MN 55057, USA
- 2366 <sup>154</sup>University of Szeged, Dóm tér 9, Szeged 6720, Hungary
- 2367 <sup>155</sup>OzGrav, Swinburne University of Technology, Hawthorn VIC 3122, Australia
- 2368 <sup>156</sup>INFN Cagliari, Physics Department, Università degli Studi di Cagliari, Cagliari 09042, Italy
- 2369 <sup>157</sup>Università degli Studi di Cagliari, Via Università 40, 09124 Cagliari, Italy
- 2370 <sup>158</sup>Université Libre de Bruxelles, Brussels 1050, Belgium
- 2371 <sup>159</sup>INAF, Osservatorio Astronomico di Brera sede di Merate, I-23807 Merate, Lecco, Italy
- 2372 <sup>160</sup>Departamento de Matemáticas, Universitat de València, E-46100 Burjassot, València, Spain
- 2373 <sup>161</sup>Montana State University, Bozeman, MT 59717, USA
- 2374 <sup>162</sup>The University of Utah, Salt Lake City, UT 84112, USA
- 2375 <sup>163</sup>Johns Hopkins University, Baltimore, MD 21218, USA
- 2376 <sup>164</sup>University of Rhode Island, Kingston, RI 02881, USA
- 2377 <sup>165</sup>The University of Texas Rio Grande Valley, Brownsville, TX 78520, USA
- 2378 <sup>166</sup>Université de Liège, B-4000 Liège, Belgium
- 2379 <sup>167</sup>DIFA- Alma Mater Studiorum Università di Bologna, Via Zamboni, 33 - 40126 Bologna, Italy
- 2380 <sup>168</sup>Istituto Nazionale Di Fisica Nucleare - Sezione di Bologna, viale Carlo Berti Pichat 6/2 - 40127 Bologna, Italy
- 2381 <sup>169</sup>University of Manitoba, Winnipeg, MB R3T 2N2, Canada
- 2382 <sup>170</sup>INFN-CNAF - Bologna, Viale Carlo Berti Pichat, 6/2, 40127 Bologna BO, Italy
- 2383 <sup>171</sup>Università degli Studi di Sassari, I-07100 Sassari, Italy
- 2384 <sup>172</sup>INFN, Laboratori Nazionali del Sud, I-95125 Catania, Italy
- 2385 <sup>173</sup>Université de Normandie, ENSICAEN, UNICAEN, CNRS/IN2P3, LPC Caen, F-14000 Caen, France
- 2386 <sup>174</sup>Laboratoire de Physique Corpusculaire Caen, 6 boulevard du maréchal Juin, F-14050 Caen, France
- 2387 <sup>175</sup>The University of Sheffield, Sheffield S10 2TN, United Kingdom
- 2388 <sup>176</sup>Université Claude Bernard Lyon 1, CNRS, Laboratoire des Matériaux Avancés (LMA), IP2I Lyon / IN2P3, UMR 5822, F-69622 Villeurbanne, France
- 2389 <sup>177</sup>Università di Firenze, Sesto Fiorentino I-50019, Italy
- 2390 <sup>178</sup>IGFAE, Universidade de Santiago de Compostela, E-15782 Santiago de Compostela, Spain
- 2391 <sup>179</sup>Dipartimento di Scienze Matematiche, Fisiche e Informatiche, Università di Parma, I-43124 Parma, Italy
- 2392 <sup>180</sup>INFN, Sezione di Milano Bicocca, Gruppo Collegato di Parma, I-43124 Parma, Italy
- 2393 <sup>181</sup>California State University, Los Angeles, Los Angeles, CA 90032, USA
- 2394 <sup>182</sup>Marquette University, Milwaukee, WI 53233, USA

- 2395 <sup>183</sup>Perimeter Institute, Waterloo, ON N2L 2Y5, Canada
- 2396 <sup>184</sup>Corps des Mines, Mines Paris, Université PSL, 60 Bd Saint-Michel, 75272 Paris, France
- 2397 <sup>185</sup>Dipartimento di Fisica, Università di Trieste, I-34127 Trieste, Italy
- 2398 <sup>186</sup>Université Côte d'Azur, Observatoire de la Côte d'Azur, CNRS, Lagrange, F-06304 Nice, France
- 2399 <sup>187</sup>National Center for Nuclear Research, 05-400 Świerk-Otwock, Poland
- 2400 <sup>188</sup>Vrije Universiteit Brussel, 1050 Brussel, Belgium
- 2401 <sup>189</sup>University of Zurich, Winterthurerstrasse 190, 8057 Zurich, Switzerland
- 2402 <sup>190</sup>Canadian Institute for Theoretical Astrophysics, University of Toronto, Toronto, ON M5S 3H8, Canada
- 2403 <sup>191</sup>Stony Brook University, Stony Brook, NY 11794, USA
- 2404 <sup>192</sup>Center for Computational Astrophysics, Flatiron Institute, New York, NY 10010, USA
- 2405 <sup>193</sup>Montclair State University, Montclair, NJ 07043, USA
- 2406 <sup>194</sup>HUN-REN Institute for Nuclear Research, H-4026 Debrecen, Hungary
- 2407 <sup>195</sup>Indian Institute of Technology Bombay, Powai, Mumbai 400 076, India
- 2408 <sup>196</sup>Centro de Física das Universidades do Minho e do Porto, Universidade do Minho, PT-4710-057 Braga, Portugal
- 2409 <sup>197</sup>Aix Marseille Univ, CNRS/IN2P3, CPPM, Marseille, France
- 2410 <sup>198</sup>CNR-SPIN, I-84084 Fisciano, Salerno, Italy
- 2411 <sup>199</sup>Scuola di Ingegneria, Università della Basilicata, I-85100 Potenza, Italy
- 2412 <sup>200</sup>Western Washington University, Bellingham, WA 98225, USA
- 2413 <sup>201</sup>SUPA, University of the West of Scotland, Paisley PA1 2BE, United Kingdom
- 2414 <sup>202</sup>Barry University, Miami Shores, FL 33168, USA
- 2415 <sup>203</sup>Eötvös University, Budapest 1117, Hungary
- 2416 <sup>204</sup>Institute for Cosmic Ray Research, KAGRA Observatory, The University of Tokyo, 5-1-5 Kashiwa-no-Ha, Kashiwa City, Chiba 277-8582, Japan
- 2417 <sup>205</sup>Department of Physics, Graduate School of Science, Osaka Metropolitan University, 3-3-138 Sugimoto-cho, Sumiyoshi-ku, Osaka City, Osaka 558-8585, Japan
- 2418 <sup>206</sup>University of Sannio at Benevento, I-82100 Benevento, Italy and INFN, Sezione di Napoli, I-80100 Napoli, Italy
- 2419 <sup>207</sup>University of California, Berkeley, CA 94720, USA
- 2420 <sup>208</sup>Instituto de Física Teórica UAM-CSIC, Universidad Autónoma de Madrid, 28049 Madrid, Spain
- 2421 <sup>209</sup>Laboratoire d'Acoustique de l'Université du Mans, UMR CNRS 6613, F-72085 Le Mans, France
- 2422 <sup>210</sup>University of Southampton, Southampton SO17 1BJ, United Kingdom
- 2423 <sup>211</sup>University of California, Riverside, Riverside, CA 92521, USA
- 2424 <sup>212</sup>Dipartimento di Ingegneria Industriale, Elettronica e Meccanica, Università degli Studi Roma Tre, I-00146 Roma, Italy
- 2425 <sup>213</sup>University of Nevada, Las Vegas, Las Vegas, NV 89154, USA
- 2426 <sup>214</sup>University of Nottingham NG7 2RD, UK
- 2427 <sup>215</sup>Ariel University, Ramat HaGolan St 65, Ari'el, Israel
- 2428 <sup>216</sup>The University of Mississippi, University, MS 38677, USA
- 2429 <sup>217</sup>Graduate School of Science, Institute of Science Tokyo, 2-12-1 Ookayama, Meguro-ku, Tokyo 152-8551, Japan
- 2430 <sup>218</sup>Institute of Physics, Academia Sinica, 128 Sec. 2, Academia Rd., Nankang, Taipei 11529, Taiwan
- 2431 <sup>219</sup>The Chinese University of Hong Kong, Shatin, NT, Hong Kong
- 2432 <sup>220</sup>American University, Washington, DC 20016, USA
- 2433 <sup>221</sup>Dipartimento di Fisica, Università degli studi di Milano, Via Celoria 16, I-20133, Milano, Italy
- 2434 <sup>222</sup>INFN, sezione di Milano, Via Celoria 16, I-20133, Milano, Italy
- 2435 <sup>223</sup>Department of Applied Physics, Fukuoka University, 8-19-1 Nanakuma, Jonan, Fukuoka City, Fukuoka 814-0180, Japan
- 2436 <sup>224</sup>University of Cambridge, Cambridge CB2 1TN, United Kingdom
- 2437 <sup>225</sup>University of Lancaster, Lancaster LA1 4YW, United Kingdom
- 2438 <sup>226</sup>College of Industrial Technology, Nihon University, 1-2-1 Izumi, Narashino City, Chiba 275-8575, Japan
- 2439 <sup>227</sup>Faculty of Engineering, Niigata University, 8050 Ikarashi-2-no-cho, Nishi-ku, Niigata City, Niigata 950-2181, Japan
- 2440 <sup>228</sup>Department of Physics, Tamkang University, No. 151, Yingzhuan Rd., Danshui Dist., New Taipei City 25137, Taiwan
- 2441 <sup>229</sup>Rutherford Appleton Laboratory, Didcot OX11 0DE, United Kingdom
- 2442 <sup>230</sup>Department of Physical Sciences, Aoyama Gakuin University, 5-10-1 Fuchinobe, Sagami City, Kanagawa 252-5258, Japan
- 2443 <sup>231</sup>Helmut Schmidt University, D-22043 Hamburg, Germany
- 2444 <sup>232</sup>Nambu Yoichiro Institute of Theoretical and Experimental Physics (NITEP), Osaka Metropolitan University, 3-3-138 Sugimoto-cho, Sumiyoshi-ku, Osaka City, Osaka 558-8585, Japan
- 2445 <sup>233</sup>Directorate of Construction, Services & Estate Management, Mumbai 400094, India
- 2446 <sup>234</sup>Observatoire Astronomique de Strasbourg, 11 Rue de l'Université, 67000 Strasbourg, France
- 2447 <sup>235</sup>Faculty of Physics, University of Białystok, 15-245 Białystok, Poland
- 2448 <sup>236</sup>National Astronomical Observatories, Chinese Academic of Sciences, 20A Datun Road, Chaoyang District, Beijing, China
- 2449 <sup>237</sup>School of Astronomy and Space Science, University of Chinese Academy of Sciences, 20A Datun Road, Chaoyang District, Beijing, China
- 2450 <sup>238</sup>Sungkyunkwan University, Seoul 03063, Republic of Korea
- 2451

- 2452 <sup>239</sup>Department of Physics, Ulsan National Institute of Science and Technology (UNIST), 50 UNIST-gil, Ulju-gun, Ulsan 44919, Republic of Korea  
 2453 <sup>240</sup>Institute for Cosmic Ray Research, The University of Tokyo, 5-1-5 Kashiwa-no-Ha, Kashiwa City, Chiba 277-8582, Japan  
 2454 <sup>241</sup>Chung-Ang University, Seoul 06974, Republic of Korea  
 2455 <sup>242</sup>University of Washington Bothell, Bothell, WA 98011, USA  
 2456 <sup>243</sup>Laboratoire de Physique et de Chimie de l'Environnement, Université Joseph KI-ZERBO, 9GH2+3V5, Ouagadougou, Burkina Faso  
 2457 <sup>244</sup>Ewha Womans University, Seoul 03760, Republic of Korea  
 2458 <sup>245</sup>National Institute for Mathematical Sciences, Daejeon 34047, Republic of Korea  
 2459 <sup>246</sup>Korea Astronomy and Space Science Institute, Daejeon 34055, Republic of Korea  
 2460 <sup>247</sup>Department of Astronomy and Space Science, Chungnam National University, 9 Daehak-ro, Yuseong-gu, Daejeon 34134, Republic of Korea  
 2461 <sup>248</sup>Institute of Particle and Nuclear Studies (IPNS), High Energy Accelerator Research Organization (KEK), 1-1 Oho, Tsukuba City, Ibaraki 305-0801, Japan  
 2462 <sup>249</sup>Division of Science, National Astronomical Observatory of Japan, 2-21-1 Osawa, Mitaka City, Tokyo 181-8588, Japan  
 2463 <sup>250</sup>Nagoya University, Nagoya, 464-8601, Japan  
 2464 <sup>251</sup>Department of Physics, Aristotle University of Thessaloniki, 54124 Thessaloniki, Greece  
 2465 <sup>252</sup>Bard College, Annandale-On-Hudson, NY 12504, USA  
 2466 <sup>253</sup>Technical University of Braunschweig, D-38106 Braunschweig, Germany  
 2467 <sup>254</sup>Institute of Mathematics, Polish Academy of Sciences, 00656 Warsaw, Poland  
 2468 <sup>255</sup>Astronomical Observatory, Jagiellonian University, 31-007 Cracow, Poland  
 2469 <sup>256</sup>Department of Physics and Astronomy, University of Padova, Via Marzolo, 8-35151 Padova, Italy  
 2470 <sup>257</sup>Sezione di Padova, Istituto Nazionale di Fisica Nucleare (INFN), Via Marzolo, 8-35131 Padova, Italy  
 2471 <sup>258</sup>Department of Physics, Nagoya University, ES building, Furocho, Chikusa-ku, Nagoya, Aichi 464-8602, Japan  
 2472 <sup>259</sup>Université de Montréal/Polytechnique, Montreal, Quebec H3T 1J4, Canada  
 2473 <sup>260</sup>Indian Institute of Science Education and Research, Kolkata, Mohanpur, West Bengal 741252, India  
 2474 <sup>261</sup>Seoul National University, Seoul 08826, Republic of Korea  
 2475 <sup>262</sup>Department of Computer Simulation, Inje University, 197 Inje-ro, Gimhae, Gyeongsangnam-do 50834, Republic of Korea  
 2476 <sup>263</sup>NAVIER, Ecole des Ponts, Univ Gustave Eiffel, CNRS, Marne-la-Vallée, France  
 2477 <sup>264</sup>Gravitational Wave Science Project, National Astronomical Observatory of Japan (NAOJ), Mitaka City, Tokyo 181-8588, Japan  
 2478 <sup>265</sup>Department of Physics, National Cheng Kung University, No.1, University Road, Tainan City 701, Taiwan  
 2479 <sup>266</sup>St. Thomas University, Miami Gardens, FL 33054, USA  
 2480 <sup>267</sup>Scuola Normale Superiore, I-56126 Pisa, Italy  
 2481 <sup>268</sup>Institució Catalana de Recerca i Estudis Avançats, E-08010 Barcelona, Spain  
 2482 <sup>269</sup>Institut de Física d'Altes Energies, E-08193 Barcelona, Spain  
 2483 <sup>270</sup>Institut fuer Theoretische Astrophysik, Zentrum fuer Astronomie Heidelberg, Universitaet Heidelberg, Albert Ueberle Str. 2, 69120 Heidelberg, Germany  
 2484 <sup>271</sup>Institució Catalana de Recerca i Estudis Avançats (ICREA), Passeig de Lluís Companys, 23, 08010 Barcelona, Spain  
 2485 <sup>272</sup>Research Center for Space Science, Advanced Research Laboratories, Tokyo City University, 3-3-1 Ushikubo-Nishi, Tsuzuki-Ku, Yokohama, Kanagawa 224-8551, Japan  
 2486 <sup>273</sup>Tsinghua University, Beijing 100084, China  
 2487 <sup>274</sup>Department of Physics, National Institute of Technology, Calicut, 673601, Kerala, India  
 2488 <sup>275</sup>Institut des Hautes Etudes Scientifiques, F-91440 Bures-sur-Yvette, France  
 2489 <sup>276</sup>Faculty of Law, Ryukoku University, 67 Fukakusa Tsukamoto-cho, Fushimi-ku, Kyoto City, Kyoto 612-8577, Japan  
 2490 <sup>277</sup>Phenikaa Institute for Advanced Study (PIAS), Phenikaa University, Yen Nghia, Ha Dong, Hanoi, Vietnam  
 2491 <sup>278</sup>University of Stavanger, 4021 Stavanger, Norway  
 2492 <sup>279</sup>Physics Program, Graduate School of Advanced Science and Engineering, Hiroshima University, 1-3-1 Kagamiyama, Higashihiroshima City, Hiroshima 739-8526, Japan  
 2493 <sup>280</sup>GRAPPA, Anton Pannekoek Institute for Astronomy and Institute for High-Energy Physics, University of Amsterdam, 1098 XH Amsterdam, Netherlands  
 2494 <sup>281</sup>University College London, London WC1E 6BT, United Kingdom  
 2495 <sup>282</sup>Observatoire de Paris, 75014 Paris, France  
 2496 <sup>283</sup>Laboratoire Univers et Théories, Observatoire de Paris, 92190 Meudon, France  
 2497 <sup>284</sup>Graduate School of Science and Technology, Niigata University, 8050 Ikarashi-2-no-cho, Nishi-ku, Niigata City, Niigata 950-2181, Japan  
 2498 <sup>285</sup>University of Maryland, Baltimore County, Baltimore, MD 21250, USA  
 2499 <sup>286</sup>CSIR-Central Glass and Ceramic Research Institute, Kolkata, West Bengal 700032, India  
 2500 <sup>287</sup>Consiglio Nazionale delle Ricerche - Istituto dei Sistemi Complessi, I-00185 Roma, Italy  
 2501 <sup>288</sup>Department of Astronomy, Yonsei University, 50 Yonsei-Ro, Seodaemun-Gu, Seoul 03722, Republic of Korea  
 2502 <sup>289</sup>Department of Physics, University of Guadalajara, Av. Revolucion 1500, Colonia Olimpica C.P. 44430, Guadalajara, Jalisco, Mexico  
 2503 <sup>290</sup>Hobart and William Smith Colleges, Geneva, NY 14456, USA  
 2504 <sup>291</sup>INAF, Osservatorio Astronomico di Padova, I-35122 Padova, Italy  
 2505 <sup>292</sup>Dipartimento di Ingegneria, Università del Sannio, I-82100 Benevento, Italy  
 2506 <sup>293</sup>Museo Storico della Fisica e Centro Studi e Ricerche "Enrico Fermi", I-00184 Roma, Italy

- 2509 <sup>294</sup>*Kennesaw State University, Kennesaw, GA 30144, USA*
- 2510 <sup>295</sup>*Subatech, CNRS/IN2P3 - IMT Atlantique - Nantes Université, 4 rue Alfred Kastler BP 20722 44307 Nantes CÉDEX 03, France*
- 2511 <sup>296</sup>*Universidad de Antioquia, Medellín, Colombia*
- 2512 <sup>297</sup>*Departamento de Física - ETSIDI, Universidad Politécnica de Madrid, 28012 Madrid, Spain*
- 2513 <sup>298</sup>*Department of Electronic Control Engineering, National Institute of Technology, Nagaoka College, 888 Nishikataai, Nagaoka City, Niigata 940-8532, Japan*
- 2514 <sup>299</sup>*Trinity College, Hartford, CT 06106, USA*
- 2515 <sup>300</sup>*Dipartimento di Fisica e Scienze della Terra, Università Degli Studi di Ferrara, Via Saragat, 1, 44121 Ferrara FE, Italy*
- 2516 <sup>301</sup>*Faculty of Science, Toho University, 2-2-1 Miyama, Funabashi City, Chiba 274-8510, Japan*
- 2517 <sup>302</sup>*Indian Institute of Technology, Palaj, Gandhinagar, Gujarat 382355, India*
- 2518 <sup>303</sup>*Kavli Institute for Astronomy and Astrophysics, Peking University, Yiheyuan Road 5, Haidian District, Beijing 100871, China*
- 2519 <sup>304</sup>*Laboratoire MSME, Cité Descartes, 5 Boulevard Descartes, Champs-sur-Marne, 77454 Marne-la-Vallée Cedex 2, France*
- 2520 <sup>305</sup>*Faculty of Information Science and Technology, Osaka Institute of Technology, 1-79-1 Kitayama, Hirakata City, Osaka 573-0196, Japan*
- 2521 <sup>306</sup>*NASA Goddard Space Flight Center, Greenbelt, MD 20771, USA*
- 2522 <sup>307</sup>*Faculty of Science and Technology, Kochi University, 2-5-1 Akebono-cho, Kochi-shi, Kochi 780-8520, Japan*
- 2523 <sup>308</sup>*Laboratoire de Physique de l'École Normale Supérieure, ENS, (CNRS, Université PSL, Sorbonne Université, Université Paris Cité), F-75005 Paris, France*
- 2524 <sup>309</sup>*Faculty of Physics, University of Warsaw, Ludwika Pasteura 5, 02-093 Warszawa, Poland*
- 2525 <sup>310</sup>*Laser Interferometry and Gravitational Wave Astronomy, Max Planck Institute for Gravitational Physics, Callinstrasse 38, 30167 Hannover, Germany*
- 2526 <sup>311</sup>*The Hakubi Center for Advanced Research, Kyoto University, Yoshida-honmachi, Sakyou-ku, Kyoto City, Kyoto 606-8501, Japan*
- 2527 <sup>312</sup>*Department of Physics, Kyoto University, Kita-Shirakawa Oiwake-cho, Sakyou-ku, Kyoto City, Kyoto 606-8502, Japan*
- 2528 <sup>313</sup>*Yukawa Institute for Theoretical Physics (YITP), Kyoto University, Kita-Shirakawa Oiwake-cho, Sakyou-ku, Kyoto City, Kyoto 606-8502, Japan*
- 2529 <sup>314</sup>*University of Catania, Department of Physics and Astronomy, Via S. Sofia, 64, 95123 Catania CT, Italy*
- 2530 <sup>315</sup>*National Institute of Technology, Fukui College, Geshi-cho, Sabae-shi, Fukui 916-8507, Japan*
- 2531 <sup>316</sup>*Department of Communications Engineering, National Defense Academy of Japan, 1-10-20 Hashirimizu, Yokosuka City, Kanagawa 239-8686, Japan*
- 2532 <sup>317</sup>*Eindhoven University of Technology, 5600 MB Eindhoven, Netherlands*
- 2533 <sup>318</sup>*Kavli Institute for the Physics and Mathematics of the Universe (Kavli IPMU), WPI, The University of Tokyo, 5-1-5 Kashiwa-no-Ha, Kashiwa City, Chiba*
- 2534 *277-8583, Japan*
- 2535 <sup>319</sup>*Department of Astronomy, Beijing Normal University, Xijiekouwai Street 19, Haidian District, Beijing 100875, China*
- 2536 <sup>320</sup>*School of Physics and Technology, Wuhan University, Bayi Road 299, Wuchang District, Wuhan, Hubei, 430072, China*